UNIVERSIDAD COMPLUTENSE DE MADRID

FACULTAD DE CIENCIAS MATEMÁTICAS

DEPARTAMENTO DE MATEMÁTICA APLICADA

TESIS DOCTORAL

Estudios Analíticos y Numéricos de un Modelo de Vegetación de Tierras Secas
Analytical and Numerical Studies of a Dryland Vegetation Model

MEMORIA PARA OPTAR AL GRADO DE DOCTOR

PRESENTADA POR

Paris Kyriazopoulos

Directores

Jesús Ildefonso Díaz
Danielle Hilhorst
Ehud Meron

Madrid, 2014

Universidad Complutense de Madrid

FACULTA DE CIENCIAS MATEMÁTICAS

Departamento de Matemática Aplicada

Estudios Analiticos y Numericos de un modelo de vegetacion de tierras secas

Analytical and Numerical Studies of a Dryland Vegetation Model

Tesis doctoral realizada por:

Paris Kyriazopoulos

Bajo la direccnion de:

Jesús Ildefonso Díaz
Danielle Hilhorst
Ehud Meron

Madrid 2014

Resumen

La vegetación en ambientes de agua muy limitada ha atrado la atención de varios investigadores debido, entre otras razones, a la variedad de mosaicos de vegetación espaciales que se producen en tales áreas y los problemas ambientales que surgen en una época de rápidos cambios climáticos. En las últimas dos décadas, diversos modelos teóricos han sido formulados y usados para tratar cuestiones abiertas tales como la relativas a la formación de patrones de vegetación, desertificación, composición de la comunidad vegetal y la competencia en los ecosistemas de recursos limitados.

En esta tesis se considera un modelo de vegetación genrico que recoge un conjunto de relaciones esenciales entre agua y biomasa que se producen en ambientes secos. El modelo describe las interacciones entre múltiples especies de plantas, el agua subterranea del suelo y las aguas superficiales, a través de un sistema de ecuaciones de reacción-difusión, donde en particular la incognita dada por la concentración del agua superficial se rige por una ecuación cuasilineal de tipo medios porosos.

En el primer capítulo de la tesis, nos ocupamos de un problema estacionario simplificada para una forma unica de vida vegetal. En primer lugar, consideramos una ecuación escalar para la variable biomasa y mostramos que, bajo condiciones apropiadas en los parámetros fijos del problema, existen múltiples soluciones positivas para un rango del parámetro precipitación. En la segunda parte, nos ocupamos de un sistema de dos componentes de la biomasa y el suelo-agua que muestra la existencia de un continuo de soluciones fijas no uniformes que emanan de la rama de soluciones uniformes positivos utilizando la longitud del intervalo espacial como un parámetro de bifurcación. En la última sección, nos ocupamos del problema estacionario para la biomasa y el agua superficial y analizamos los frentes generados por esta incognita. En particular, suponiendo que la precipitación se distribuye de forma no homogénea en el espacio y se desvanece en una subregión de un dominio dado, estudiamos la transición de la altura del agua superficial en un entorno de la zona de cambio de precipitación.

En el segundo capítulo se estudia numéricamente un sistema ampliado teniendo en cuenta también la competencia por la luz. El sistema captura la competencia espacial entre dos especies de plantas distintas que hacen diferentes com-

promisos en la captación de agua en el suelo y la luz solar. Identificamos un rango del parámetro de precipitación para el que dos estados estables alternativos coexisten. El primero de los estado describe una distribución uniforme de una especie de planta que se especializa en la captura de agua en el suelo, mientras que el segundo estado describe un patrón peridico de una especie que se especializa en la captura de la luz. Se demuestra que este rango de biestabilidad generalmente se divide en tres partes: una que corresponde a bajo rango de precipitación, donde el competidor superior para el agua desplaza al competidor superior para la luz, un alto rango de precipitación donde se invierte el desplazamiento, y un rango intermedio donde ninguna de las especies desplaza a la otra. La gama intermedia permite la coexistencia de las especies en la forma de una multitud de soluciones localizadas estables que consisten en dominios fijos de una especie en zonas ocupadas por las otras especies.

En el tercer capítulo, consideramos un sistema modificado para una sola forma de vida vegetal. La difusión no lineal en la ecuación del agua superficial contiene ahora un trmino de absorción fuerte que modeliza procesos peculiares de infiltracin de aguas superficiales. Mostramos la de existencia de soluciones débiles para el problema de valor inicial en un dominio acotado y para condiciones iniciales acotadas: tanto para el caso del problema de condiciones de contorno de tipo Dirichlet como para el caso del problema de Neumann. En el primer caso, aproximamos el problema degenerado mediante problemas regularizados convenientes y obtenemos adecuadas estimaciones a priori que nos permite pasar al límite. En el segundo caso, la existencia de soluciones se prueba mediante el uso de un teorema de punto fijo. Por último, estudiamos algunas propiedades cualitativas de la componente de agua superficial para períodos secos, es decir, cuando la precipitación es insignificante o inexistente.

Índice General

Dedication

To my mom, dad and brother

Acknowledgements

I owe my deepest gratitude to my advisors: Ildefonso Diaz, Danielle Hilhorst and Ehud Meron, for their constant support and assistance in all the stages of this thesis. Without their encouragement this thesis would not have been possible.

There were many other people that supported me during my doctoral studies. Starting from the beginning, I am thankful to Michael Stich for the discussions we had in Madrid. He was the first who made me realize and appreciate the physicists perspective about research, this helped me a lot much later when I met Ehud Meron and his reasearch group in Israel. Also, I could not forget my friends in spain Alberto, Javier, Gonzalo, my mates Alex and Tommaso who have always been tolerant with my peculiarities.

I would like to thank the Technion in Haifa and Université Paris Sud for the facilities they offered to me, for my six month visit in Israel (Haifa) and one year visit in France (Orsay), respectively.

In Israel, I will never forget the time I spent in Sede Boker. I am grateful to Ehud Meron's research group for everything. I appreciate every group meeting I joined and every piece of knowledge they shared with me. My special thanks go to Yonatan as his ideas were the main ingredient of the second chapter of this thesis, to Yuval for helping me with the continuation package AUTO, to Yair and Shai for the numerous discussions we had. In Haifa, I also wish to thank Elad for his company and the things he taught me about Israel.

Finally, for the year I spent in Orsay I wish to express my appreciation to Danielle Hilhorst's research group: Yueyuan , Cuong, Thanh Nam, who brought me back to the mathematical way of thinking. Also, many thanks to my greek friend Filodamos who made me feel like home during my one year stay in France.

Abstract

Vegetation in water limited environments has attracted the attention of several researchers due to the variety of spatial vegetation mosaics that occur in such areas and the environmental issues that arise in a time of rapid climatic changes. The last two decades various theoretical models have been formulated and used to address open questions concerning vegetation pattern formation, desertification, plant community composition and competition in resource limited ecosystems.

In this thesis we consider a generic vegetation model that captures a set of essential feedbacks between water and biomass that take place in dry environments. The model describes the interactions among multiple plant species, soil-water and surface-water through a system of reaction-diffusion equations, where the surface-water variable, in particular, is governed by a porous medium type equation.

In the first chapter of the thesis, we are concerned with a simplified stationary problem for a single life form. We first consider a scalar equation for the biomass variable and show that under appropriate conditions on fixed parameters of the problem, multiple positive solutions exist for a range of the precipitation parameter. In the second part, we deal with a two-component system of biomass and soil-water showing the existence of continua of nonuniform stationary solutions which emanate from the branch of positive uniform solutions using the length of the spatial interval as a bifurcation parameter. In the last section, we deal with the complete water-biomass stationary problem focusing on the profiles of the surface-water solution. In particular, assuming that precipitation is inhomogeneously distributed in space and vanishes in a subregion of a given domain, we study the transition of the surface-water height in a neighborhood of the vanishing region.

In the second chapter, we study numerically an extended system taking into account competition for light, too. The system captures spatial competition between two distinct plant species that make different compromises in capturing soil water and sunlight. We identify a precipitation range along the rainfall gradient where two alternative stable states coexist. The first state describes a uniform distribution of a plant species that specializes in capturing soil water, whereas the second state describes a periodic pattern of a species that specializes in capturing light. We show that this bistability range generally divides into three parts:

a low precipitation range where the superior competitor for water displaces the superior competitor for light, a high precipitation range where the displacement is reversed, and an intermediate range where neither species displaces the other. The intermediate range allows for species coexistence in the form of a multitude of stable localized solutions consisting of fixed domains of one species in areas otherwise occupied by the other species.

In the third chapter, we consider a modified system for a single life form. The nonlinear diffusion in the surface-water equation is combined with a strong absorption term modeling the surface water infiltration process. We give existence proofs for the initial value problem in a bounded domain for bounded initial conditions treating the case of the Dirichlet and Neumann boundary conditions, separately. In the first case, we approximate the degenerate problem by regularized ones and obtain some a priori estimates of the approximating solutions which allow us to pass to the limit. In the second case, existence of solutions is proved by using a fixed point theorem. Finally, we study the qualitative properties of the surface-water solution for dry periods i.e when precipitation is negligible or absent.

Contents

Introduction

In a time of climate change and global warming the understanding of the response of vegetation to environmental changes and the impact that this may have on ecosystems has become crucial. The growth of plants as well as the distribution of vegetation depends strongly on the presence of various resources including nutrients, water and light. Among these resources, water is commonly accepted as a fundamental ingredient of life which is often in limited supply and depletes rapidly. As a result, dry, sub-humid, semi-arid, arid and hyper-arid regions of the planet, collectively known as drylands, have attracted the attention of vegetation ecologists and numerous other scientists. This interest is reenforced by the fact that drylands cover more than 40 percent of the earth's land surface and are home to more than two billion people. A common approach in the study of dryland vegetation involves mathematical models consisting of systems of partial differential equations which capture an essential part of the complex processes that take place in water limited environments. The analysis of such systems may provide an insight about the underlying causes of several observed phenomena such as spatial vegetation patterns and desertification. In addition, they can act as tools to address issues concerning species coexistence and biodiversity. The objective of this thesis is to study different aspects of a generic vegetation model which describes interactions between biomass and water in drylands.

Empirical evidence support that vegetation in drylands forms a variety of spatial patterns. Many of these patterns seem to be self-organized exhibiting characteristic length scales. Perhaps the most studied vegetation communities of this type are the tiger-bush patterns (TB). The TB are composed of regularly spaced vegetation bands interspersed with bare soil that form along the contours of gently slopped semi-arid regions and migrate uphill with constant speed that depends on the type of vegetation [22]. Diverse spatial vegetation patterns can also form in the absence of any environmental anisotropy. They include almost periodic patterns of vegetation spots, labyrinths, and vegetation gaps [20]. Such vegetation structures are not confined to a specific type of vegetation, but rather the can consist of trees, shrubs and grasses. Moreover, they have been reported worldwide at the edges of tropical deserts and they occur in a wide range of soils: from sandy and silty to heavy soils. This regular nonuniform character of

dryland vegetation was the motivation for the formulation of several continuum vegetation models that exhibit pattern formation properties. The first to introduce such a model were Lefever and Lejeune [46]. In their model, the evolution of vegetation is governed by a fourth order partial differential equation[1] which captures the interactions and redistribution of plants' biomass. Although, no water variable is present in the model, the resource scarcity can be controlled by a mortality rate parameter which may act as an aridity gradient. In particular, regular spatial patterns emerge for a subrange of this gradient: periodic patterns of spots, gaps and stripes are predicted for completely isotropic conditions (flat terrains), whereas moving banded structures develop when a topographic anisotropy is added (slopped terrains). After a few years, Klausmeier proposed a different vegetation model to investigate the TB phenomenon focusing on terrains of constant slope putting a water state variable in the picture [43]. In this model the biomass-water dynamics are captured by a reaction-diffusion equation for the biomass variable and a reaction advection equation for the water variable modeling the downhill flow of run-off water. Water supply is controlled by a precipitation rate parameter which allows us to investigate the response of vegetation to rainfall fluctuations. Within a precipitation range the model predicts spatial patterns which resemble satisfactorily the moving TB patterns [70]. Research efforts in this direction have given numerous pattern forming models describing biomass-water dynamics in both flat and non-flat topographies [9, 36, 60, 79].

The primary concern in the study of dryland vegetation models is the detection of different vegetation states which depict the spatial distribution of biomass under various environmental conditions. On a flat terrain (2d domain) and using the precipitation rate as the key control parameter, model studies have shown that a sequence of five basic stationary vegetation states arise along the precipitation gradient: the bare soil, the spot pattern, the stripe pattern, the gap pattern and the uniform vegetation state [51]. The bare soil state is realizable (stable) when precipitation rate is very low and represents the absence of biomass throughout a region under conditions of extreme water scarcity. For increased values of the parameter periodic spotted patterns of hexagonal symmetry arise which are composed of sparse vegetation spots alternating with bare soil. Crossing a higher precipitation threshold periodic stripe patterns emerge consisting of bands of vegetation separated by bare soil. When precipitation is further increased periodic gap patterns appear which are comprised of vegetation cover punctuated by spots of bare soil. Finally, at sufficiently high precipitation rates the uniform vegetation state becomes realizable and it corresponds to the homogeneous vegetation coverage under conditions of water abundance. The emergence of the periodic inhomogeneous states is a result of symmetry breaking phenomenon also known

[1]This PDE is actually an approximation of a more general no-local integro-differential equation

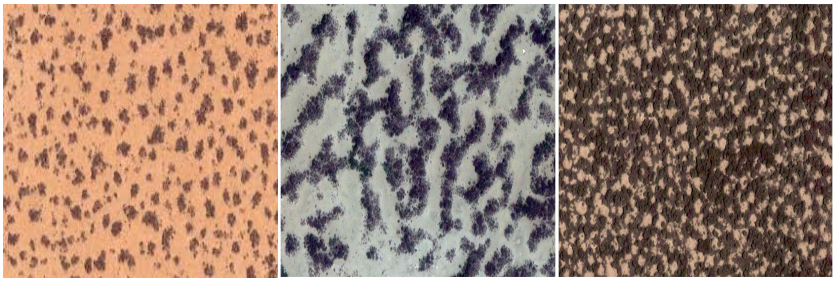

(a) Spotted patterns (b) Striped patterns (c) Gapped patterns

Figure 1: (a) Spotted vegetation patterns in Sudan (11.5331794N 27.9360008E), (b) striped patterns (labyrinths) in Niger (13.0724868N 2.2034025E), (c) gaps in vegetation cover in Senegal (15.20331N 14.8940384W). The images have been taken from google maps.

as Turing pattern formation mechanism. These states are in conformity with the vegetation patterns observed in fields for the corresponding rainfall values (Fig. 1). The sequence of basic states is often represented on a bifurcation diagram which displays branches of stationary biomass states versus the precipitation rate parameter. In such a diagram, parameter ranges can be located where two consecutive stable states coexist. Within these bistability ranges more spatially inhomogeneous solutions may emerge consisting of spatial mixtures of two basic stable states. These can be combinations of vegetation stripes and spots, or gaps. In other cases, the solutions are localized structures which consist of fronts separating domains of two alternative stable states. Depending on the parameter values, contracting or spreading fronts can generally be found. However, localized solutions can also be stabilized for some range of the control parameter as a result of front pinning.

Localized vegetation structures frequently arise in water limited regions. They have a well-defined size and shape, and occur at different scales. Some typical examples, that have been studied only recently, include spot and ring shaped vegetation patches of clonal plants [69, 52, 13] and holes in the vegetation cover, also known as fairy circles [75, 86] (see also Fig. 3 and Fig. 2). Unlike the periodic vegetation patterns, localized structures have no tendency to spread or invade the whole territory accessible to them. They can be either isolated patches or groups of patches which are restricted to subdomains of large fields and they can consist of the same or different life forms surrounded by uniform vegetation or bare soil. In many cases, the localized spots and the vegetation gaps seem to be stable for constant environmental conditions. On the other hand, the ring structures originate from circled vegetation patches (spots) which expand in the radial direction losing biomass in the middle part (this phenomenon is known as

'central die-back'). Beside the periodic and localized patterns, irregular patterns are also reported in field studies, for which no characteristic length scale can be identified. These type of scale-free structures can also be predicted by some mathematical models [80].

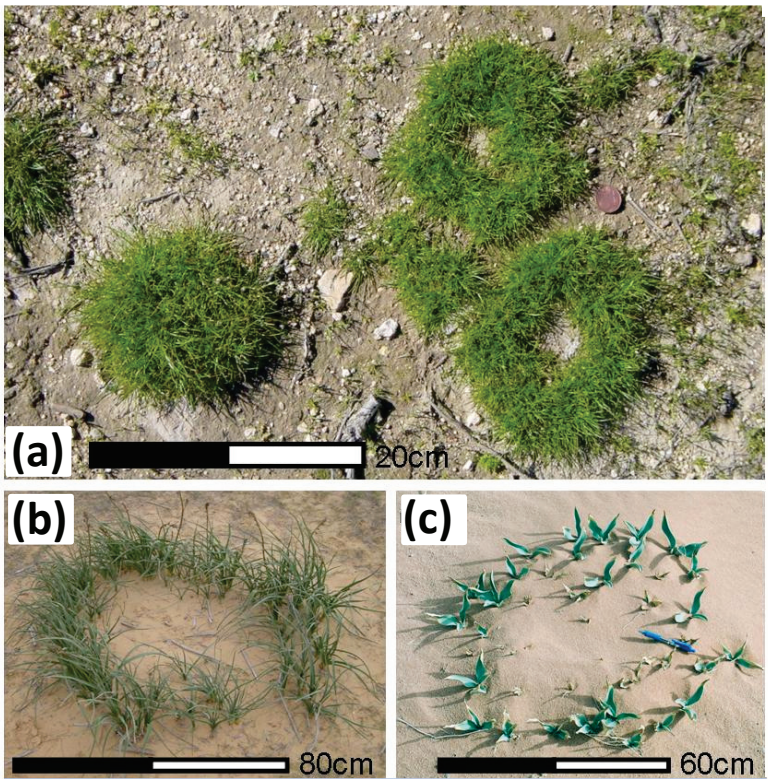

Figure 2: The pictures demonstrate examples of localized vegetation structures at different scales. (a) Mixture of rings and spots of Poa bulbosa observed in the Northern Negev (rainfall: 250 mm/yr). (b) A ring of Asphodelus ramosus observed in the Negev desert (170 mm/yr) (c) A ring of Urginea maritima observed in Wadi Rum, Jordan (50 mm / yr). These type of localized structures can vary in diameter from centimeters to meters. Pictures are taken from [68], photography by J. von Hardenberg (a) and H. Yizhaq (b), (c).

Desertification

A lot of attention has been paid on the use of mathematical models to understand the desertification phenomenon. Desertification is generally defined as an irreversible decrease of biological productivity in drylands which is induced by environmental changes. These changes may be climate variations as well as an-

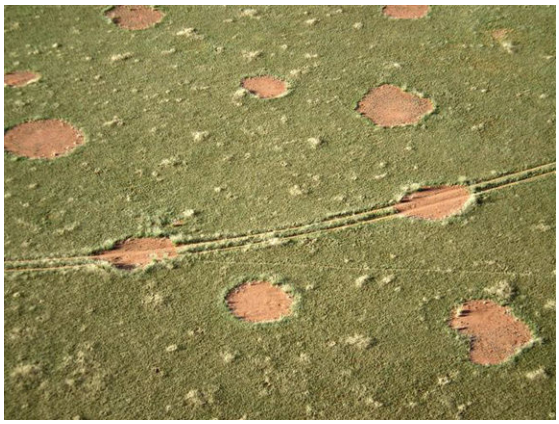

Figure 3: The picture depicts the so-called fairy circles which are common in the grasslands of southern Africa, specifically in Namibia, and they can grow from 2 to 15 meters in diameter.

thropogenic disturbances which in many cases accelerate the phenomenon. The complex nature and multiple temporal and spatial scales of the processes that take place in water limited ecosystems render the field and laboratory studies inadequate to provide complete understanding of desertification. In this effort mathematical models play a crucial role as they can predict the long term spatio-temporal dynamics of vegetation and its variations with respect to environmental parameters. In addition, they are capable to predict the various spatial vegetation patterns observed in drylands which may act as an indicator for imminent desertification [42]. This is based on the perception of desertification as a catastrophic shift involving abrupt transitions from a perennial vegetated state (high productivity state) to lower productivity states [64]. The critical states are vegetation patterns which are sensitive to a decrease of an environmental parameter or a disturbance which involves removal of vegetation biomass. Consequently, slight variations of the environmental conditions can cause a transition from one state to another. The transition is catastrophic as recovery of previous conditions is not enough to move the ecosystem back to high productivity levels [61]. This is usually illustrated by a hysterisis loop on a bifurcation diagram depicting the vegetation states versus the rainfall gradient. In such a diagram and within a given parameter range, the stable bare soil state (desert) coexists with at least one stable low productivity vegetated state, then a shift can occur from the vegetated state towards the bare soil state as precipitation is decreased below the left edge of the bistability range. It is notable that recent model studies have recognized patterns consisting of vegetation spots as the lowest productivity transitional states. Further research is conducted in this direction seeking the development of prevention and restoration policies.

Pattern formation and localized structures

In many cases, the spatial patterns that appear in nature are a result of self-organization processes. This kind of inhomogeneous structures have been studied in chemistry and biology using systems of reaction-diffusion equations, inspired by the celebrated paper of Turing on morphogenesis [77]. The original work of Turing refers to two interacting chemical substances, called morphogens, which diffuse throughout a given domain. The central idea behind his theory is that, under certain conditions, a spatially homogeneous steady state of the two substances which is stable (realizable) with respect to uniform perturbations may become unstable when the disturbances are nonuniform leading the system to some spatially inhomogeneous stationary state. In order for this instability to occur, the productive and degradative interactions between the two substances must be of a certain type and most importantly the two substances need to diffuse at different rates. This diffusion driven instability, also known as symmetry-breaking instability, constitutes a first mathematically recognized pattern formation mechanism. Based on this idea, Hans Meinhardt held the research on pattern formation a step forward by introducing a typical activator-inhibitor system, setting forth the so-called 'short-range-activation long-range-inhibition'pattern forming principle [33]. Reaction-diffusion systems inducing patterns also include the resource-consumer systems with their main representative being the Gray-Scott equations which in its original form describes simple autocatalytic reactions [38]. It is noteworthy that the Klausmeier's vegetation model and its extensions are actually a variation of the Gray-Scott model where the role of the resource is played by the soil-water and that of the consumer by the vegetation biomass [79]. Finally, reaction-diffusion systems have been used to generate animal coats patterns on growing domains [4, 53], while emergence of spatial patterns is also observed in fourth-order scalar evolution equations such as the extended Fisher-Kolmogorov equation [21, 55] and the Swift-Hohenberg equation [16, 72].

An important tool to study pattern formation properties of a reaction-diffusion system is the linear stability analysis (LSA) which we sketch below for a two-component system in a bounded domain. In particular, let $F : \mathbb{R}^2 \to: \mathbb{R}^2$ be a continuously differentiable vector field with $F(u) = (f(u), g(u))$, $\Omega \subset \mathbb{R}^2$ be a smooth bounded domain and consider the following reaction diffusion-system (RD)

$$\begin{cases} u_t - D\Delta u = \gamma F(u) & \text{in } \mathbb{R}^+ \times \Omega, \\ \\ u(0,x) = u_0(x) & \text{for } x \in \Omega, \end{cases} \tag{1}$$

along with the zero Neumann boundary conditions, where

$$D = \begin{pmatrix} \delta & 0 \\ 0 & 1 \end{pmatrix},$$

$\delta, \gamma > 0$ and $u(t,x) = (u_1(t,x), u_2(t,x))$. Suppose that u_s is a uniform steady state of the system, that is $F(u_s) = 0$. Let J denote the linearization matrix of F (Jacobian matrix) about the steady state and assume that all the eigenvalues of J have negative real part, i.e

$$\det(J) > 0 \text{ and } \mathrm{tr}\,(J) < 0. \tag{2}$$

The latter assumption essentially implies that u_s is linearly stable in the absence of diffusion. The primary aim of the LSA is to determine conditions under which u_s becomes linearly unstable to spatially inhomogeneous perturbations. For this we let $u = u_s + w$ and linearize (1) about u_s obtaining the following equation supposing that $|w|$ is small:

$$w_t = D\Delta w + \gamma J w,\ w(0,x) = w_0(x). \tag{3}$$

To solve this linear system we first consider the scalar eigenvalue problem

$$\Delta\phi + \mu\phi = 0,\ \nabla\phi \cdot \mathbf{n} = 0 \text{ on } \partial\Omega, \tag{4}$$

which admits a increasing sequence of eigenvalues, μ_n, and the corresponding eigenfunctions, ϕ_n, for $n \in \mathbb{N}$, where $\mu_0 = 0$ [71]. Next we take the Fourier expansion of the initial distribution of the perturbation, namely $w_0(x) = \sum_{n=0}^{\infty} \psi_n \phi_n$, where $\psi_n \in \mathbb{R}^2$ are the Fourier coefficients, and we look for solutions of the form

$$w(x,t) = \sum_{n=0}^{\infty} c_n(t)\phi_n(x),$$

where $c_n(t) \in \mathbb{R}^2$. By substituting $w(x,t)$ into (3) and using the fact that the eigenpair $\{\mu_k, \phi_k(x)\}$ satisfies (4), we conclude that for each n, $c_n(t)$ are the solutions of the system of ordinary differential equations

$$\frac{d}{dt}c_n = \gamma J c_n - \mu_n D c_n,\ c_n(0) = \psi_n.$$

To determine the temporal growth or decay of an eigenfunction $\phi_k(x)$ it suffices to investigate the eigenvalues of the matrix

$$\gamma J - \mu_n D,$$

which are given by the roots of the quadratic characteristic polynomial

$$\det\left(\lambda I - \gamma J + \mu_n D\right) = 0, \tag{5}$$

with I being the identity matrix. An instability can occur when for some n the real part of an eigenvalue $\lambda_n = \lambda(\mu_n)$ becomes positive for given values of

the parameters δ and γ. Note that this cannot be the case for the zero spatial eigenvalue, $\mu_0 = 0$, as this corresponds to a uniform perturbation. Moreover, due to the assumption (2), $\mathrm{tr}\,(\gamma J - \mu_n D) < 0$, and so the positivity of $\mathrm{Re}(\lambda(\mu_n))$ follows only if

$$\det\,(\gamma J - \mu_n D) < 0.$$

From this, we can conclude that the following conditions are necessary in order for a Turing instability to occur:

$$f_{u_1} + \delta g_{u_2} > 0 \text{ and } \frac{(f_{u_1} + \delta g_{u_2})^2}{4\delta} > f_{u_1} g_{u_2} - f_{u_2} g_{u_1}, \tag{6}$$

where f_{u_i} and g_{u_i} denote partial derivatives with respect to u_i of f and g, respectively, evaluated at the uniform steady state, u_s. In fact, the above conditions along with (2) imply that f_{u_1} and g_{u_2} must be of opposite signs, and that δ needs to be different than unity, which reveals that the two interacting quantities must diffuse at different rates. Roughly speaking, the formation of the spatially inhomogeneous stationary solution is attributed to the exponential growth with time of an eigenfunction $c_n(t)\phi_n(x)$ corresponding to a temporal unstable eigenvalue λ_n, which is eventually bounded by the nonlinearities in the reaction-diffusion equations. The above analysis can also be carried out for other boundary conditions (e.g. periodic BC) and infinite domains. Finally, it worths to mention that the LSA is also used for fourth-order scalar equations, cross-diffusion equations, where D is not a diagonal matrix, integro-differential equations and systems of three or more equations. In the latter case, difficulties arise due to the higher order polynomials that occur, examples and treatment of such systems can be found in [83].

Patterned solutions also occur in parameter regimes where a uniform steady state remains stable. To detect such regimes bifurcation analysis is usually involved to investigate the likelihood and behavior of continua of nontrivial stationary solutions (inhomogeneous solutions) lying on a space of functions versus a control parameter. These are branches of solutions emanating from the curve of uniform (trivial) solutions. Bifurcation analysis can be performed using numerical tools such as continuation methods [30], or analytical methods such as local and global bifurcation theory [15, 59]. In both cases, stability of some stationary solutions is always a challenging issue that needs to be addressed. On the other hand, spatial inhomogeneous distribution of a substance governed by a reaction-diffusion system can also be a result of interactions between different stationary states which give rise to localized solutions. An example exhibiting such solutions is the Swift-Hohenberg (SH) equation. A well studied form of this equation, in one spatial dimension, reads

$$\partial_t u = \lambda u + \mu u^2 - u^3 - (\partial_x^2 + k_0^2)^2 u. \tag{7}$$

The SH exhibits multiple stationary states among which regular patterns. In fact, using λ as a control bifurcation parameter various bistability ranges can be identified. For instance, such a range is formed between spatial periodic solutions and the uniform steady state, $u_s = 0$, near $\lambda = 0$ (see Figure 4). Within this bistability region localized structures emerge consisting of two oscillatory fronts confining a region of the patterned state in a zero background. The fronts can be stationary over a range of the control parameter leading to stable pulses, double-pulse and multi-pulse solutions as depicted in Figure 4. These are symmetric solutions which lie on the so-called homoclinic-snaking region [44].

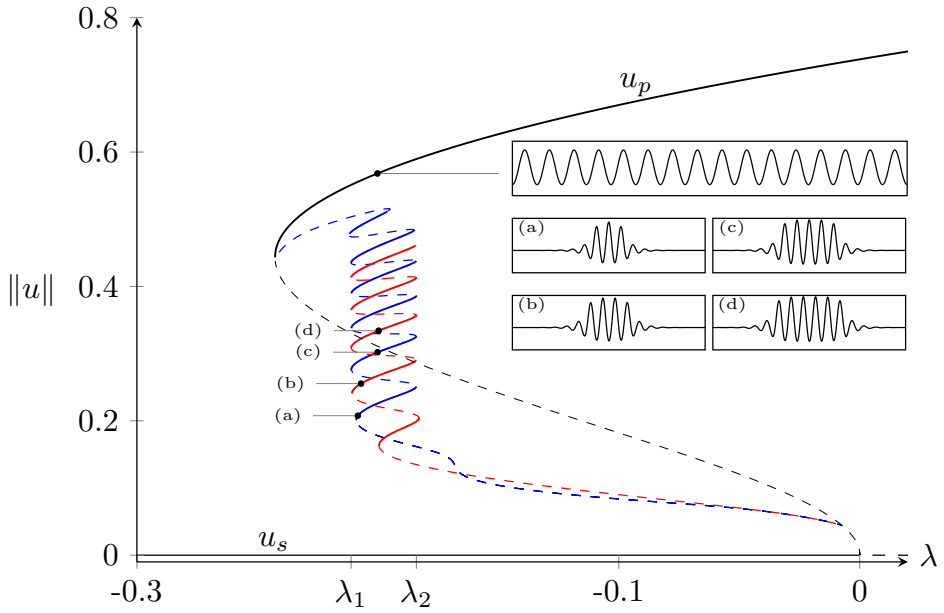

Figure 4: The bifurcation diagram of equation (7) endowed with the zero Neumann boundary conditions in a spatial interval of length L where x is rescaled so that $x \in (0, 1)$ and $\mu = 1.6$, $k_0 = 1$ are fixed. The diagram depicts the $L^2(0, 1)$ norm of stationary states vs the parameter λ. Solid (dashed) lines represent stable (unstable) states. The branch of periodic solutions, u_p, bifurcates subctitically from the line of trivial solutions, $u_s = 0$, at $\lambda = 0$. Near that point two branches of localized solutions with odd (blue) and even (red) number of humps emanate which form a snaking region situated within the parameter values λ_1 and λ_2. On the inset some nonuniform solutions are plotted vs the space variable x which correspond to particular points of the bifurcation diagram: on the top a periodic solution, underneath odd and even localized solutions. The odd solutions consist of one (a) and three picks (c) while the even ones consist of two (b) and four picks (d). The diagram has been produced using the continuation package AUTO [30].

0.1 The Model studied in this thesis

In this thesis, we consider different forms of a vegetation model introduced in [36]. The original model consists of equations for the above-ground biomass densities b_i of N interacting species ($i = 1, \ldots, N$), the soil water content per unit ground area w and the height of a surface-water layer above ground level h. The equations in dimensionless form read

$$\begin{cases} \partial_t b_i = d_{b_i}\Delta b_i + G_{b_i}(b, w)(1 - b_i)b_i - \mu_i b_i, \\ \partial_t w = d_w \Delta w - (L(b) + G_w(b))\, w + I(b)h, \\ \partial_t h = d_h \Delta h^2 - I(b)h + p, \end{cases} \tag{8}$$

where $b = (b_1, \cdots b_N)$ and in general x lies in $\Omega \subset \mathbb{R}^2$.

In the equation for b_i, the nonlinear growth rate of the i-th species involves a water dependent factor, $G_{b_i}(b_i, w)$, that represents water uptake by the plants' roots. The growth rate of grown plants is limited by genetic factors, such as stem strength, modeled by the term $(1 - b_i)$. In fact, in the dimensional model, these factors are captured by the parameter K_i which has been eliminated after rescaling ($b_i = B/K_i$, Table 2). Spatial biomass expansion is accounted for by a diffusion term that represents short-distance seed dispersal or clonal growth, where the "biomass diffusivity", d_{b_i}, is assumed to be a constant parameter. The term μ_i represents biomass loss rate by mortality and grazing which in the original model is a constant parameter but in general can also depend on x and/or t, or even on the above-ground biomass density. Note that in the case of inhomogeneous mortality rate $\mu(x)$, a different rescaling needs to be used (see Table 2). In particular, assuming $\bar{M} \geq M_1(x) \geq M_{0,1}$ is a bounded inhomogeneous mortality rate in dimensional quantities with $M_{0,1} > 0$, we set $t = M_{0,1}T$. Then, the constant M_1 in Table 2 is replaced by $M_{0,1}$ in all the associated terms.

In the equation for w, $I(b)$ accounts for the infiltration rate of the surface water into the soil. $L(b)$ represents the loss rate of soil-water due to evaporation while $G_w(b)$ stands for the total soil water uptake rate by all the life forms. The linear diffusion term describes water diffusion in non-saturated soil with constant water diffusivity d_w.

The equation for h models the flow of a thin surface water layer. Here p is a source term representing the precipitation rate which can be either a constant parameter or a variable depending on t and/or x. On the other hand, $-I(b)h$ is a loss term representing the infiltration of surface water into the soil. The nonlinear diffusion term $d_h\Delta h^2$ models the surface-water flow in flat topographies resulting from shallow water theory using a linear bottom friction term.

There are several feedbacks that this model captures which are accounted for by the explicit forms of the various terms of the system.

Shading effect

Evaporation in vegetated patches is reduced due to shading effect of above-ground biomass. This is a positive feedback between above-ground biomass and soil-water which is captured by the loss term $-L(b)w$ in the equation for w, where

$$L(b) = \frac{\nu}{\sum_{i=1}^{N}(1+\rho_i b_i)}.$$

Here, ν represents the constant evaporation rate in the absence of vegetation, while ρ_i accounts for the reduction of evaporation due to the shading effect of the ith plant species. For a weak shading feedback the above term can be simplified by assuming that $\rho_i \ll 1$, and so we may consider the linear approximation $\frac{\nu}{\sum_{i=1}^{N}(1-\rho_i b_i)}$. Moreover, if the feedback is essentially negligible, we take $\rho_i = 0$, and the evaporation rate becomes constant.

Infiltration rate

The water infiltration rate is not constant throughout the sparsely vegetated drylands. This is mainly attributed to the formation of biogenic soil crusts in unvegetated patches which decrease the infiltration of run-off water [84]. As a result, infiltration rate under vegetated patches is higher than in bare soil. In turn the increased soil-water under a vegetation patch benefits the plants growth accelerating further the infiltration. The above process renders a positive feedback between biomass and soil water modeled by the infiltration rate term given by

$$I(b) = \alpha \frac{\sum_i \psi_i b_i + q/c}{\sum_i \psi_i b_i + q}.$$

Here α represents the infiltration rate in a fully vegetated soil, $c \geq 1$ captures the infiltration contrast between soil and vegetated soil, and q is a biomass reference value beyond which infiltration rate under a vegetation patch approaches its maximum.

Root augmentation and water up-take

Plants capture water through their roots' system which constitutes their below-ground biomass. When the roots extent in the lateral direction the water suction is not a local process but also depends on the water availability in a zone around a plant. This process is captured by the following nonlocal form for the biomass-growth rates

$$G_{b_i}(x,t) = \nu\lambda_i \int g_i(x,x',t)w(x',t)dx',$$

$$g_i(x,x',t) = \frac{1}{\sigma_i^2 2\pi}\exp\left(-\frac{|x-x'|^2}{2\sigma_i^2(1+\eta_i b_i(x,t))^2}\right),$$

where λ_i is a parameter accounting for the biomass growth rate of the ith species per unit amount of soil water. The kernel $g_i(x', x, t)$ represents the roots architecture, where η_i quantify the root augmentation per unit of above-ground biomass which is a measure of the root-to-shoot ratio [2] and σ_i represents the lateral root-zone size of a seedling. This term also captures a positive feedback relation between the above-ground and below-ground biomass through the expression $(1+\eta_i b_i(x,t))^2$ which expresses the root system in terms of the above-ground biomass b.

For laterally extended root zones the water uptake is also nonlocal and is captured by the form

$$G_w(x,t) = \sum_{i=1}^{N} \gamma_i \int_\Omega g_i(x', x, t) b_i(x', t) dx'.$$

where γ_i represents the soil-water uptake rate per unit of above ground biomass. Here, the water loss at x is due to the water uptake of all the plants located at x' that extend their roots up to x. It is important to notice that g is asymmetric as $g_i(x, x', t) \neq g_i(x', x, t)$ because of the biomass dependence. Moreover, we remark that in both forms the integration is over Ω but in practice the integration can be over the entire domain $\mathbb{R}^2$ when the spatial scale of the roots' zone is much smaller than the region that is considered.

When the roots' system is narrow in the lateral direction, simplifications of the above terms can be considered. Roughly, using the dimensional quantities (see Table 2) we may suppose that S_i tends to zero so that $W(X) \approx W(X')$ and $B(X) \approx B(X')$ within the roots' zone. Then the biomass-growth and water-uptake rate are given by the local terms

$$G_{B_i} = \Lambda_i (1 + E_i B_i)^2 W \;\text{ and }\; G_W = \sum_{i=1}^{N} \Gamma_i (1 + E_i B_i)^2 B_i,$$

respectively. In this case, scaling in Table 2 needs to be reconsidered since the terms S_i vanish. An option is to let $x = X\sqrt{M_1/D_{B_1}}$, then $d_{B_i} = D_{B_i}/D_{B_1}$, $d_w = D_W/D_{B_1}$ and $d_h = D_H N(\Lambda_1 D_{B_1})^{-1}$ while the rest of the rescaled quantities in Table 2 remain the same.

[2] that is the analogy between below and above-ground biomass

Quantity	Units	Description
S_i	m	Lateral root size of a seedling
K_i	$\mathrm{kg/m^2}$	Maximum standing biomass
E_i	$(\mathrm{kg/m^2})^{-1}$	Root augmentation per unit biomass
N	yr^{-1}	Soil water evaporation rate
P	$\mathrm{kg/m^2\ yr}^{-1}$	Precipitation rate
D_{B_i}	$\mathrm{m^2/yr}$	Seed dispersal coefficient
D_W	$\mathrm{m^2/yr}$	Soil water diffusivity coefficient
D_H	$\mathrm{m^2/yr(kg/m^2)}^{-1}$	Surface water transport coefficient
R_i	–	Evaporation reduction due to shading
Q	$\mathrm{kg/m^2}$	Biomass reference value beyond which infiltration rate under a patch approaches its maximum
A	yr^{-1}	Infiltration rate in uniformly vegetated soil
M_i	yr^{-1}	Biomass decay rates
Λ_i	$(\mathrm{kg/m^2})^{-1}\mathrm{yr}^{-1}$	Biomass growth rate per unit soil water
Γ_i	$(\mathrm{kg/m^2})^{-1}\mathrm{yr}^{-1}$	Soil water uptake rate per unit biomass

Table 1: A list of dimensional quantities (state variables, space and time coordinates, parameters), their units and meanings. The subscript i refers to traits of the ith species.

Quantity	Scaling
b_i	B_i/K_i
w	$\Lambda_1 W/N$
h	$\Lambda_1 H/N$
x	X/S_1
t	$M_1 T$
η_i	$E_i K_i$
λ_i	Λ_i/Λ_1
p	$\Lambda_1 P/N M_1$
σ_i	S_i/S_1

Quantity	Scaling
d_{b_i}	$D_{B_i}/M_1 S_1^2$
d_w	$D_W/M_1 S_1^2$
d_h	$D_H N/M_1 \Lambda_1 S_1^2$
μ_i	M_i/M_1
ν	N/M_1
γ_i	$\Gamma_i K_i/M_1$
ρ_i	R_i
q	Q/K_1
α	A/M_1

Table 2: A list of dimensionless quantities. The subscript i refers to traits of the ith species.

Thesis outline

In the first chapter of this thesis, we deal with the stationary problem of the vegetation model. We first examine the existence and multiplicity of biomass stationary solutions in terms of a constant precipitation rate parameter p, for a localized simplification of the system, with non-homogeneous rate of biomass loss $\mu(x)$. In fact, we show that under appropriate conditions on fixed parameters of the problem, multiple positive solutions exist for a range of the parameter p. In the second part, we deal with a two-component system of biomass and soil-water showing the existence of continua of nonuniform stationary solutions which emanate from the branch of positive uniform solutions using the length of the spatial interval as a bifurcation parameter. In the last part, we consider the case of an idealized "oasis", $\omega \subset\subset \Omega$, where we study the transition of the surface-water height in a neighborhood of the set ω. Precisely, for a constant $p_0 > 0$ we assume that $p(x) = p_0\chi_\omega(x)$ on Ω, where χ_ω denotes the characteristic function of ω.

In the second chapter, we study the spatial competition between two plant species that make different compromises in capturing soil water and sunlight using a extended model which takes into account competition for light, too. A precipitation range along the rainfall gradient is identified where two alternative stable states coexist. The first state describes a uniform distribution of a plant species that specializes in capturing soil water, whereas the second state describes a periodic pattern of a species that specializes in capturing light. We show that this bistability range generally divides into three parts according to the dynamics of the front or ecotone that separates the two plant populations: a low precipitation range where the superior competitor for water displaces the superior competitor for light, a high precipitation range where the displacement is reversed, and an intermediate range where neither species displaces the other. While in the low and high precipitation ranges one species outcompetes the other, the intermediate range allows for species coexistence in the form of a multitude of stable localized solutions consisting of fixed domains of one species in areas otherwise occupied by the other species. These localized solutions can only be realized when one of the alternative stable states is spatially patterned. We further study two factors that affect the size of the species coexistence range: the strength of the competition for light and the form of the tradeoff between the competitive abilities to capture water and light.

The third chapter is devoted to the mathematical analysis of the time-dependent system with local biomass growth and water uptake rate terms but with a non-linear modified infiltration rate term. The existence of solutions is studied for the case of Dirichlet (DBC) and Neumann (NBC) boundary conditions for given essentially bounded initial data. The main difficulty in the study of the system arises from the degeneracy in the diffusion term of the equation for the surface

water variable h. To overcome this difficulty, in the case of DBC, the problem is approximated by a family of regularized systems for which existence of unique solutions is guaranteed. Next using some a priori bounds of the approximating solutions we obtain a solution of the original system by passing to the limit. For the case of NBC, we use a different approach based on a fixed point argument. In particular, we define an operator on a convex weakly closed subset into itself. Then the weak compactness properties of a mapping defined by the solutions of a decoupled inhomogeneous system, with fixed bounded initial data, induce that the operator has a weakly closed graph which ensures the existence of at least one fixed point. Finally, in the remainder of this chapter we examine the response of the system to long dry periods, that is $p(t) = 0$ for $t \in (0, T]$ for T large enough. We show that depending on the initial data and the boundary condition surface-water component either vanishes or forms vanishing regions which shrink gradually.

Chapter 1

On the elliptic system

1.1 Introduction

We study a system of elliptic equations which is the stationary version of the dryland vegetation model proposed by [37]. Precisely, the stationary problem is given by the following elliptic system:

$$\begin{cases} -\delta_b \Delta b = -\mu b + G_b b(1-b) & \text{in } \Omega, \\ -\delta_w \Delta w = -G_w w - \mathcal{L}_b w + \mathcal{I}_b h & \text{in } \Omega, \\ -\delta_h \Delta h^2 = -\mathcal{I}_b h + p & \text{in } \Omega, \\ \dfrac{\partial b}{\partial n} = \dfrac{\partial w}{\partial n} = \dfrac{\partial h}{\partial n} = 0 & \text{on } \partial\Omega, \end{cases} \tag{1.1}$$

where we suppose that $\Omega \subset \mathbb{R}^d$ is an open bounded domain for $d = 1$ or 2. Here, b represents the biomass, w the soil-water content and h the surface-water height after suitable non-dimensionalization. The growth rate G_b and the soil-water uptake rate G_w are non-local terms given by

$$G_b(b,w) = \nu \int_\Omega g(x,y) w(y)\, dy \quad \text{and} \quad G_w(b) = \gamma \int_\Omega g(y,x) b(y)\, dy,$$

where

$$g(x,y) = c_d \exp\big[-\frac{|x-y|^2}{2(1+\eta b)^2}\big], \text{ for } x, y \in \Omega,$$

with c_d being a normalization constant so that $\int_{\mathbb{R}^d} g(x,y)\, dy = 1$, for $\eta = 0$, i.e. $c_1 = \frac{1}{\sqrt{2\pi}}$ and $c_2 = \frac{1}{2\pi}$. The non-dimensional quantity $\mu \geq 1$ represents the biomass loss rate, which can be either a bounded inhomogeneous term, or a constant equal to unity when the mortality rate is supposed to be uniform. The

term $\mathcal{L}_b(b) = \dfrac{\nu}{1+\rho b}$ stands for the evaporation rate of the soil water, and $\mathcal{I}_b(b) = \alpha\dfrac{b+q/c}{b+q}$ represents the infiltration rate of the surface-water. The third equation of the parabolic system is a porous medium type equation that describes the overland flow of a thin water layer and involves the precipitation rate parameter $p > 0$. The rest of the parameters are positive, and in fact, $c > 1$. As we shall see, in special cases, some of the parameters may also be taken to be equal to zero.

In section 1, we consider the case of plant species with negligible below-ground biomass. In that case we may assume that the root extension parameter η is equal to zero. Since the minimal root size of a seedling for such plant species tends to zero, the non-local effect of the root system is insignificant. As a result, we may replace $g(x, y)$ with the Dirac delta based on x. Furthermore, for suitable scaling of the dimensional quantities we may assume that $\delta_b = 1$. Then we arrive at the following local coupled system

$$\begin{cases} -\Delta b = -\mu b + \nu w b(1-b) & \text{in } \Omega, \\ -\delta_w \Delta w = -\gamma b w - \mathcal{L}_b w + \mathcal{I}_b h & \text{in } \Omega, \\ -\delta_h \Delta h^2 = -\mathcal{I}_b h + p & \text{in } \Omega, \\ \dfrac{\partial b}{\partial n} = \dfrac{\partial w}{\partial n} = \dfrac{\partial h}{\partial n} = 0 & \text{on } \partial\Omega. \end{cases} \tag{1.2}$$

Moreover, we shall limit ourselves to the case where infiltration feedback and soil-water diffusion are not present. Roughly, this corresponds to $\delta_w = \delta_h = 0$. Finally, we consider an inhomogeneous biomass loss rate μ, which cannot exceed a minimal loss rate due to natural mortality and a maximal total loss rate. Precisely, in dimensionless quantities, we suppose that $\mu \in C^1(\bar{\Omega})$ is such that $1 \le \mu(x) \le \bar{\mu}$, for $x \in \bar{\Omega}$. On the basis of the considerations described above, in the first section we shall investigate the existence of positive solutions in terms of the precipitation parameter p, when $\Omega \subset \mathbb{R}^2$ is a bounded domain with C^2 boundary.

In the second part, we study the existence of nonuniform solutions for a simplified coupled system of the biomass variable b and the soil-water variable w in 1d. This is done by using a global bifurcation theorem and treating the length of the spatial interval as a bifurcation parameter. In particular, we show that continua of positive nonuniform solutions emanate from points of a branch of uniform (constant) solutions, for parameter values determined by particular eigenvalues of an associated linear problem.

In the third part, we consider system (1.1) in a bounded two dimensional domain assuming that the precipitation rate is inhomogeneous. Particularly, we assume that p is constant in a closed subset $\omega \subset\subset \Omega$ and vanishes outside ω.

Here, one may think of $p(\cdot)$ as a distributed water resource which is not negligible only on a sub-region ω of Ω. Moreover, in contrast with section 1, in this section we suppose that $\delta_w, \delta_h > 0$ and that the loss rate is a constant. In that occasion, we investigate the free boundary of the surface-water solution component h, in terms of the parameters involved in the third equation of (1.1).

1.2 A multiplicity result for a scalar biomass equation

In this section, we seek non-negative solutions of (1.2), depending on the parameter p, when $\delta_w = \delta_h = 0$ and $\mu(x)$ is a smooth function in Ω such that $1 \leq \mu(x) \leq \bar{\mu}$, where Ω is two dimensional bounded domain with a C^2 boundary. Thus, we study the following elliptic problem

$$\begin{cases} -\Delta b + \mu(x) b = p f(b) & \text{in } \Omega, \\ \\ \dfrac{\partial b}{\partial n} = 0 & \text{on } \partial\Omega, \end{cases} \tag{$\mathcal{P}_p$}$$

for

$$f(b) = \frac{\nu b(1-b)(1+\rho b)}{\gamma b(1+\rho b) + \nu}.$$

Clearly, $f(\cdot) \in C^2(\mathbb{R}^+)$,

$$0 \leq f(s) \leq M \quad \text{for all} \quad s \in [0,1],$$

and

$$f(s) < 0 \quad \text{for} \quad s \geq 1.$$

We also note, that $b \equiv 0$ is a solution of $(\mathcal{P}_p)$ for all $p > 0$, such a solution will be called the trivial. We shall first consider a subclass of weak solutions, namely, the so-called variational solutions. So, let us consider the set

$$K = \{v \in H^1(\Omega) \,|\, 0 \leq v \leq 1 \,\text{in}\, \Omega\},$$

and let

$$F_p(v) = p \int_0^v f(s)\, ds\,.$$

We define the variational functional

$$J_p(v) = \frac{1}{2} \int_\Omega \left(|\nabla v|^2 + \mu(x) v^2 \right) dx - \Phi_p(v),$$

where

$$\Phi_p(v) := \int_\Omega F_p(v(x))\, dx.$$

Definition 1. *We shall call a function $v \in H^1(\Omega)$, a variational solution of $(\mathcal{P}_p)$, if v is a minimum of the functional J_p on the set K.*

Remark 1. *It can be easily verified that any variational solution is a weak solution of a multivalued equation involving the subdifferential, ∂I_K of the convex function*

$$I_K(x) = \begin{cases} 0 & \text{if } x \in K \\ +\infty & \text{if } x \notin K \end{cases}$$

As it is proved in [23, Chapter 4] this multivalued equation satisfies the same comparison principle with the Euler-Lagrange equation which does not involve ∂I_K (i.e. equation $(\mathcal{P}_p)$). Thus if the solutions of $(\mathcal{P}_p)$ are greater than 0 or less than 1 in Ω the same holds for the multivalued equation.

We have:

Theorem 1. *For each $p > 0$, there exists at least one variational solution of $(\mathcal{P}_p)$.*

Proof. Since K is a convex closed subset of $H^1(\Omega)$, in order to show that J_p attains a minimum (due to a version of the Weierstrass theorem, see [85] p.513), it suffices to show that J_p is weakly lower semicontinuous and weakly coercive defined on K.

(i) J_p is weakly lower semicontinuous. Indeed, the norm on $H^1(\Omega)$ is weakly lower semicontinuous. On the other hand, the embedding $H^1(\Omega) \hookrightarrow L^q(\Omega)$ is compact for $1 \leq q < \infty$, since $N = \dim(\Omega) = 2$. Therefore, if v_n is a sequence in K that converges weakly in $H^1(\Omega)$ to a function v, we know that (up to a subsequence) $v_n \to v$ strongly in $L^q(\Omega)$. This actually implies that

$$\Phi_p(v_n) \to \Phi_p(v)$$

and so the map $\Phi_p : K \subset H^1(\Omega) \to R$ is weakly continuous. Thus $J_p(v)$ is weakly lower semicontinuous.

(ii) J_p is coercive. Indeed, for $u \in K$ we have $\Phi_p(v) \leq pM\|v\|_{L^1(\Omega)} \leq pM|\Omega|$ so for some constant $C(p,\Omega) > 0$, $J_p(v) \geq \frac{1}{2}\|v\|^2_{H^1} - C(p,\Omega)$ which implies that $J(v) \to \infty$ as $\|v\|^2_{H^1} \to \infty$. This ends the proof of the Theorem 1. □

We now proceed to consider solutions of $(\mathcal{P}_p)$ which are not necessarily variational solutions. Our study is inspired by a previous one arising in a completely different context: some simple climate models [25].

Before stating our main result, it is useful to consider the following auxiliary algebraic equations which provide us with positive constant super and sub-solutions of $(\mathcal{P}_p)$ for a range of the parameter p.

$$s = pf(s), \quad s \in \mathbb{R}, \tag{E_1}$$

$$\bar{\mu}s = pf(s), \quad s \in \mathbb{R}. \tag{E_2}$$

So, let us make some observations and introduce notation related to the set of non-negative solution of (E_1) and (E_2). We first observe that for all $p > 0$, $s = 0$ satisfies both equations and any possible positive solution of the auxiliary equations has to be lower than unity. We shall denote by Γ_1 and Γ_2 the (bifurcation) curves of nontrivial positive solutions corresponding to the algebraic equations (E_1) and (E_2), respectively. Now, let

$$T_1(p, s) = s - pf(s)$$

and

$$T_2(p, s) = \bar{\mu}s - pf(s).$$

Clearly, if p_i is such that

$$\frac{\partial}{\partial s} T_i(p_i, 0) = 0, \tag{1.3}$$

then Γ_i bifurcates from the line of trivial solutions at $(p_i, 0)$, for $i = 1, 2$. One can easily check that $p_1 = 1$ and $p_2 = \bar{\mu}$. Moreover, if the following condition is satisfied

$$\rho > 1 \quad \text{and} \quad \gamma < \nu(\rho - 1), \tag{C1}$$

then $\dfrac{\partial^2}{\partial s^2} T_i(p_i, 0) < 0$ and the bifurcation at $(p_i, 0)$ is subrcritical. In fact, (C1) also assures that Γ_i has a unique "turning point" (p_i^*, s^*) which satisfies

$$T_i(p_i^*, s^*) = 0 = \frac{\partial}{\partial s} T_i(p_i^*, s^*) \tag{1.4}$$

as well as

$$\frac{\partial^2}{\partial s^2} T_i(p_i^*, s^*) > 0 \text{ and } \frac{\partial}{\partial p} T_i(p_i^*, s^*) < 0,$$

for $i = 1, 2$, where

$$s^* = \frac{-(\gamma + \nu) + \sqrt{\nu^2 + \gamma\nu + \rho\gamma\nu}}{\gamma\rho} > 0.$$

Finally, we point out that for fixed $p \in (p_i^*, p_i)$, (E_i) has two distinct positive solutions denoted by $s_{i,p}^1$ and $s_{i,p}^2$, which are such that

$$s_{i,p}^1 < s^* < s_{i,p}^2,$$

while for $p \geq p_i$, (E_i) has a unique positive solution denoted again by $s_{i,p}^2$.

Theorem 2. *Let p_1, p_2 be the bifurcation points of (E_1), (E_2) given by (1.3). Also, assume that (C1) holds true and let p_i^* be the unique points that satisfy (1.4) for $i = 1, 2$. Then,*

(i) if $p \in (0, p_1^*)$, the trivial solution $b \equiv 0$ is the only possible non-negative solution of $(\mathcal{P}_p)$.

(ii) if $p_2^* < p_1$ and $p \in (p_2^*, p_1)$, $(\mathcal{P}_p)$ has at least two positive solutions, besides the trivial solution $b \equiv 0$.

(iii) if $p \in (\max\{p_1, p_2^*\}, \infty)$, then besides the trivial solution, $(\mathcal{P}_p)$ has at least one positive solution. In fact, for p large enough, there exists $\xi \in (0, 1)$ and a unique non-trivial positive solution of $(\mathcal{P}_p)$ satisfying $\xi \leq b(x) < 1$ in Ω. Moreover, this unique solution is also a variational solution of $(\mathcal{P}_p)$.

Proof. (i) By $(C1)$, there exists a unique pair $(p_1^*, s^*) \in \Gamma_1$ such that $f'(s^*) > 0$. In fact, we have that

$$f(s) \leq s f'(s^*) \quad \text{for all} \quad s \geq 0. \tag{1.5}$$

Therefore, if $b \in H^1(\Omega)$ is a non-negative solution of $(\mathcal{P}_p)$, by multiplying $(\mathcal{P}_p)$ by b and integrating over Ω, since $\mu(x) \geq 1$, we have that

$$\int_\Omega b^2 \, dx \leq \int_\Omega \left(|\nabla b|^2 + b^2 \right) dx \leq \int_\Omega f(b) b \, dx \leq p f'(s^*) \int_\Omega b^2 \, dx.$$

So, a non-negative solution which is not the trivial may exist only for $p > p_1^*$. In order to obtain (ii) and (iii), we now focus on positive constant super and sub-solutions of $(\mathcal{P}_p)$. Clearly, for $p > 0$ any positive solutions of the following problems

$$\begin{cases} -\Delta U_p + U_p = p f(U_p) & \text{in } \Omega, \\ \frac{\partial U_p}{\partial n} \geq 0 & \text{on } \partial\Omega, \end{cases}$$

and

$$\begin{cases} -\Delta V_p + \bar{\mu} V_p = p f(V_p) & \text{in } \Omega, \\ \frac{\partial V_p}{\partial n} \leq 0 & \text{on } \partial\Omega, \end{cases}$$

are respectively, sup or sub-solutions of $(\mathcal{P}_p)$. So, for every $p > p_1^*$ positive solutions of (E_1) form a family of positive constant super-solutions and for every $p > p_2^* > 0$ positive solutions of (E_2) form a family of sub-solutions of $(\mathcal{P}_p)$. Namely, we let

$$U_p^1 \equiv s_{1,p}^1, \; U_p^2 \equiv s_{1,p}^2 \text{ and } V_p^2 \equiv s_{2,p}^2.$$

(ii) If $p_2^* < p_1$, for each $p \in (p_2^*, p_1)$, we consider the ordered intervals $[0, U_p^1]$ and $[V_p^2, U_p^2]$, then from [1, Theorem 15.2, p.668], $(\mathcal{P}_p)$ has at least three distinct

solutions b_1, b_2 and b_3 such that $0 \leq b_1 < b_2 < b_3 < U_p^2$. Since b_1 may be identically zero (ii) follows.

(iii) For each $p \in (\max\{p_1, p_2^*\}, \infty)$, we consider the ordered interval $[V_p^2, U_p^2]$ where V_p and U_p are such that $V_p < U_p$. It is easy to check that the conditions of the results in [1] hold true and so there exist a minimal and a maximal solution in $[V_p^2, U_p^2]$. Moreover, for p large enough, any such positive weak solution takes values in an interval $[\xi, 1)$ where $f(\cdot)$ is decreasing which implies the uniqueness of any possible weak solution taking values in that interval. Finally, the energy of such weak solution is less than zero. Therefore, we deduce that for p large enough u_p is also a variational solution of $(\mathcal{P}_p)$. □

It is actually natural to ask whether the set of positive solutions consists of a connected closed set in $R \times X$ for some function space X. To this end, we let $X = C(\bar{\Omega})$ and recall that X possesses a positive cone P induced by the natural ordering. In fact, since P has non-empty interior, P is total i.e., $\{u - v : u, v \in P - 0\}$ is dense in X. We denote by K the solution operator of $-\Delta + \mu(x)$ together with the homogeneous Neumann boundary conditions, and by $F : P \to X$ the Nemiskii operator given by $F(u) = f^+(u(\cdot))$ where $f^+ = \max\{f, 0\}$. Note that $f^+ \in C^{0,\alpha}(R)$ and F is continuous and clearly, if $u \in P$, then $F(u) \in P$. Now let us consider the following auxiliary problem.

$$\begin{cases} -\Delta b + \mu(x) b = p f^+(b) & \text{in } \Omega, \\ \dfrac{\partial b}{\partial n} = 0 & \text{on } \partial\Omega. \end{cases} \tag{$\mathcal{P}_p^+$}$$

Since K is a linear positive compact operator from X to itself, we have that for $p > 0$ the map

$$pK \circ F : P \to X$$

is completely continuous and positive, where the latter means that $pK \circ F(P) \subset P$. Finally, the fixed point equation $u = pK \circ Fu$ for $u \in X$, is equivalent to equation $(\mathcal{P}_p^+)$. It can be checked that $K \circ F$ is right Frechet differentiable at $u = 0$, with K being the Frechet derivative from the right. Therefore by Theorem 18.3 in [1] (see also [17]), we conclude that:

Theorem 3. *The problem $(\mathcal{P}_p^+)$ possesses an unbounded continuum of positive solutions $\mathcal{C}^+$ in $R^+ \times P$, emanating from the line of trivial solutions $(p, 0)$ at $(p^*, 0)$, where p^* is the unique positive eigenvalue with a positive eigenvector of the following eigenvalue problem:*

$$\begin{cases} -\Delta b + \mu(x) b = \lambda b & \text{in } \Omega, \\ \dfrac{\partial b}{\partial n} = 0 & \text{on } \partial\Omega. \end{cases} \tag{1.6}$$

Remark 2. *By standard regularity theory and the strong maximum principle, we have that* $\max_{\bar{\Omega}} b(x) < 1$. *Therefore, since* $f(s) = f^+(s)$ *for* $s \in [0,1]$, *we have that* $(p,b) \in \mathcal{C}^+$ *also satisfies* $(\mathcal{P}_p)$. *Note that this is true for all* $\nu, \gamma, \rho > 0$.

1.3 A coupled water-biomass system

In this section, we study the existence of nonuniform solutions for a coupled system of the biomass variable b and the soil water variable w in a bounded interval. In particular, to obtain a two-component system and we ignore the infiltration feedback by setting $\delta_h = 0$ in (1.1) (the infiltration feedback can be neglected in sandy soils where the infiltration of surface water uniform and fast). Then we assume that the plant species with biomass b does not extend its roots in the lateral direction. As a result, we can consider local biomass growth and water-uptake rate terms which are given by the forms $G_b = \nu w(1+\eta b)$ and $G_w = \gamma b(1+\eta b)$, respectively. Furthermore, we assume that the biomass loss rate μ is uniform. We note that under the preceding assumptions, we may take $\delta_b = \mu = 1$, by choosing appropriately the rescaled quantities in the non-dimensionalization process. Finally, we also assume that a weak shading feedback is present in the system. In other words, $\rho \ll 1$ (note that ρ represents the water evaporation reduction due to shading of the plants) and so we can use a linear approximation of the evaporation rate term, namely, $\mathcal{L}_b \approx \nu(1-\rho b)$. The simplified coupled system then reads

$$\begin{cases} -b_{xx} = \nu w b(1-b)(1+\eta b) - b, \\ -\delta_w w_{xx} = p - w\left(\nu(1-\rho b) + \gamma b(1+\eta b)\right), \end{cases} \tag{1.7}$$

for x in $\Omega = (0,l)$

Next, in order to study the existence of spatially nonuniform solutions with respect to the length of the spatial domain, we rescale the spatial variable x letting $\tilde{x} = xl^{-1}$. By dropping the tilde notation and letting $\xi = l^2$, (1.7) can be transformed into the system

$$\begin{cases} -b_{xx} = \xi\left(\nu w b(1-b)(1+\eta b) - b\right), \\ -\delta_w w_{xx} = \xi\left(p - w\left(\nu(1-\rho b) + \gamma b(1+\eta b)\right)\right), \end{cases} \tag{1.8}$$

where $x \in (0,1)$ and ξ plays the role of a parameter in the system which carries information about the size of the spatial interval. We recall that system (1.8) is considered together with the homogeneous NBC:

$$b_x(0) = b_x(1) = 0 = w_x(0) = w_x(1). \tag{1.9}$$

Next we find conditions under which the above system possesses positive uniform solutions.

1.3.1 Uniform solutions

It is clear, that the pair $(b_0, w_0) = (0, p/\nu)$ is a trivial uniform nonnegative solution of (1.8). In addition, we can find pairs of positive uniform solutions of the system for specific choices of the parameters. Precisely, real pairs of constants $(b_s^{\pm}, w_s^{\pm})$ satisfying (1.8) exist when

$$\mathrm{dis}(p,\nu,\eta,\gamma,\rho) := (p\nu(\eta-1)-\gamma+\nu\rho)^2 - 4\eta\nu(1-p)(p\nu+\gamma) \geq 0\,, \qquad (1.10)$$

and are given by the expressions

$$b_s^{\pm} = \frac{(\eta-1)p\nu-\gamma+\nu\rho \pm \sqrt{\mathrm{dis}}}{2\eta(p\nu+\gamma)},$$

$$w_s^{\pm} = \frac{p}{b_s^{\pm 2}\gamma\eta + b_s^{\pm}(\gamma-\nu\rho)+\nu}.$$

We further need to determine the parameter values for which these solutions are positive. To simplify exposition in what follows we will assume that

$$\rho < \min\{\gamma/\nu, 1\}. \qquad (H1)$$

Then it is enough to find a parameter regime where $b_s^{\pm}$ is positive since this induces positivity of $w_s^{\pm}$, too. To this end, we distinguish two cases given that (1.10) is satisfied for $p,\nu,\eta,\gamma,\rho > 0$:

1. if $p\nu(\eta-1)-\gamma+\nu\rho \geq 0$, then b_s^+ is positive for $p > 1$, while $b_s^- < 0$. Note that, in this case, for $p = 1$, b_s^+ coincides with the solution $b_0 = 0$ and $b_s^{\pm} = b_0$ when $p\nu(\eta-1)-\gamma+\nu\rho = 0$.

2. if $p\nu(\eta-1)-\gamma+\nu\rho < 0$, then setting

$$p_c := \frac{2\sqrt{\eta\nu(\eta+\rho)(\gamma\eta+\gamma-\nu\rho+\nu)} - \gamma(\eta+1) - \eta\nu(\rho-2)+\nu\rho}{(\eta+1)^2\nu}\,,$$

   we have that $b_s^{\pm} > 0$ for $p_c < p < 1$, while $b_s^+ > 0$ and $b_s^- < 0$ for $p > 1$. Note that in this case, necessarily $\eta > 1$. Moreover, for $p = 1$, b_s^- coincides with the solution $b_0 = 0$.

Next we focus only on the uniform solutions (b_s^+, w_s^+), for the parameter values that they are positive and we drop the "+" notation. Our aim is to examine the rise of non-uniform solutions, emanating from the branch of uniform solutions using ξ as a bifurcation parameter. To apply a global bifurcation theorem, which is stated in the next section, it is convenient to set $u = b - b_s$ and $v = w - w_s$, so

that the constant solutions of the system are shifted to the origin. In particular, the shifted system is given by,

$$\begin{cases} -u_{xx} = \xi\left(J_{11}u + J_{12}v + f(u,v)\right), \\ -\delta_w v_{xx} = \xi\left(J_{21}u + J_{22}v + g(u,v)\right), \end{cases} \tag{1.11}$$

along with the zero Neumann boundary conditions

$$u_x(0) = u_x(1) = 0 = v_x(0) = v_x(1), \tag{1.12}$$

where

$$J_{11} := \nu w_s(1 + 2b_s(\eta - 1) - 3b_s^2\eta) - 1, \tag{1.13}$$
$$J_{12} := \nu b_s(1 - b_s)(1 + \eta b_s), \tag{1.14}$$
$$J_{21} := -2b_s w_s\gamma\eta - w_s\gamma + w_s\nu\rho, \tag{1.15}$$
$$J_{22} := -\gamma b_s^2\eta - b_s\gamma + b_s\nu\rho - \nu, \tag{1.16}$$

are the coefficients of the linear reaction part and

$$\begin{aligned} f(u,v) :=& uv\left(-3b_s^2\eta\nu + 2b_s\eta\nu - 2b_s\nu + \nu\right) - 3b_s u^2 v\eta\nu \\ &- 3b_s u^2 w_s\eta\nu - u^3 v\eta\nu - u^3 w_s\eta\nu \\ &+ u^2 v\eta\nu - u^2 v\nu + u^2 w_s\eta\nu - u^2 w_s\nu, \\ g(u,v) :=& -vu^2\gamma\eta - uv(2b_s\gamma\eta + \gamma - \nu\rho) - u^2 w_s\gamma\eta. \end{aligned}$$

are the non-linear reaction parts. It is also meaningful to consider the linear problem associated to (1.11), (1.12), namely, the eigenvalue problem

$$\begin{cases} -u_{xx} = \xi\left(J_{11}u + J_{12}v\right), \\ -\delta_w v_{xx} = \xi\left(J_{21}u + J_{22}v\right), \\ u_x(0) = u_x(1) = 0 = v_x(0) = v_x(1). \end{cases} \tag{1.17}$$

Note that a necessary condition for a point ξ^* to be a bifurcation point of (1.11), (1.12) is (1.17) to possess a non-trivial solution at ξ^*. Problem (1.17) admits non-nontrivial solutions for values of ξ such that

$$\det\begin{pmatrix} J_{11}\xi - \sigma_i & J_{12}\xi \\ J_{21}\xi & J_{22}\xi - \delta_w\sigma_i \end{pmatrix} = 0\,,$$

where σ_i are the eigenvalues of $-\partial_{xx}$ with the zero Neumann boundary conditions. In particular, these values are given by the pairs:

$$\xi_i^{\pm} = \sigma_i \frac{\delta_w J_{11} + J_{22} \pm \sqrt{(\delta_w J_{11} + J_{22})^2 - 4\delta_w(J_{11}J_{22} - J_{12}J_{21})}}{2(J_{11}J_{22} - J_{12}J_{21})}, \tag{1.18}$$

In order for the $\xi_i^{\pm}$ to be distinct real and positive numbers for each $i \geq 1$, we assume that

$$(\delta_w J_{11} + J_{22})^2 - 4\delta_w(J_{11}J_{22} - J_{12}J_{21}) > 0 \qquad (H2)$$

and

$$J_{11}J_{22} - J_{12}J_{21} > 0 \text{ and } \delta_w J_{11} + J_{22} > 0, \qquad (H3)$$

respectively, for fixed values of the parameters $p, \gamma, \eta, \nu, \rho, \delta_w$. It can be checked that these conditions are satisfied for a range of the parameters given that $\delta_w > 1$.

1.3.2 Nonuniform solutions

In order to investigate the existence of nonuniform solutions we first state an extension of the celebrated global bifurcation theorem of Rabinowitz [59], introduced by Blat and Brown in [8]. In this theorem the notion of the index of an isolated fixed point of a mapping is used. This can be defined in terms of the Leray-Schauder degree of the mapping in an neighborhood of the isolated fixed point [2, 48, 71]. In particular, let F be a continuously differentiable compact operator defined on a Banach space to itself, and let $F'_u(u_0)$ denote the Fréchet derivative of F at u_0. We recall that if $I - F'_u(u_0)$ is invertible, then u_0 is an isolated fixed point of F, and the index of $I - F$ at u_0 is given by

$$\text{ind}\,(I - F, u_0) = (-1)^{\beta},$$

where β is the sum of the algebraic multiplicities of the eigenvalues of $F'_u(u_0)$ which are greater than unity.

Theorem 4. *Let X be a Banach space and let $F : \mathbb{R} \times X \to X$ be a compact, continuously differentiable operator such that $F(\xi, 0) = 0$. Suppose that F can be written as,*

$$F(\xi, u) = K(\xi)u + R(\xi, u)$$

where $K(\xi)$ a linear compact operator and the Fréchet derivative of $R_u(\xi, 0) = 0$. Let ξ^* be such that $I - K(\xi)$ is invertible when $0 < |\xi - \xi^*| < \epsilon$ for some $\epsilon > 0$. Suppose ind$\,(I - F(\xi, \cdot), 0)$ is constant on $(\xi^* - \epsilon, \xi^*)$ and $(\xi^*, \xi^* + \epsilon)$ such that if $\xi^* - \epsilon < \xi_1 < \xi^* < \xi_2 < \xi^* + \epsilon$, then ind$\,(I - F(\xi_1, \cdot), 0) \neq$ ind$\,(I - F(\xi_2, \cdot), 0)$. Then there exists a continuum, $\mathcal{C}$, in the $\xi - u$ plane of solutions of $u = F(\xi, u)$, such that one of the following alternatives holds true

1. *either $\mathcal{C}$ joins $(\xi^*, 0)$ to $(\hat{\xi}, 0)$ where $I - K(\lambda)$ is not invertible,*
2. *or $\mathcal{C}$ joins $(\xi^*, 0)$ to infinity in $\mathbb{R}$.*

Let us now put our problem into the context of the preceding theorem. This can be achieved by rewriting (1.11) as an integral equation. For this we introduce the following Hölder spaces

$$Y = \{(f_1, f_2) |\, f_1, f_2 \in C^{2,\alpha}([0,1]) \text{ and } f_{1x}(0) = f_{1x}(1) = 0 = f_{2x}(0) = f_{2x}(1)\},$$

$$Z = \{(f_1, f_2) |\, f_1, f_2 \in C^{\alpha}([0,1])\}.$$

First we define the operator $\mathcal{L} : Y \to Z$ given by $\mathcal{L}(u.v) = (-\partial_{xx}u, -\delta_w \partial_{xx} v)$. Next we let $N : Z \to Z$ be the operator defined by the nonlinear reaction parts, namely

$$N(u, v) := (f(u, v), g(u, v)),$$

and the operators $J : Z \to Z$ and $D : Z \to Z$ defined, respectively, by the action of

$$J = \begin{pmatrix} J_{11} & J_{12} \\ J_{21} & 1_{22} \end{pmatrix}$$

and

$$D = \begin{pmatrix} 1 & 0 \\ 0 & \delta_w \end{pmatrix}$$

on elements of Z, where we have used the same notation for the operators defined on Z and the corresponding matrices. Then, finding solutions of system (1.11), (1.12) is equivalent to finding an element of Y satisfying the equation

$$\mathcal{L}(u, v) = \xi J(u, v) + \xi N(u, v). \tag{1.19}$$

Note that because of the zero Neumann boundary conditions, $\mathcal{L}$ is not invertable, so we cannot pass to the integral equation problem at this point. However, adding D in both sides the new operator defined by

$$\tilde{\mathcal{L}}(u, v) := \mathcal{L}(u, v) + D(u, v)$$

is invertible since the problem

$$\begin{cases} -c_1 y_{xx} + c_2 y = z, \\ y_x(0) = y_x(1) = 0, \end{cases} \tag{1.20}$$

with $z \in C^{\alpha}([0,1])$ has a unique solution $y \in C^{2,\alpha}([0,1])$ for all $c_1, c_2 > 0$. Therefore, solving (1.11), (1.12) is finally equivalent to solving the equation

$$(u, v) = \xi \tilde{\mathcal{L}}^{-1} J(u, v) + \tilde{\mathcal{L}}^{-1} D(u, v) + \xi \tilde{\mathcal{L}}^{-1} N(u, v) =: F(\xi, u, v). \tag{1.21}$$

We remark that $F : \mathbb{R} \times Z \to Y$ is continuous operator and as Y is compacted embedded into Z, in fact, $F : \mathbb{R} \times Z \to Z$ is compact (see for instance [2]). Then,

setting $K(\xi)(u,v) := \xi\tilde{\mathcal{L}}^{-1}J(u,v) + \tilde{\mathcal{L}}^{-1}D(u,v)$ and $R(\xi,u,v) := \xi\tilde{\mathcal{L}}^{-1}N(u,v)$, F is in the form of Theorem 4 for $Z = X$. In addition, $F(\xi,0,0) = 0$ for all ξ, the Fréchet derivative of $R(\xi,u,v)$ at $(0,0)$ is zero and the linear operator $K(\xi) : Z \to Z$ is compact. To apply Theorem 4, we need to find the critical values of ξ for which $\mathrm{ind}(I - K(\xi))$ changes sign. To evaluate the indices we look for eigenvalues of $K(\xi)(u,v)$, thus we search for nontrivial solutions of $K(\xi)(u,v) = \lambda(u,v)$. Writing the latter problem in terms of the differential operators we see that its nontrivial solutions occur for the pairs of eigenvalues $\lambda_i^{\pm}(\xi) = \frac{1+\sigma_i\xi/\xi_i^{\pm}}{1+\sigma_i}$ with $i \geq 1$. Clearly, $\lambda_i^{\pm}(\xi)$ are increasing functions of ξ and they cross 1 when ξ passes through $\xi_i^{\pm}$. Moreover, it can be shown that if $\xi_i^{\pm} \neq \xi_j^{\mp}$ for $i \neq j$ (i.e. excluding eigenvalues with algebraic multiplicity different than 1) $\lambda_i^{\pm}$ are simple eigenvalues (see for instance [12] and references therein). Therefore evaluating the index of $K(\xi)$ in the right and left neighborhood of such $\xi_i^{\pm}$, Theorem 4 can be applied with $\xi^* = \xi_i^{\pm}$ and $\epsilon > 0$ sufficiently small.

We conclude, that there exist continua $\mathcal{C}_i^{\pm}$ in $\mathbf{R} \times Z$ which bifurcate from $(\xi_i^{\pm}, 0, 0)$. Moreover, a triple $(\xi,u,v) \in \mathcal{C}_i^{\pm}$ satisfies (1.11), (1.12), therefore since the solutions of the original problem (1.8),(1.9) are given by $b = u + b_s$ and $w = v + w_s$, the branches $\mathcal{C}_i^{\pm}$, define continua of solutions of the original problem, bifurcating from $(\xi_i^{\pm}, b_s, w_s)$, which we denote by $\tilde{\mathcal{C}}_i^{\pm}$. Finally, the solutions lying on $\tilde{\mathcal{C}}_i^{\pm}$ are positive for $\xi > 0$. This is a consequence of the maximum principle and the use of local bifurcation theory [59], which ensures that the solutions are nonnegative sufficiently close to the bifurcation point. We also note that a continuum can cross the $\xi = 0$ axis only at $(0, b_s, w_s)$. To prove that this cannot be the case, and so $\tilde{\mathcal{C}}_i^{\pm}$ are defined only for $\xi > 0$, a priori estimates need to be derived for the solutions of the problem. Such estimates can also provide information about the global behavior of the branches of nonuniform solutions.

1.4 Surface water transition

In this section, we study the third equation of system (1.1), assuming that $\delta_w, \delta_h > 0$ and that the precipitation rate is not completely constant in Ω, but vanishes outside a closed subset $\omega \subset\subset \Omega$. For $p_0 > 0$, we let $p(x) = p_0\chi_\omega(x)$ on Ω, where χ_ω denotes the characteristic function of ω. We recall that the non-linear term of the equation involves the so-called infiltration contrast parameter $c > 1$. Now, supposing that b is a given non-negative solution of the corresponding equation of system (1.1) for the given boundary conditions, we set

$$\theta(x) := \alpha\frac{b(x) + q/c}{b(x) + q} \quad \text{in } \Omega.$$

Obviously, we have that $\frac{\alpha}{c} \leq \theta(x) \leq \alpha$ on Ω. On the other hand, letting $\tilde{h} = h^2$, if $h \geq 0$ and $\delta_h > 0$, then the third equation can be written as

$$\begin{cases} -\Delta\tilde{h} + \dfrac{\theta(x)}{\delta_h}\sqrt{\tilde{h}} = \phi(x) & \text{in } \Omega, \\ \dfrac{\partial\tilde{h}}{\partial n} = 0 & \text{on } \partial\Omega, \end{cases} \tag{1.22}$$

with $\phi(x) := \dfrac{p_0}{\delta_h}\chi_\omega(x)$.

We point out that, in general, we cannot ensure the uniqueness of function $\tilde{h}$ (in fact, in the preceding section, we exhibit a case of multiplicity of b and so of h). Nevertheless, for fixed b the non-negative solution of (1.22) is unique. Furthermore, by the maximum principle, we know that a possible solution $\tilde{h}$ must satisfy that

$$\|\tilde{h}\|_{L^\infty(\Omega)} \leq \left(\frac{p_0 c}{\alpha}\right)^2.$$

The following theorem provides an estimate on the location of the null set of a solution component h. This estimate depends on c, α, δ_h and p_0.

Theorem 5. *Let h be the third component of any non-negative solution of the system (1.1). Then, necessarily, $h(x) = 0$ for all $x \in \Omega - \omega$ such that*

$$d(x, \partial\Omega \cup \partial\omega) > 4\sqrt{p_0}\frac{c\sqrt{\delta_h}}{\alpha}.$$

In fact, at least one of those possible solutions verifies that $h(x) = 0$ for any $x \in \Omega - \omega$ such that $d(x, \partial\omega) > 4\sqrt{p_0}\dfrac{c\sqrt{\delta_h}}{\alpha}$.

Proof. We set $m = \dfrac{\alpha/c}{\delta_h}$. Following [23], we look for a local comparison function $\tilde{h}_m$ such that $\tilde{h} \leq \tilde{h}_m$ on the ball $B_R(x_0)$ and $\tilde{h}_m(x_0) = 0$, where $R \geq 4\sqrt{p_0}\dfrac{c\sqrt{\delta_h}}{\alpha}$ so that $B_R(x_0) \subset \Omega - \omega$. Then, since $\tilde{h} \geq 0$ clearly $\tilde{h}(x_0) = 0$ (and in a weak sense if $\tilde{h}$ is not continuous). In fact, if $\tilde{h}_m \in H^1(\Omega)$ satisfies

$$-\Delta\tilde{h}_m + m\sqrt{\tilde{h}_m} \geq 0 \qquad \text{in} \quad B_R(x_0), \tag{1.23}$$

$$\tilde{h}_m \geq \left(\frac{p_0 c}{\alpha}\right)^2 \qquad \text{on} \quad \partial B_R(x_0), \tag{1.24}$$

then, since

$$-\Delta\tilde{h} + m\sqrt{\tilde{h}} = \left(m - \frac{\theta(x)}{\delta_h}\right)\sqrt{\tilde{h}} \leq 0 \leq -\Delta\tilde{h}_m + m\sqrt{\tilde{h}_m} \text{ in } B_R(x_0),$$

by the comparison principle, we have that $\tilde{h} \leq \tilde{h}_m$.
Now, for such $x_0 \in \Omega - \omega$, we consider the function $\tilde{h}_m(x) = C_m|x - x_0|^4$ where $C_m = \left(\frac{m}{16}\right)^2$. Then it is not difficult to check (see [23]) that

$$-\Delta\tilde{h}_m + m\sqrt{\tilde{h}_m} \geq 0 \quad \text{in} \quad B_R(x_0),$$

and so the first conclusion holds. The second assertion holds merely by extending by zero some of those solutions on the set of $x \in \Omega - \omega$ such that $d(x, \partial\omega) > 4\sqrt{p_0}\dfrac{c\sqrt{\delta_h}}{\alpha}$ (since, obviously it also satisfies the Neumann boundary conditions). □

Remark 3. *In fact, it is possible to give a sharper estimate (near $\partial\Omega$) depending on the geometry of the domain Ω [23, ch. 2] but we shall not detail it here.*

Remark 4. *From the estimate of the preceding theorem we deduce that the distance of the free boundary from the set ω increases when one of the parameters p_0, δ_h or c increases or when α decreases. Moreover, the same answer remains true when the variation of the parameters is not necessarily monotone in each of them but the combination of them given by the expression $\dfrac{\sqrt{p_0}c\sqrt{\delta_h}}{\alpha}$ increases.*

Chapter 2

Species coexistence by front pinning

2.1 Introduction

Water-limited vegetation is generally patchy. According to the traditional view, vegetation patchiness is a result of an underlying physical template, often formed by slow geologic and geomorphologic processes, that creates favorable vegetation-growth areas [67]. A different view of vegetation patchiness has been motivated by recent field observations of banded vegetation and other forms of regular vegetation patterns in nearly homogeneous landscapes [76, 19]. According to this view vegetation patterns can result from small-scale biomass-water feedbacks that give rise to self-organization at large scales even in spatially uniform systems [62, 51]. Mathematical models that capture these feedbacks have been very instrumental in understanding the causes of self-organized vegetation patchiness and the specific forms it takes along the rainfall gradient [9]. Studies of such models have first identified five basic vegetation states along the rainfall gradient [81, 60]: uniform vegetation, hexagonal gap patterns, stripes or labyrinthine patterns, hexagonal spot patterns, and bare soil, which are in good agreement with field observations. They further suggest richer forms of self-organized vegetation patchiness: disordered spatial mixtures of basic states in bistability ranges, and amorphous patches that span wide patch-size distributions under conditions of global competition [80, 51].

Most model studies have considered a single plant species, overlooking the large plant communities that generally exist in water-limited landscapes [66]. The tendency of water-limited ecosystems to self-organize in patchy landscapes raises the question: what impact does vegetation pattern formation have on species coexistence and diversity? This is a significant question, particularly nowadays, when transitions between different vegetation states become more likely due to the

ongoing global climate change and the environmental fluctuations associated with it [32]. Understanding the response of plant communities to such transitions is important for maintaining the diversity of water-limited ecosystems and securing their function and stability.

Very few model studies have addressed the interaction between different species in water-limited vegetation, taking into account mechanisms of vegetation pattern formation. All of them have considered a pattern-forming species that acts as an ecosystem engineer [40, 41] by concentrating the water resource, thereby facilitating the growth of the other species understory [58, 39, 49]. One set of studies has focused on the interplay between biomass-water feedbacks that have opposite effects on the soil-water distribution, and the development ecosystem engineering under conditions of water stress [36, 34, 51]. Two other studies focused on species coexistence where a pattern-forming ecosystem engineer is an inferior competitor that survives the competition with a superior competitor because of the highly dispersive character of the latter [5, 54].

In this paper we propose a new pattern-formation mechanism of species coexistence that is based on a generic mathematical property associated with bistability of a uniform state and a periodic-pattern state - the possible existence of a multitude of stable localized structures (or homoclinic orbits in an appropriately defined dynamical system) [44]. These structures consist of confined domains of the patterned state in a background of the other, spatially uniform, alternative stable state, and vice versa. Their existence is related to the dynamics of the transition zones that separate the two alternative stable states, i.e. the fronts that are bi-asymptotic to the two states [57]. When the two alternative stable states are spatially uniform the fronts propagate in one direction or another, except for a particular value of the control parameter (the Maxwell point) at which the fronts are stationary [56]. By contrast, when one of the alternative stable states is spatially patterned there might exist a finite range of the control parameter within which fronts are stationary or pinned. It is within this range that localized structures are found. The mathematical property described above is commonly referred to as "homoclinic snaking", because of the snake-like forms of the solution branches that describe the localized structures in the corresponding bifurcation diagrams [44]. Localized structures of this kind were found also in a vegetation model for a single plant species in a bistability range of periodic vegetation pattern and bare soil [47, 86].

To study species coexistence associated with bistability of uniform and patterned states we consider two plant species in water limited ecosystems that are related to one another by a tradeoff between investment in growing taller shoots and investment in increasing root-to-shoot ratio. Taller plants have an advantage in capturing light whereas plants with higher root-to-shoot ratios have an advantage in capturing soil water. We study the interaction between these two

species along a rainfall gradient using a modified version of the vegetation model introduced by Gilad et al. [35] that includes inter-specific competition for light. Since the proposed coexistence mechanism is based on a generic mathematical property of bistable pattern-forming systems, the results presented here may be applicable to many other contexts of ecological communities.

2.2 Modeling community dynamics

The model we study is based on the multi-species vegetation model introduced by Gilad et al. [34, 50]. The Gilad et al. model describes the evolution of a plant community in a water limited system where species interact through competition for water. In its most general form the model consists of a system of integro-differential equations that models non-local water uptake by laterally extended root zones. Here we study a modified version of this model that takes into account competition for light too, but simplifies it in other respects.

2.2.1 Model equations

The original model consists of equations for the above-ground biomass densities B_i of N interacting species ($i = 1, \ldots, N$), the soil water content per unit ground area W and the height of a surface-water layer above ground level H. We simplify it first by assuming that the infiltration rate of surface water into the ground is approximately constant, independent of the plants' biomass. Quite often the infiltration rate in bare soil is lower than that in vegetated soil because it is covered by physical and biogenic crust that makes the infiltration slower [31]. This effect can be negligible in sandy soils which are often uncrusted. When the infiltration rate is constant the equation for H decouples from the equations for W and the B_is and the variable H can be eliminated [86]. The model equations in one dimension (1d) then read

$$\frac{\partial B_i}{\partial t} = \Lambda_i(B) G_{B_i}(B_i, W)(1 - B_i/K_i)B_i - M_i B_i + D_{B_i}\frac{\partial^2 B_i}{\partial x^2}, \tag{2.1a}$$

$$\frac{\partial W}{\partial t} = P - LW - G_W(B)W + D_W\frac{\partial^2 W}{\partial x^2}\,, \tag{2.1b}$$

where $B = (B_1, \ldots, B_N)$ and x represents a 1d lateral direction. The nonlinear growth rate of the i-th species includes a water dependent factor, $G_{B_i}(B_i, W)$, that represents water uptake by the plants' roots, and a biomass dependent factor, $\Lambda_i(B)$, that accounts for light attenuation by competing plant species. The growth rate of grown plants is also limited by genetic factors, such as stem strength, whose effects are lumped in the parameter K_i. In the case of annuals K_i can also represent the limited size a plant can develop in its life cycle. Biomass growth is

also limited by mortality and grazing that are represented by the parameter M_i. Spatial biomass expansion is accounted for by a diffusion term that represents short-distance seed dispersal or clonal growth, where the "biomass diffusivity", D_{B_i}, is assumed to be a constant parameter. In the soil water equation (2.1b), the parameter P represents the precipitation rate while L represents the evaporation rate, which in general may also depend on the above-ground biomass to account for reduced evaporation by shading. The factor $G_W(B)$ is the rate of water uptake by the plants' roots, and its biomass dependence reflects the increase in the root-zone size as the above-ground increases, i.e. the root-to-shoot ratio. Lastly, the term $D_W \partial^2 W/\partial x^2$ models water transport in a non-saturated soil with D_W being a diffusivity constant.

2.2.2 Competition for water

Plants compete for water through water uptake by their roots. For laterally extended root zones the uptake is nonlocal and is captured by the following form [36],

$$G_W(x,t) = \sum_{i=1}^{N} \Gamma_i \int g_i(x',x,t) B_i(x',t) dx',$$

where the kernel $g_i(x',x,t)$ represents the roots architecture, and the integration is over the root zone of plants located at x. We use the form

$$g_i(x,x',t) = \frac{1}{\sigma_i \sqrt{2\pi}} \exp\left(-\frac{|x-x'|^2}{2\sigma_i^2 (1+E_i B_i(x,t))^2}\right),$$

where E_i quantify the root augmentation per unit of above-ground biomass, which is a measure of the root-to-shoot ratio. Note that $g_i(x,x',t) \neq g_i(x',x,t)$ because of the biomass dependence. The biomass growth rates have nonlocal forms too

$$G_{B_i}(x,t) = \int g_i(x,x',t) W(x',t) dx',$$

since they depend on water availability at all points where the plants' roots extend to.

Another simplification we make here is the assumption of laterally confined root zones. This assumption is consistent with the assumption of sandy soil (used to eliminate the surface water variable) because its high soil-water diffusivity combined with gravity gives an advantage to plants with roots extending vertically to deep soil layers. To implement this simplification we take the limits $\sigma_i \to 0$ (vanishingly small lateral root sizes of seedlings) in which the biomass growth rates and the water uptake rate become

$$G_{B_i}(B_i, W) = (1 + E_i B_i)W, \tag{2.2}$$

$$G_W(B) = \sum_{i=1}^{N} \Gamma_i B_i (1 + E_i B_i)\,. \tag{2.3}$$

Competition for water can be inter-specific, occurring between individuals that belong to different plant species, or intra-specific, occurring between individuals that belong to the same plant species. Inter-specific competition is captured by the rate forms (2.2) and (2.3), which give advantage to species with higher E_i values, for they grow faster and leave less water for other species. Intra-specific competition is also captured but in a spatial context; the biomass density of a given species, B_i, does not resolve the different individuals that contribute to the biomass $B_i(x,t)dx$ within a small length element (area element in 2d) around the point x, but does distinguish between groups of individuals that occupy different length elements.

An important manifestation of intra-specific competition occurring between distinct spatial locations is spatial instabilities leading to vegetation patterns. Intra-specific competition leading to vegetation pattern formation is captured by the soil-water diffusion term and the water uptake term in (2.1b), which together with the water-dependent biomass growth rate form a positive feedback between local vegetation growth and water transport towards the growing vegetation. The water uptake by a patch of growing vegetation depletes the local soil water content and induces water diffusion from the patch surroundings. The supply of water by diffusion accelerates the vegetation growth in the patch, but also inhibits the growth in the patch surroundings, thereby favoring the growth of nonuniform perturbations and the formation of vegetation patterns.

2.2.3 Competition for light

When the productivity of a system is sufficiently high, taller plants reduce the availability of light to shorter plants by shading. The positive feedback between shoot growth and light availability results in an inter-specific competition for light that can lead to the dominance of the taller plant species [74] [1]. To capture competition for light we introduce the following form for the biomass growth rate of the i-th plant species:

[1] Note that the biomass variable represents the overall biomass per unit area of the i-th species, irrespective of the number of individuals contributing to it. Thus, the modeling approach used here does not resolve local intra-specific competition. However, it does take into account nonlocal intra-specific competition as explained in Section 2.2.

$$\Lambda_i(B) = \Omega_i \left(1 - \frac{\Sigma_{j\neq i} B_j}{\Sigma B_j + h}\right) . \tag{2.4}$$

Here, Ω_i represents the growth rate of the i-th species in the absence of competitors and h is a positive constant serving as a reference value for the total biomass beyond which light becomes a limiting resource for small plants.

2.2.4 Trait tradeoff

We consider species that make different tradeoffs between investment in shoot growth and investment in root growth. To define this tradeoff we quantify the investment in shoot growth by the parameter K and the investment in root growth by the parameter E, and describe them parametrically as

$$\begin{aligned} K = K(\chi;\alpha) =& K_{\min} + (K_{\max} - K_{\min})(1-\chi)^{\alpha}, \\ E = E(\chi;\alpha) =& E_{\min} + (E_{\max} - E_{\min})\chi^{\alpha}, \end{aligned} \tag{2.5}$$

where $\chi \in [0,1]$ is a dimensionless tradeoff parameter, which describes the community of interest. The ith species is defined by the pair (K_i, E_i) or, alternatively, by the point χ_i on the tradeoff axis[2]. The parameter $\alpha > 0$ delimits tradeoff curves in the rectangle $R = [E_{\min}, E_{\max}] \times [K_{\min}, K_{\max}]$ that describe different species pools as Fig. 2.1 illustrates.

2.2.5 Parameter values and units

The model equations are presented in dimensional form. The dimensions of the state variables, the independent space and time variables, and the model parameters are presented in Table 1. Table 1 also displays the numerical values used in this study for the various parameters. No attempt has been made to fit the parameter values to a specific ecosystem; the values used rather represent the correct orders of magnitude for herbaceous or small woody vegetation (e.g. shrubs) in general. For simplicity, in what follows we drop the units notation from numerical values of parameters and variables and refer the reader to Table 1 for that purpose.

[2]More precisely, the point χ_i, including a small length element $\Delta\chi$ around it, describes a functional group whose species share the same values, K_i and E_i, of the functional traits K and E.

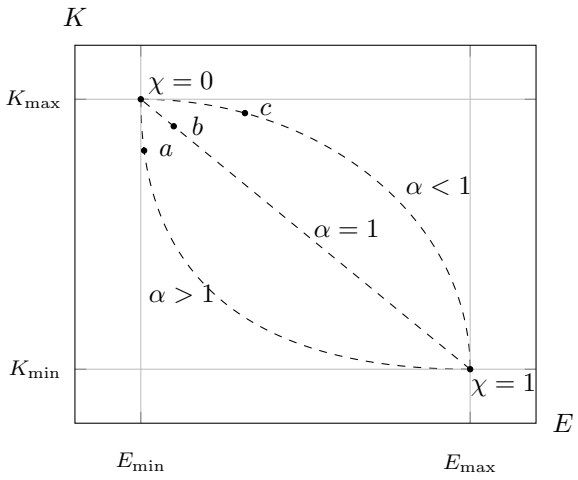

Figure 2.1: The tradeoff between soil-water capture, as quantified by E, and sunlight capture, as quantified by K (see (2.5)). Shown are three typical tradeoff lines in the rectangle $[E_{\min}, E_{\max}] \times [K_{\min}, K_{\max}]$ that are parameterized by $\chi \in [0, 1]$ and represent different species pools: diagonal ($\alpha = 1$), subdiagonal ($\alpha > 1$) and supdiagonal ($\alpha < 1$). The solid circles represent the two species to be considered, $\chi = 0$ (biomass B_1) and $\chi = 1$ (biomass B_2) for most of the studies, and $\chi \ll 1$ (the circles a, b, c) and $\chi = 1$ for studying the effect of the species pools (or α) on species coexistence (Section 2.5.2).

Quantity	Units	Description	Value
B_i	$\mathrm{kg/m^2}$	Biomass density	–
W	$\mathrm{kg/m^2}$	Soil water density	–
x	m	Space coordinate	[0,5]
t	yr	Time coordinate	–
K_{min}	$\mathrm{kg/m^2}$	Minimal standing biomass limit	0.5
K_{max}	$\mathrm{kg/m^2}$	Maximal standing biomass limit	3
E_{min}	$(\mathrm{kg/m^2})^{-1}$	Minimal root augmentation per unit biomass	0.5
E_{max}	$(\mathrm{kg/m^2})^{-1}$	Maximal root augmentation per unit biomass	3
χ_1	–	Tradeoff parameter for superior light competitor	$\chi_1 \ll 1$
χ_2	–	Tradeoff parameter for superior water competitor	1
L	$\mathrm{yr^{-1}}$	Soil water evaporation rate	6
P	$\mathrm{kg/m^2\ yr^{-1}}$	Precipitation rate	variable
h	$\mathrm{kg/m^2}$	Reference total-biomass value for light to become a limiting resource	variable
D_W	$\mathrm{m^2/yr}$	Soil water diffusivity	6.25×10^{-1}
$D_{B_1} = D_{B_2}$	$\mathrm{m^2/yr}$	Seed dispersal coefficient	6.25×10^{-5}
$M_1 = M_2$	$\mathrm{yr^{-1}}$	Biomass decay rates	2
$\Omega_1 = \Omega_2$	$(\mathrm{kg/m^2})^{-1}\mathrm{yr^{-1}}$	Biomass growth rate per unit soil water	0.1
$\Gamma_1 = \Gamma_2$	$(\mathrm{kg/m^2})^{-1}\mathrm{yr^{-1}}$	Soil water uptake rate per unit biomass	2.2

Table 2.1: A list of dimensional quantities (state variables, space and time coordinates, parameters), their units, meanings and numerical values. The subscript i refers to traits of the ith species.

2.3 Stationary solutions

We consider the system (2.1) for two interacting plant species, that is, the set of equations

$$\begin{aligned}
\frac{\partial B_1}{\partial t} &= \Lambda_1(B) G_{B_1}(B_1, W)(1 - B_1/K_1)B_1 - M_1 B_1 + D_{B_1}\frac{\partial^2 B_1}{\partial x^2}, \\
\frac{\partial B_2}{\partial t} &= \Lambda_2(B) G_{B_2}(B_2, W)(1 - B_2/K_2)B_2 - M_2 B_2 + D_{B_2}\frac{\partial^2 B_2}{\partial x^2}, \\
\frac{\partial W}{\partial t} &= P - LW - G_W(B)W + D_W\frac{\partial^2 W}{\partial x^2}\,,
\end{aligned} \tag{2.6}$$

where G_{B_i}, $G_W(B)$ and $\Lambda_i(B)$ are given, respectively, by (2.2), (2.3) and (2.4) for $i = 1, 2$ and $B = (B_1, B_2)$. We study this system on a finite spatial interval imposing periodic boundary conditions. Analogous results can be obtained for the homogeneous Newmann boundary conditions. Since we are primarily interested in species that make different compromises in their investments in above and below-ground biomass, we characterize them by χ values close to zero and close to unity. Specifically, we assign a value $\chi_1 \ll 1$ to the species with biomass B_1, and a value $\chi_2 = 1$ to the species with biomass B_2. The χ_1 species represents a superior competitor for light (high K and low E) while the χ_2 species represents a superior competitor for water (high E and low K). The two species are kept identical in regard to all other trait parameters.

2.3.1 Uniform states

The system (2.6) possesses three types of uniform equilibria $U = (B_1, B_2, W)$:

- The trivial bare soil state $U_0 = (0, 0, W_0)$
- Pure population states $U_1^* = (B_1^*, 0, W_1^*)$ and $U_2^* = (0, B_2^*, W_2^*)$,
- Coexistence states of the form $\bar{U} = (\bar{B}_1, \bar{B}_2, \bar{W})$.

A linear stability analysis of these solutions is described in Appendix A. The results are summarized in the bifurcation diagram in Fig. 2.2, which shows the existence and stability ranges of selected stationary uniform states (excluding, in particular, the coexistence states which are unstable in the parameter range considered here). At very low precipitation values P, the bare-soil state, U_0, is the only stable state. At sufficiently high P values there is a bistability range of the two uniform pure-population states, U_1^* and U_2^*. The latter loses stability at $P = P_2^M$ to a mixed-population state, leaving the pure-population state U_1^* of the superior light competitor, $\chi_1 \ll 1$, as the only stable state in the range $P > P_2^M$. The stability range of the uniform state U_1^* is bounded below by a nonuniform stationary instability at P_1^T (see Fig. 2.2) that leads to a stationary periodic pattern. The uniform state U_2^* can also go through such an instability but at lower precipitation values. These are Turing instabilities [77] that in the present context require strong water uptake and fast soil-water diffusion relative to the rate of seed dispersal or clonal growth.

2.3.2 Spatially periodic states

To study the solutions that appear below the Turing instability at P_1^T we resort to numerical continuation and stability methods. Applying the continuation package AUTO [30] with P as a bifurcation parameter we find the spatially periodic solution $U_{1,p}^* = (B_1^*(x), 0, W_1^*(x))$ that emanates from the U_1^* uniform-solution

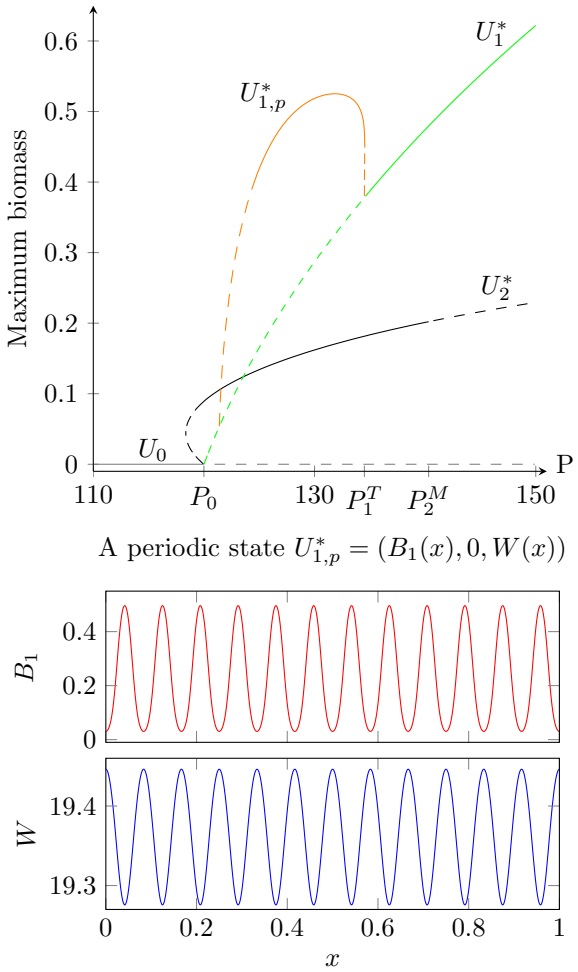

Figure 2.2: Bifurcation diagram (top) showing biomass-precipitation solution branches for the bare-soil state, U_0, the two pure-population uniform states, U_1^* and U_2^*, and for the pure-population periodic-pattern state, $U_{1,p}^*$, for which the maximum biomass is plotted. Solid (dashed) lines denote stable (unstable) states. The two uniform states bifurcate from the bare-soil state at $P = P_0$. The periodic-pattern state bifurcates from the corresponding uniform state at $P = P_1^T$ and reconnects to it at a lower precipitation value. The spatial dependence of the biomass $B_1(x)$ and soil-water $W(x)$ associated with the periodic-pattern state $U_{1,p}^* = (B_1(x), 0, W(x))$ are shown at the bottom part of the figure. Note the existence of a bistability precipitation range of the uniform U_2^* solution and of the periodic $U_{1,p}^*$ solution. Parameters are as in Table 1 with $\chi_1 = 0$. Note that the spatial domain is scaled down by a factor 5.

branch at P_1^T, and additional periodic solutions, not shown in Fig. 2.2, that emanate from the U_1^* branch at $P < P_1^T$. All solution branches reconnect to the U_1^* branch at lower P values. Figure 2.2 also shows typical spatial biomass and soil-water profiles associated with these periodic solutions. As Fig. 2.2 indicates there is a wide bistability range of the uniform U_2^* state and the periodic $U_{1,p}^*$ pattern.

2.3.3 Localized states

As discussed in the Introduction section, bistability ranges of uniform and periodic-pattern states often give rise to stable localized solutions involving confined domains of one state in a system otherwise occupied by the alternative state. In the bistability range of the uniform U_2^* state and the periodic $U_{1,p}^*$ pattern such solutions correspond to confined patterns of the species χ_1 that specializes in capturing light in an otherwise uniform distribution of the species χ_2 that specializes in capturing soil water. The bifurcation diagram in Fig. 2.3 shows the solution branches associated with several localized solutions of increasing size and their stability properties. The localized solution branches snake up towards the periodic-pattern solution, acquiring an additional hump in each turn as the panels (a-f) show. Unlike some other examples of homoclinic snaking [44, 6, 18] there appears to be a single family of localized solutions containing both odd and even numbers of humps [10], rather than two distinct families of odd solutions and of even solutions.

2.4 Species coexistence and spatial displacement

The multiplicity of stable localized solutions implies the possible coexistence of the two species in the same area and under the same environmental conditions. This is a new species coexistence mechanism in uniform environments associated with pattern formation [54]. The mechanism is related to the inability of either species to displace the other, or to the pinning of the front that is bi-asymptotic to U_2^* and $U_{1,p}^*$. The front pinning can be viewed as resulting from the interplay between competition for light and water; because of the different tradeoffs the two species make in capturing these resources, each species has an advantage and disadvantage in attempting to displace the other, which balance one another. The physical and ecological processes that maintain this balance over a precipitation range rather than at a single precipitation value (the Maxwell point) are not clear yet.

The localized structures occupy a limited subrange within the bistability precipitation range of the two pure-population states U_2^* and $U_{1,p}^*$. Outside this subrange, but still within the bistability range, one species displaces the other as Figs. 2.4a,d show. At relatively high precipitation water is no longer a strong

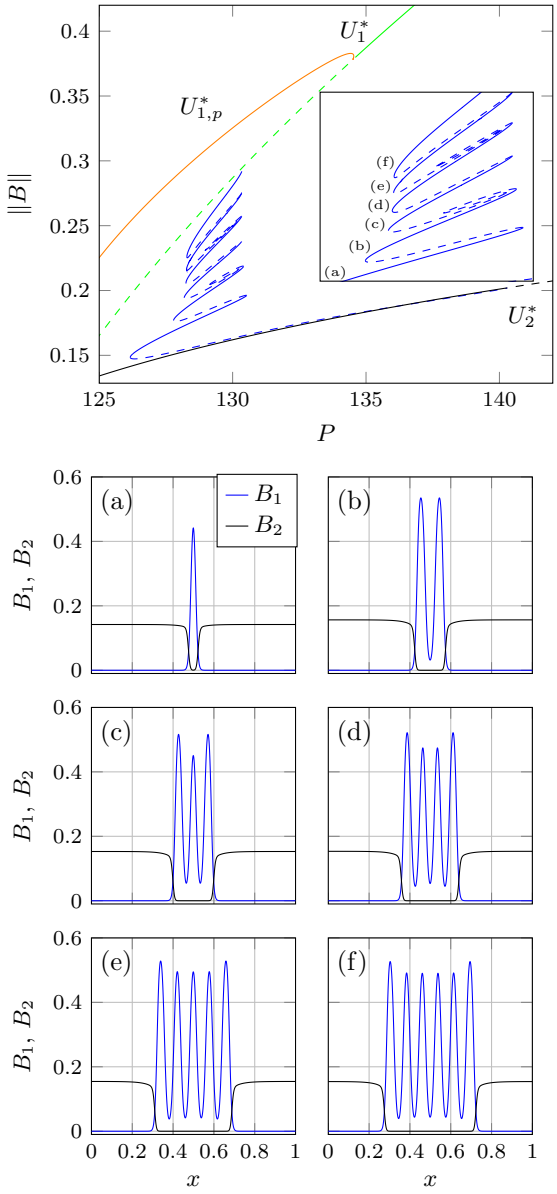

Figure 2.3: A bifurcation diagram that includes localized solution branches (top). The vertical axis is chosen here to be the L_2 norm of the biomass variables defined as $\|B\| = (\int B_1^2 + B_2^2 dx)^{1/2}$. The inset shows a blow up of the localized solution branches labeled in ascending order of localized-solution sizes as the spatial solution forms in panels (a-f) show. The blue and black graphs denote B_1 and B_2, respectively. Parameters are as in Table 1 except that the spatial domain is scaled down by a factor 5.

limiting factor and competition for light becomes more important. As a result, the $U^*_{1,p}$ state, which represents a periodic pattern of the better competitor for light, invades into areas occupied by the U^*_2 state (2.4d). At relatively low precipitation the vegetation is less dense and light is no longer a strong limiting factor. As a result the competition for water becomes more important, and the U^*_2 state, which represents the better competitor for water, invades into areas occupied by the $U^*_{1,p}$ state (Fig. 2.4a).

Within the range of localized structures there is a significant subrange in which the only stable localized structure is a single hump solution, and a smaller subrange where only single-hump and two-hump solutions are stable. In these subranges, large initial domains of the patterned state $U^*_{1,p}$ first contract but do not disappear; they rather converge to a single-hump or two-hump solutions, as Fig. 2.4b demonstrates. Most of the remaining subrange of stable localized solutions contains a high multiplicity of localized structures of increasing sizes. Within

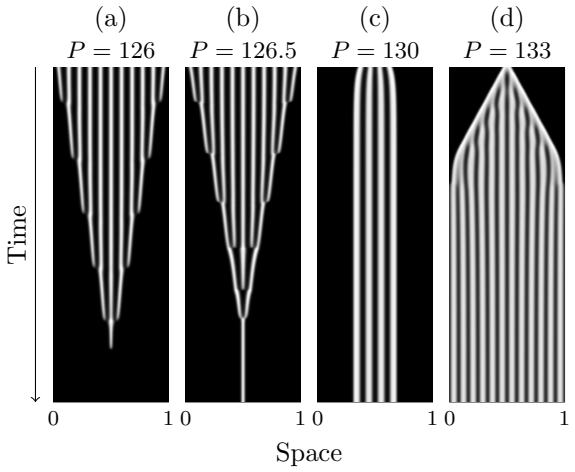

Figure 2.4: Space-time plots showing different dynamical behaviors within the bistability range of the U^*_2 state (uniform distribution of the χ_2 species) and the $U^*_{1,p}$ state (periodic pattern of the χ_1 species). At low precipitation outside the range of stable localized solutions the U^*_2 state invades into the $U^*_{1,p}$ state, leading asymptotically to a U^*_2 state occupying the whole domain (a). At higher precipitation the U^*_2 state still invades into large domains of the $U^*_{1,p}$ state, but the invasion process culminates in a stable single-hump localized solution (b). At yet higher precipitation a multitude of stable localized solutions exists and any localized initial condition converges to a nearby localized solution (c). Finally, at sufficiently high precipitation the $U^*_{1,p}$ state invades into the U^*_2 state, leading asymptotically to a $U^*_{1,p}$ state occupying the whole domain (d). Parameters are as in Table 1 with P as specified in the figure.

this subrange most initial conditions have "nearby" stable localized solutions to which they converge on a relative short time scale without noticeable contraction or expansion, as Fig. 2.4c demonstrates.

2.5 Factors controlling species coexistence

The precipitation range of stable localized structures defines the species coexistence range; domains of periodic distributions of the χ_1 species embedded in an otherwise uniform distribution of the χ_2 species or vice versa. The size of this range naturally depends on model parameters that affect the competition for light and water. Two parameters of this kind are investigated below, the reference biomass value h, which controls the intensity of the competition for light, and the species pool parameter α.

2.5.1 Competition for light

The strength of the competition for light can be controlled using the parameter h that appears in equation (2.4) for the biomass growth rate $\Lambda_i(B)$. Smaller values of h imply lower biomass growth rate for the shaded species and thus a stronger competition effect. Conversely, as h is increased the competition for light becomes weaker and completely disappears when $h \to \infty$ as Λ_i approaches a constant value independent of B. Figure 2.5 shows the effect of increasing h on the species-coexistence range as measured by the existence range of the one-hump solution. Apart from a small range of low h values, the species-coexistence range is found to decrease as h is increased. The reduction in the coexistence range occurs mostly through a shift of its low precipitation edge to higher precipitation values. As the competition for light decreases the advantage of χ_1 over χ_2 weakens and χ_2 is able to displace χ_1. The balance between the two competitive abilities (capturing light vs. capturing water) that leads to front pinning, is then regained only at higher precipitation values.

2.5.2 Species pool

We recall that E and K are the biotic parameters that control the competitive abilities to capture water and light, respectively. The actual values that these parameters can take in the rectangle $R = [E_{\min}, E_{\max}] \times [K_{\min}, K_{\max}]$ are determined by the tradeoff curves obtained for different α values, as Fig. 2.1 illustrates. Each curve is parameterized by $\chi \in [0, 1]$ and represents a different species pool.

In order to study how does the species pool affect coexistence in 2-species communities we fix the species with biomass density B_2 at $\chi_2 = 1$ and vary the species with biomass density B_1 from $\chi_1 = 0$ to a small positive value. In other words, we reduce the gap between the two species by weakening the ability to

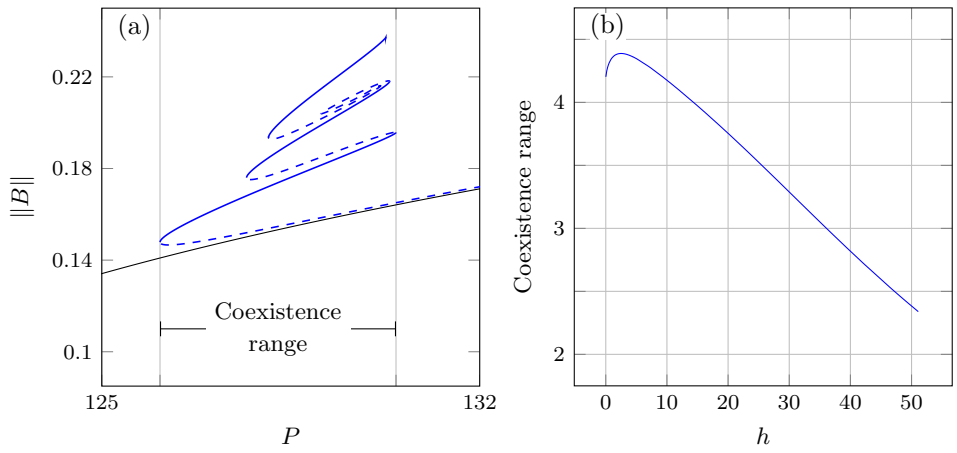

Figure 2.5: Dependence of the species coexistence range, as defined by the existence range of the one-hump solution (see panel a), on the parameter h that controls the competition for light. The coexistence range decreases as h increases or as the competition for light weakens (b). Parameters are as in Table 1 with $h = 4$ in panel (a).

capture light and strengthening the ability to capture water of the species that specializes in capturing light. We reduce the gap for three representative values of α: $\alpha = 1$ (diagonal curve), $\alpha < 1$ (sup-diagonal curve) and $\alpha > 1$ (sub-diagonal curve). In a species pool represented by a sup-diagonal tradeoff curve, increasing χ from zero involves a sharp increase in E, i.e. in the ability to capture water, which comes at the expense of a small decrease in K, i.e. in the ability to capture light (see point c in Fig. 2.1). That is, the overall competitive ability is bettered with respect to the reference case represented by the diagonal tradeoff line (point b in Fig. 2.1). In a species pool represented by a sub-diagonal tradeoff curve, the increase of χ involves a sharp decrease in K, which is compensated only by a small increase in E (point a in Fig. 2.1). That is, the overall competitive ability is worsened with respect to the reference case.

Figure 2.6 shows the localized solution branches for three representative values of α. Two trends can be identified with respect to the reference diagonal tradeoff curve ($\alpha = 1$); the range of localized solutions moves to higher (lower) precipitation and narrows down (widens up) as α is increased (decreased). These trends can be understood by comparing the dynamics of the fronts that separate the two stable states (U_2^* and $U_{1,p}^*$) when $\alpha \neq 1$ with the front dynamics in the reference case $\alpha = 1$, as explained below. Recall that at precipitation rates below (above) the range of localized solutions the χ_2 (χ_1) species displaces by front propagation the χ_1 (χ_2) species.

When $\alpha > 1$ the species χ_1 is significantly less competitive in capturing light

compared to the reference case $\alpha = 1$ because of its smaller K value. It is also less competitive in capturing water because it is significantly less better off in water capture compared with the reference case (see Fig. 2.1). As a result, there exists a precipitation range (just below $P = 130$ in Fig. 2.6) where the species χ_1 displaces χ_2 when $\alpha = 1$ but fails to displace χ_2 and forms localized structures when $\alpha > 1$. Likewise, there exists a precipitation range (around $P = 125$) where χ_2 is unable to displace χ_1 when $\alpha = 1$ but succeeds when $\alpha > 1$. This explains the shift of the localized solutions range to higher P as α increases beyond unity. It also explains the narrowing down of the localized solutions range because the advantage of χ_2 over χ_1 is stronger at lower P than the converse advantage at higher P and therefore the contraction of the localized solutions range at the lower P edge is larger than the extension of the range at the upper P edge. Similar arguments explain the shift of the localized solutions range to lower P and its widening as α decreases below unity.

Finally, we note that if we reduce the gap between the two species by fixing $\chi_1 = 0$ and decreasing slightly χ_2 away from unity along the different trait curves, using again the diagonal ($\alpha = 1$) as a reference curve, the effect on the localized solutions range compared to Fig. 2.6 is qualitatively the same with respect to the widening of the localized solutions range, while it is the inverse with respect to the shift of the range.

2.6 Conclusion

We used a spatially explicit mathematical model to study conditions for spatial coexistence of two plant species that make different tradeoffs in capturing two limiting resources, soil water and sun light. We focused on a parameter regime that gives rise to bistability of two pure-population states over a range of precipitation rates: a uniform state of a species that specializes in capturing water and a patterned state of a species that specializes in capturing light. Within the bistability range we identified a sub-range where localized solutions exist, describing fixed domains of the patterned states in a system otherwise occupied by the uniform state. Stable solutions of this kind imply long-term spatial coexistence of the two species. We found that the size of the coexistence precipitation range size reduces as the competition for light becomes weaker. We further found that the size of this range and its position along the precipitation axis vary with the form of the tradeoff curve, which defines the nature of the species pool.

Localized structures in bistability ranges of uniform and patterned states have been found in various physical contexts [44], and are likely to occur in ecological contexts too. The context considered in this paper, i.e. a plant community distributed along a tradeoff axis of above-ground vs. below-ground resource-capture capabilities, may be applicable to herbaceous plant communities in which one or

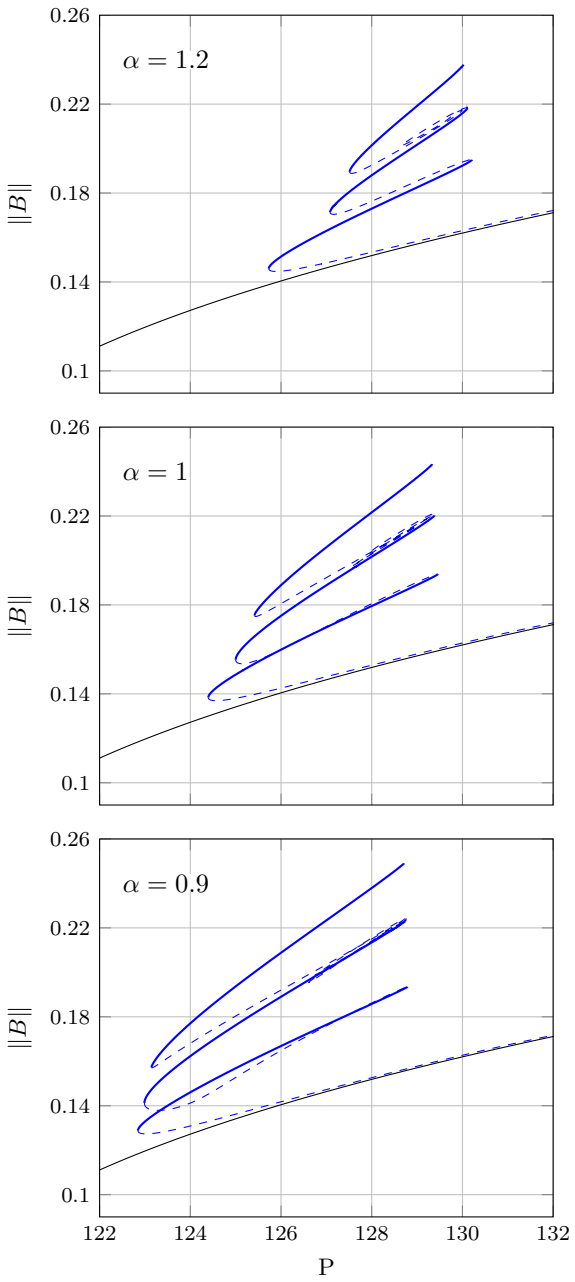

Figure 2.6: Species-pool effects on the species-coexistence range. The range moves to higher (lower) precipitation and narrows down (widens up) as α is increased (decreased) with respect to the reference value $\alpha = 1$. Parameters are as in Table 1 with $\chi_1 = 0.01$.

more species are capable of forming patterns [68, 52]. Woody-herbaceous systems, such as Savanna landscapes [63], provide another possible example. Here, the pattern-forming woody life form constitutes the stable periodic-pattern state and the herbaceous vegetation forms the alternative stable uniform state - the grassland [34]. Localized structures consisting of confined domains of the woody pattern in an otherwise uniform grassland then create savanna-like landscapes. A related problem is shrubland-grassland transitions, e.g. the displacement of black grama (*Bouteloua eriopoda*) grassland by creosotebush (*Larrea tridentata*) shrubland [78]. Here, the displacement process is a front propagation problem, which indicates the possible realization of pinned fronts and localized structures under different environmental conditions. In all these examples identifying bistability ranges of uniform and patterned population states may shed new light on the possible dynamical responses of the corresponding plant communities to environmental changes. We note that the assumption of sandy soil, which we used to simplify the model equations by eliminating overland water flow, applies to several examples of pattern-forming herbaceous and woody-herbaceous systems, e.g. herbaceous gap patterns (fairy circles) [14] and savanna landscapes [65] in southern Africa. We believe, however, that the coexistence mechanism is general and applies to other soil types in bistability ranges of uniform and patterned vegetation states.

A basic assumption underlying the model equations is translational invariance, that is, the absence of any external heterogeneity, such as non-uniform rainfall. Such heterogeneities can lead to front pinning and species coexistence even in the case of bistability of uniform states; a non-uniform rainfall that shifts the precipitation rate from one side of the Maxwell point to another can lead to front pinning at the spatial location of the Maxwell point. The significance of the results reported here is that front pinning and species coexistence can occur even in uniform (translationally invariant) systems. In the current study the precipitation range of species coexistence is pretty narrow. Further studies are needed in order to identify biotic and abiotic circumstances that lead to wider coexistence ranges.

2.7 Appendices

2.7.1 Uniform steady states and their stability properties

Uniform steady states

We focus in this appendix on the trivial uniform state, $U_0 = (0, 0, W_0)$ with $W_0 = P/L$, and on the two pure-population uniform states $U_1^* = (B_1^*, 0, W_1^*)$ and $U_2^* = (0, B_2^*, W_2^*)$ for B_1^*, $B_2^* > 0$. We do not study mixed states of the form (B_1, B_2, W) as they are unstable in the parameter range we consider in this study.

The uniform pure-population states, for $i = 1, 2$, are given by

$$B_i^{*\pm} = \frac{\pm\sqrt{\Delta_i} + P\Omega_i(K_iE_i - 1) - \Gamma_iK_iM_i}{2E_i\left(\Gamma_iK_iM_i + PN_i\right)},$$

and

$$W_i^{*\pm} = \frac{P}{L + \Gamma_iB_i^{\pm}(1 + E_iB_i^{\pm})},$$

with

$$\Delta_i(P) = \left(K_i\left(\Gamma_iM_i - PE_i\Omega_i\right) + P\Omega_i\right)^2 - 4K_iE_i\left(LM_i - P\Omega_i\right)\left(\Gamma_iK_iM_i + P\Omega_i\right),$$

where a necessary condition for these states to exist is Δ_i being non-negative. Let,

$$P_i^0 := LM_i/\Omega_i \tag{2.7}$$

and

$$P_i^F := \frac{M_i(2K_iE_i\sqrt{L\Gamma_iK_i(K_iE_i + 1) + L^2} - K_i\left(\Gamma_i - 2LE_i\right) - \Gamma_iK_i^2E_i)}{\Omega_i\left(K_iE_i + 1\right)^2}, \tag{2.8}$$

be the largest root of $\Delta_i(P) = 0$. Note that $B_i^{*\pm}$ is a double root at P_i^F and $d^2/dP^2(\Delta_i(P)) > 0$ which implies that $\Delta_i(P) > 0$ for $P > P_i^F$. Therefore, if

$$(K_iE_i - 1) > 0 \ \text{ and } \ P_i^F\Omega_i(K_iE_i - 1) - \Gamma_iK_iM_i > 0, \tag{2.9}$$

$$B_i^{*\pm} > 0, \text{ for } P_i^F \le P < P_i^0, \tag{2.10}$$

and

$$B_i^{*-} \le 0 < B_i^{*+}, \text{ for } P \ge P_i^0\,. \tag{2.11}$$

On the other hand, when (2.9) is not satisfied, B_i^{*+} is positive for $P > P_i^0$ while B_i^{*-} is negative for all $P > P_i^F$. We use these criteria to define parameter ranges where $U_i^{*\pm} = (B_i^{*\pm}, 0, W_i^{*\pm})$ $(i = 1, 2)$ are positive, and thus can represent realistic quantities. In what follows, we refer to $U_i^{*\pm}$ only in parameter ranges where they are positive.

Stability

To study the stability of a uniform state U^* to uniform and nonuniform perturbation we consider an unbounded domain and an infinitesimally small sinusoidal perturbation with wavenumber k:

$$U(x,t) = U^* + \hat{U}\exp\left(ikx + \lambda t\right) + c.c., \tag{2.12}$$

where $U(x,t) = (B_1(x,t), B_2(x,t), W(x,t))$ represents the perturbed state and "c.c" stands for the complex conjugate. We then study the linear problem obtained by inserting the form (2.12) into (2.1) keeping only terms that are linear in $\hat{U}$.

To simplify the presentation, we first study the stability of U^* to uniform perturbations for which $k = 0$. In this case, the linear stability of U^* is determined by the eigenvalues of a 3×3 Jacobian matrix associated with the reaction terms of (2.1). For the trivial uniform state $U^* = U_0$ the Jacobian reads,

$$J^0(0,0,W_0) = \begin{pmatrix} P\Omega_i/L - M_i & 0 & 0 \\ 0 & P\Omega_i/L - M_i & 0 \\ -\Gamma_i P/L & -\Gamma_i P/L & -L \end{pmatrix} \tag{2.13}$$

which readily implies that U_0 is stable for $P < P_0 := \min\{P_1^0, P_2^0\}$, where P_1^0, P_2^0 are given by (2.7), and becomes unstable for $P > P_0$.

For the pure uniform states, $U_1^{*\pm}$ and $U_2^{*\pm}$, the corresponding Jacobian matrices $J^{1\pm}(B_1^{*\pm}, 0, W_1^{*\pm})$ and $J^{2\pm}(0, B_2^{*\pm}, W_2^{*\pm})$ have, respectively, the following entries:

$$\begin{aligned}
{J_{21}^1}^{\pm} &= {J_{23}^1}^{\pm} = 0 \\
{J_{11}^1}^{\pm} &= \Omega_1 B_1^{*\pm}(E_1 - 1/K_1 - 2E_1 B_1^{*\pm}/K_1) W_1^{*\pm} \\
{J_{13}^1}^{\pm} &= \Omega_1(1 - B_1^{*\pm}/K_1)(1 + E_1 B_1^{*\pm}) B_1^{*\pm} \\
{J_{31}^1}^{\pm} &= -(\Gamma_1(1 + 2E_1 B_1^{*\pm}) W_1^{*\pm}) \\
{J_{33}^1}^{\pm} &= -(L + \Gamma_1 B_1^{*\pm}(1 + E_1 B_1^{*\pm})) \\
{J_{22}^1}^{\pm} &= \Omega_2 \frac{h}{(B_1^{*\pm} + h)} W_1^{*\pm} - M_2
\end{aligned} \tag{2.14}$$

and

$$\begin{aligned}
{J_{12}^2}^{\pm} &= {J_{13}^2}^{\pm} = 0 \\
{J_{22}^2}^{\pm} &= \Omega_2 B_2^{*\pm}(E_2 - 1/K_2 - 2E_2 B_2^{*\pm}/K_2) W_2^{*\pm} \\
{J_{23}^2}^{\pm} &= \Omega_2(1 - B_2^{*\pm}/K_2)(1 + E_2 B_2^{*\pm}) B_2^{*\pm} \\
{J_{32}^2}^{\pm} &= -(\Gamma_2(1 + 2E_2 B_2^{*\pm})) W_2^{*\pm} \\
{J_{33}^2}^{\pm} &= -(L + \Gamma_2 B_2^{*\pm}(1 + E_2 B_2^{*\pm})) \\
{J_{11}^2}^{\pm} &= \Omega_1 \frac{h}{(B_2^{*\pm} + h)} W_2^{*\pm} - M_1 \,.
\end{aligned} \tag{2.15}$$

The stability of $U_1^{*\pm}$ and $U_2^{*\pm}$ is determined by the roots of the characteristic polynomials

$$\left({J_{22}^1}^{\pm} - \lambda_1\right)\left({\lambda_1}^2 - ({J_{11}^1}^{\pm} + {J_{33}^1}^{\pm})\lambda_1 - {J_{13}^1}^{\pm}{J_{31}^1}^{\pm} + {J_{11}^1}^{\pm}{J_{33}^1}^{\pm}\right) = 0\,, \tag{2.16}$$

$$\left(J_{11}^{2\,\pm} - \lambda_2\right)\left(\lambda_2{}^2 - (J_{22}^{2\,\pm} + J_{33}^{2\,\pm})\lambda_2 - J_{23}^{2\,\pm}J_{32}^{2\,\pm} + J_{22}^{2\,\pm}J_{33}^{2\,\pm}\right) = 0\,. \tag{2.17}$$

We first examine the roots of the polynomial

$$\lambda_i{}^2 - (J_{ii}^{i\,\pm} + J_{33}^{i\,\pm})\lambda_i + J_{ii}^{i\,\pm}J_{33}^{i\,\pm} - J_{i3}^{i\,\pm}J_{3i}^{i\,\pm} = 0. \tag{2.18}$$

which appears in (2.16) and (2.17) for $i = 1$ and 2, respectively. For this we note that

$$J_{ii}^{i\,+}J_{33}^{i\,+} - J_{i3}^{i\,+}J_{3i}^{i\,+} > 0, \tag{2.19}$$

and

$$J_{ii}^{i\,-}J_{33}^{i\,-} - J_{i3}^{i\,-}J_{3i}^{i\,-} < 0\,. \tag{2.20}$$

To see this, recall that $B_i^{*\pm}$ are roots of the polynomial

$$f_i(s) := \Omega_i P(1 - s/K_i)(1 + E_i s) - M_i(L + \Gamma_i s(1 + E_i s)), \tag{2.21}$$

and note that

$$f_i'(s) = -\left(\Gamma_i M_i\,(2sE_i + 1) - P\Omega_i\left(-\frac{2sE_i}{K_i} - \frac{1}{K_i} + E_i\right)\right).$$

Let

$$g_i(s) := -sf_i'(s),$$

then we observe that

$$J_{ii}^{i\,\pm}J_{33}^{i\,\pm} - J_{i3}^{i\,\pm}J_{3i}^{i\,\pm} = g_i(B_i^{*\pm})\,.$$

Since $g_i''(s) = 4E_i\left(\Gamma_i K_i M_i + P\Omega_i\right)/K_i > 0$, $g_i(s)$ is convex. Moreover, $g_i(s)$ has one zero at $s = 0$ and the other coincides with the point at which $f_i(s)$ achieves a maximum. Therefore, we easily conclude that $J_{ii}^{i\,+}J_{33}^{i\,+} - J_{i3}^{i\,+}J_{3i}^{i\,+} = g_i(B_i^{*+}) > 0$ and $J_{ii}^{i\,-}J_{33}^{i\,-} - J_{i3}^{i\,-}J_{3i}^{i\,-} = g_i(B_i^{*-}) < 0$, whenever B_i^{*-} is positive. Consequently, from (2.20) the characteristic polynomial for the linearization around U_i^{*-}, possesses at least one eigenvalue with positive real part, and thus U_i^{*-} is unstable. On the other hand, from (2.19) both eigenvalues of the linearization around U_i^{*+}, which correspond to the roots of (2.18), have negative real part when

$$(J_{ii}^{i\,+} + J_{33}^{i\,+}) < 0, \tag{2.22}$$

for $i = 1$ or 2.

It remains to determine the signs of the other eigenvalues that arise from (2.16) and (2.17), namely $\lambda_1 = J_{22}^{1\,+}$ and $\lambda_2 = J_{11}^{2\,+}$. For simplicity, we assume that

$$M_1 = M_2 \text{ and } \Omega_1 = \Omega_2, \tag{2.23}$$

which is compatible with the parameter values considered in Table 1. Then,

$$\lambda_i(B_i^+; P) = \frac{P\Omega_1 h}{(B_i^+ + h)(L + \Gamma_i B_i^+(1 + E_i B_i^+)} - M_1.$$

Moreover, the algebraic system

$$\lambda_i(s; P) = 0,\ f_i(s; P) = 0, \tag{2.24}$$

with f_i given in (2.21), is solvable for a pair (s, P). We consider the solution pair (s_i, P_i^M) with

$$s_i^* := \left(E_i K_i - 1 - E_i h + \sqrt{(E_i K_i - 1 - hE_i)^2 - 4E_i(h(1 - E_i K_i) - K_i)}\right)(2E_i)^{-1},$$

and

$$P_i^M := M_1(s_i^* + h)(L + \Gamma_i s_i^*(1 + E_i s_i^*)(\Omega_1 h)^{-1}\,. \tag{2.25}$$

Then, we have that $\lambda_i(B_i^+)$ is negative for $P < P_i^M$ when

$$E_i K_i \geq 1, \tag{2.26}$$

or

$$E_i K_i < 1 \ \text{ and } \ h < K_i/(1 - E_i K_i), \tag{2.27}$$

while it is positive for $E_i K_i < 1$, $h \geq K_i/(1 - E_i K_i)$ and $P > P_0$, or for $E_i K_i \geq 1$ and $P > P_i^M$.

We conclude that when (2.22), (2.23) along with (2.26) or (2.27) are satisfied for $i = 1$ (respectively $i = 2$), U_1^{*+} (respectively U_2^{*+}) is stable, for all $P < P_1^M$ (respectively $P < P_2^M$). On the other hand, U_i^{*-} is unstable for the range of P defined in (2.10).

We are now in a position to study the stability of the trivial state, U_0, and of the two pure-population states, $U_1^{*\pm}$ and $U_2^{*\pm}$, to the growth of nonuniform perturbations characterized by nonzero wavenumbers, i.e. $k \neq 0$ in (2.12). The dynamics of such perturbation are determined by the eigenvalues of the matrix

$$J_k = J - k^2 D\,,$$

where

$$D = \mathrm{diag}(D_{B_1}, D_{B_2}, D_W),$$

and J is given by (2.13) for U_0 and by the expressions in (2.14) and (2.15) for $U_1^{*\pm}$ and $U_2^{*\pm}$. The eigenvalues of J_k are determined by the roots of the characteristic polynomial:

$$\det(J - k^2 D - \lambda I_3) = 0, \tag{2.28}$$

where I_3 is the 3×3 identity matrix. It can be easily checked that for $P < P_0 = \min\{P_1^0, P_2^0\}$ the trivial state U_0 remains stable for all k, since the diagonal elements of J^0 in (2.13) are negative.

For the pure-population state U_1^{*+} (respectively U_2^{*+}), we assume that (2.22), (2.23) along with (2.26) or (2.27) are satisfied and that $P < P_1^M$ (respectively $P < P_2^M$), so that the state is stable for $k = 0$. For the sake of clarity, in what follows we drop superscript $'+'$ in the notation of the elements (2.14), (2.15) of the Jacobian matrix. Then, the characteristic polynomial (2.28) for the two pure-population states takes the forms

$$\left(J_{22}^1 - k^2 D_{B_2} - \lambda_1\right)\left({\lambda_1}^2 - \alpha_1(k^2)\lambda_1 + \beta_1(k^2)\right) = 0\,, \tag{2.29}$$

$$\left(J_{11}^2 - k^2 D_{B_1} - \lambda_2\right)\left({\lambda_2}^2 - \alpha_2(k^2)\lambda_2 + \beta_2(k^2)\right) = 0\,, \tag{2.30}$$

where

$$\alpha_i(k^2) = (J_{ii}^i + J_{33}^i) - (D_{B_i} + D_W)k^2\,, \tag{2.31}$$

$$\beta_i(k^2) = D_{B_i} D_W k^4 - (D_{B_i} J_{33}^i + D_W J_{ii}^i)k^2 + (J_{ii}^i J_{33}^i - J_{i3}^i J_{3i}^i)\,. \tag{2.32}$$

Clearly the single eigenvalues $\lambda_1(k^2) = J_{22}^1 - k^2 D_{B_2}$ and $\lambda_2(k^2) = J_{11}^2 - k^2 D_{B_1}$ are negative for all k, and the other two eigenvalues are given by

$${\lambda_i}^{\pm}(k^2) = \frac{\alpha_i(k^2) \pm \sqrt{\alpha_i(k^2)^2 - 4\beta_i(k^2)}}{2}\,. \tag{2.33}$$

Since $\alpha_i(k^2) < 0$, the real part of $\lambda_i^-(k^2)$ remains negative for all k, while λ_i^+ may become positive, only if

$$\beta_i(k^2) < 0, \tag{2.34}$$

for some $k \neq 0$. From, (2.19), this immediately implies, that $(D_{B_i} J_{33}^i + D_W J_{ii}^i)$ needs to be positive, or

$$T(\delta) = \delta J_{33}^i + J_{ii}^i > 0\,, \qquad \delta := D_{B_i}/D_W\,. \tag{2.35}$$

Therefore, since $J_{33}^i < 0$, destabilization of S_i^{*+}, requires

$$J_{ii}^i = \Omega_i B_i^{*+}\left(E_i - 1/K_i - 2\frac{E_i}{K_i}B_i^{*+}\right)W_i^{*+} > 0\,. \tag{2.36}$$

In addition, from (2.22) $(J_{ii}^i + J_{33}^i) < 0$ and since $T(\delta) = (\delta J_{33}^i + J_{ii}^i)$ is a decreasing function of δ, we also need

$$\delta < 1. \tag{2.37}$$

Moreover, (2.32) has a minimum at

$$k_{i,c}{}^2 = \frac{(D_{B_i} J^i_{33} + D_W J^i_{ii})}{2 D_{B_i} D_W}, \tag{2.38}$$

and so (2.34) is satisfied for some $k \neq 0$, when the parameter values K_i, E_i, M_i, L, N_i, Γ, P and the diffusion coefficients D_{B_i}, D_W are such that the minimum value given by the expression

$$\beta_i(k_{i,c}{}^2) = 4 D_{B_i} D_W (J^i_{ii} J^i_{33} - J^i_{i3} J^i_{3i}) - (D_{B_i} J^i_{33} + D_W J^i_{ii})^2, \tag{2.39}$$

is negative. Finally, zeros of the right hand side of (2.39) with respect to P provide us the instability thresholds denoted by P_i^T, while the wavenumber $k_{i,c}$ growing at the instability point is given by (2.38).

2.7.2 Numerical stability analysis for nonuniform stationary solutions in a finite system

We consider a reaction-diffusion system of the form:

$$\partial_t U = D\mathcal{L}U + F(U),$$

where the spatial variable x lies in the interval $[0, 1]$, $U = (U_1, U_2, U_3)$, $D = \mathrm{diag}\,(D_1, D_2, D_3)$ for D_1, D_2, D_3 real positive numbers, $\mathcal{L} = \mathrm{diag}\,(\partial_{xx}, \partial_{xx}, \partial_{xx})$ and

$$F(U) = (f_1(U), f_2(U), f_3(U))$$

is a differentiable vector field. We consider the system either with periodic boundary conditions or homogeneous Neumann boundary conditions.

We divide the spatial interval into the uniform grid $x_j = j\Delta x$, for $j = 0, \ldots N$, with $\Delta x = 1/N$, and we let

$$U_h = (u_1^0, \ldots, u_1^N, u_2^0, \ldots, u_2^N, u_3^0, \ldots, u_3^N),$$

represent the vector of U evaluated at the grid nodes. Then we use the standard second order central difference approximation of the second derivative given by a 3 points stencil. This approximation can be represented by a $(N+1) \times (N+1)$ matrix $\mathcal{A}$. Consequently, we denote by $\delta\mathcal{A} = \mathrm{diag}(D_1\mathcal{A}, D_2\mathcal{A}, D_3\mathcal{A})$ the $3(N+1) \times 3(N+1)$ matrix approximating $D\mathcal{L}$, and by

$$F_h(U_h) = (f_1(u_1^0), \ldots, f_1(u_1^N), f_2(u_2^0), \ldots, f_2(u_2^N), f_3(u_3^0), \ldots, f_3(u_3^N))\,.$$

the vector field evaluated at the node points.

We then compute the discrete Jacobian matrix of F_h, denoted by JF_h around an inhomogeneous discretized steady state $\bar{U}(x)$ ending up with a linear operator

$$\delta\mathcal{A} + JF_h\big|_{\bar{U}_h}\,.$$

Finally, we compute the spectrum of $\delta\mathcal{A} + JF_h\big|_{\bar{U}_h}$ using MATLAB, in order to determine the linear stability of $\bar{U}(x)$ for the system $U_h' = \delta\mathcal{A}U_h + F_h(U_h)$, with $U_h(t)$, F_h in $R^{3(N+1)}$.

Chapter 3

Strong absorption

3.1 Introduction

We study a system which captures the interactions between vegetation and water in arid and semi-arid areas [37]. The system in non-dimensionalized form reads

$$\begin{cases} \partial_t b = d_b \Delta b + w G_1(b)(1-b)b - b, \\ \partial_t w = d_w \Delta w - (L(b) + G_2(b))\, w + I(b) h^\alpha, \\ \partial_t h = d_h \Delta h^m - I(b) h^\alpha + p. \end{cases} \tag{3.1}$$

Here, b represents the concentration of the above ground biomass, w the soil water content and h the height of a thin surface water layer per unit area. The equation for the evolution of biomass involves a water dependent growth rate $G(b, w)$, a mortality term with constant loss rate and a linear diffusion term modeling growth due to seeds dispersal or clonal growth. In the equation for the soil water, we have a loss term which consists of the water up-take rate by the plant's roots denoted by $G_2(b)$ and the biomass dependent evaporation rate $L(b)$. Moreover, the equation contains the source term $I(b)h^\alpha$ representing the infiltrated surface water, which is discussed in more detail below, and a linear diffusion term modeling the soil water transport. The third equation models the surface water flow and how this infiltrates into the ground. The variable h corresponds to the non-dimensionless quantity $H = \rho d$, where $d(\tilde{t}, \tilde{x})$ represents the depth in meters of the surface water where $\tilde{x} \in \Omega \subset \mathbb{R}^2$ and ρ is the constant density of the fluid. In fact, the third equation in dimensional quantities (and $m \geq 2$) can be derived by the continuity equation

$$\frac{\partial H}{\partial \tilde{t}} + \operatorname{div}(H\vec{u}) = P - \mathcal{I}H$$

and the shallow water momentum equation

$$\frac{Du}{\partial \tilde{t}} = -g\nabla(\zeta + d) + \frac{1}{\rho}F,$$

where $\vec{u}$ is the horizontal velocity of the fluid, F represents ground surface friction, P stands for the precipitation rate and $\mathcal{I}H$ is the infiltration rate of water through the soil surface. Moreover, ζ[1] denotes the height of the soil surface and g stands for the acceleration of gravity. We consider a friction term of the form $F = -k\vec{u}/d^l$, for $l \geq 0$ and $k > 0$, a biomass and surface water dependent infiltration rate term of the form $\mathcal{I}(B, H) = \mathcal{I}_B(B)\mathcal{I}_H(H)$ and we let $\zeta = 0$ which corresponds to a region with flat topography. Then

$$\frac{\partial H}{\partial \tilde{t}} - c\Delta H^m = P - \mathcal{I}(B, H)H,$$

where $m = l + 2$ and $c = \dfrac{g}{mk\rho^l}$. The biomass dependent infiltration rate $\mathcal{I}_B$ captures the infiltration contrast between vegetated regions and bare soil due to the formation of biogenic crusts in unvegetated regions which reduce the infiltration of surface water. Therefore, this term is monotonically increasing with B approaching a constant infiltration for high biomass concentrations. The counterpart $\mathcal{I}_H$ of the infiltration rate is chosen to be decreasing function of H taking the explicit form $H^{\alpha-1}$ for $\alpha \in (0, 1)$.

This chapter is organized as follows. In Section 2 we make explicit the initial and boundary conditions as well as the expressions of the function for which existence (3.1) is studied. In particular, we consider the system for two distinct cases of boundary conditions: the zero Dirichlet and Neumann boundary conditions. For the first case, we define a regularized approximating system which possesses positive bounded solutions. This allows us to pass to the limit of the approximating problem proving the existence of solutions for the original problem. For the second case, we use a different approach, specifically, existence of solutions is given by a fixed point argument employing the Arino, Gautier and Penot fixed point theorem for sequentially weakly continuous mappings in Banach spaces [3]. In Section 3 we examine the behavior of the zeroes set of the surface water component h in the absence of precipitation for sufficiently long time intervals.

3.2 Existence of solutions

In what follows, we denote by Ω a bounded domain in $\mathbb{R}^2$ with regular boundary $\partial\Omega$ and for $T > 0$ we let $Q_T = \Omega \times (0, T)$ and $S_T = \partial\Omega \times (0, T)$. Our purpose is to prove the existence of a solution $U = (b, w, h)$ of the system

$$\begin{cases} \partial_t b = d_b\Delta b + wG_1(b)(1-b)b - b, & \text{in } Q_T, \\ \partial_t w = d_w\Delta w - (L(b) + G_2(b))\, w + I(b)h^\alpha, & \text{in } Q_T, \\ \partial_t h = d_h\Delta h^m - I(b)h^\alpha + p, & \text{in } Q_T. \end{cases} \tag{3.2}$$

[1]For non-trivial land topographies $\zeta(\tilde{x})$ is a nonnegative function of the space variable $\tilde{x}$ and it is convenient to set $Z = \rho\zeta$.

together with the initial conditions,

$$b(x,0) = b_0(x),\ w(x,0) = w_0(x),\ h(x,0) = h_0(x) \text{ for } x \in \Omega. \tag{3.3}$$

and some boundary conditions which are either of Dirichlet type

$$b = w = h = 0, \text{ on } \partial\Omega \times (0,T) \tag{3.4}$$

or of Neumann type

$$\frac{\partial b}{\partial n} = \frac{\partial w}{\partial n} = \frac{\partial h^m}{\partial n} = 0, \text{ on } \partial\Omega \times (0,T). \tag{3.5}$$

We shall also assume two classes of conditions on the initial data: either their continuity

$$b_0, w_0, h_0 \in C(\bar{\Omega}), \tag{3.6}$$

or their possible discontinuity

$$b_0, w_0, h_0 \in L^\infty(\Omega), \tag{3.7}$$

but in any case we shall always assume

$$0 \le b_0 \le 1, w_0 \ge 0, h_0 \ge 0, \text{ on } \Omega. \tag{3.8}$$

Concerning the precipitation term, we assume that $p \in L^\infty(Q_T)$ is nonnegative. Moreover, we suppose that

$$I(b) = \theta \frac{b + r/c}{b + r}, \tag{3.9}$$

$$L(b) = \frac{\nu}{1 + \rho b}, \tag{3.10}$$

$$G_1(b) = \nu(1 + \eta b)^2, \tag{3.11}$$

$$G_2(b) = \gamma b(1 + \eta b)^2, \tag{3.12}$$

where $d_b, d_w, d_h, \eta, \rho, r, \nu, \theta > 0$ and $c \ge 1$ are given constants. For later use we also note that for $s \in [0,1]$, $I(s)$, $G_1(s)$, $G_2(s)$ are nondecreasing functions and $L(s)$ is nonincreasing function, so

$$I(0) \le I(s) \le I(1), \text{ for } s \in [0,1] \tag{3.13}$$

and

$$L(1) \le L(s) + G_2(s) \le L(0) + G_2(1), \text{ for } s \in [0,1]. \tag{3.14}$$

In what follows we refer to the Dirichlet problem (3.2), (3.4) and (3.3) as Problem (P_D), and to the Neumann problem (3.2), (3.4) and (3.5) as Problem (P_N). To begin with we define the notions of weak solutions of both problems.

Definition 2. *We call (b, w, h) a weak solution of Problem (P_D) on $[0, T]$, if it satisfies*

1. $(b, w, h) \in C([0, T], (L^1(\Omega))^3 \cap (L^\infty(Q_T))^3)$ *and* b, w, $h^m \in L^\infty((0, T); H_0^1(\Omega))$
2. *for all* $\psi \in C^1(\overline{Q}_T) \cap L^2(0, T; H_0^1(\Omega))$

$$\int_\Omega b(t)\psi(t) + d_b \int_0^t \int_\Omega \{\nabla b \cdot \nabla \psi - b\psi_t\}\, dxd\tau = \int_\Omega b_0\psi(0) + \\ + \int_0^t \int_\Omega \{G_1(b)w(1-b)b - b\}\psi, \tag{3.15}$$

$$\int_\Omega w(t)\psi(t) + d_w \int_0^t \int_\Omega \{\nabla w \cdot \nabla \psi - w\psi_t\} dxd\tau = \int_\Omega w_0\psi(0) + \\ + \int_0^t \int_\Omega \{-\left(L(b) + G_2(b)\right) w + I(b)h^\alpha\}\psi, \tag{3.16}$$

$$\int_\Omega h(t)\psi(t) + d_h \int_0^t \int_\Omega \{\nabla h^m \cdot \nabla \psi - h\psi_t\} dxd\tau = \int_\Omega h_0\psi(0) + \\ + \int_0^t \int_\Omega \{p - I(b)h^\alpha\}\psi\, dxd\tau. \tag{3.17}$$

Definition 3. *We call (b, w, h) a weak solution of Problem (P_N) on $[0, T]$, if it satisfies*

1. $U \in C([0, T], L^1(\Omega)^3) \cap (L^\infty(Q_T))^3)$ *and* b, w, $h^\kappa \in L^\infty((0, T); H^1(\Omega))$
2. *for all* $\psi \in C^1(\overline{Q}_T) \cap L^2(0, T; H^1(\Omega))$ b, w, h *satisfies (3.15)–(3.17)*

As a matter of fact, in the case of Dirichlet boundary conditions we shall be able to prove, additionally, that the weak solutions are continuous functions if hypothesis (3.6) holds true. In the case of Neumann boundary conditions the continuity will only be obtained with respect to the time variable:

3.2.1 The regularized system to (P_D)

The main difficulty for the study of Problem (P_D) is the fact that the equation for h is degenerate parabolic. Here, we overcome this difficulty by defining a sequence of approximating uniformly parabolic problems for which classical solutions exist. Finally, we prove existence of Problem (P_D) by passing to the limit thanks to some a priori estimates.

For $\epsilon \in (0, 1)$, $\kappa \geq 1$ and $0 < \alpha < 1$, we let

$$\phi_\epsilon(s) := (s + \epsilon)^m - \epsilon^m,$$

and

$$f_\epsilon(s) := (s+\epsilon)^\alpha - \epsilon^\alpha.$$

We consider the regularized system

$$\begin{cases} \partial_t b_\epsilon - d_b \Delta b_\epsilon + b_\epsilon = G_1(b_\epsilon) w_\epsilon (1-b_\epsilon) b_\epsilon, & \text{in } Q_T, \\ \partial_t w_\epsilon - d_w \Delta w_\epsilon + (L(b_\epsilon) + G_2(b_\epsilon))\, w_\epsilon = I(b_\epsilon) f_\epsilon(h_\epsilon), & \text{in } Q_T, \\ \partial_t h_\epsilon - d_h \Delta(\phi_\epsilon(h_\epsilon)) + I(b_\epsilon) f_\epsilon(h_\epsilon) = p_\epsilon, & \text{in } Q_T, \\ b = w = h = 0, & \text{on } S_T, \\ b_\epsilon(x,0) = b_{0,\epsilon}(x),\ w_\epsilon(x,0) = w_{0,\epsilon}(x), & \\ h_\epsilon(x,0) = h_{0,\epsilon}(x), & \text{for } x \in \Omega, \end{cases} \tag{3.18}$$

where $p_\epsilon \in C^\infty$ such that

$$0 \le p_\epsilon \le \|p\|_{L^\infty(Q_T)}, \tag{3.19}$$

$$\|p_\epsilon - p\|_{L^1(Q_T)} \to 0 \text{ as } \epsilon \to 0, \tag{3.20}$$

for $T > 0$ arbitrary and the initial conditions $b_{0,\epsilon}, w_{0,\epsilon}, h_{0,\epsilon}$, with

$$b_\epsilon(0) = b_{0,\epsilon},\ w_\epsilon(0) = w_{0,\epsilon},\ h_\epsilon(0) = h_{0,\epsilon} \in C_c^\infty(\Omega),$$

such that

$$0 \le b_{0,\epsilon}(x) \le \|b_0\|_{L^\infty(\Omega)},\ 0 \le w_{0,\epsilon}(x) \le \|w_0\|_{L^\infty(\Omega)},\ 0 \le h_{0,\epsilon}(x) \le \|h_0\|_{L^\infty(\Omega)} \tag{3.21}$$

for a.e $x \in \Omega$ and

$$(b_{0,\epsilon}, w_{0,\epsilon}, h_{0,\epsilon}) \to (b_0, w_0, h_0) \text{ in } (L^1(\Omega))^3 \text{ as } \epsilon \to 0. \tag{3.22}$$

We also note for later use that (3.19), (3.20) and (3.21), (3.22) imply

$$p_\epsilon \to p \text{ in } L^q(Q_T) \text{ as } \epsilon \to 0, \tag{3.23}$$

and

$$(b_{0,\epsilon}, w_{0,\epsilon}, h_{0,\epsilon}) \to (b_0, w_0, h_0) \text{ in } (L^q(\Omega))^3 \text{ as } \epsilon \to 0, \tag{3.24}$$

for all $q > 1$.

Under the above considerations the following result holds

Theorem 6. *For every $\epsilon \in (0,1)$, problem (3.18) possesses a unique classical solution $(b_\epsilon, w_\epsilon, h_\epsilon)$ such that*

$$0 \le b_\epsilon \le 1,\ \textit{in } Q_T \tag{3.25}$$

and there exists a positive constant $\bar{C}$ such that

$$0 \le w_\epsilon,\ h_\epsilon \le \bar{C},\ \textit{in } Q_T, \tag{3.26}$$

where $\bar{C}$ does not depend on ϵ.

Proof. The existence of classical solution of (3.18) for the non-negative initial data $(b_{0,\epsilon}, w_{0,\epsilon}, h_{0,\epsilon})$ follows from [45]. Moreover, from the classical maximum principle we have that for $b_{\epsilon,0} \in [0,1]$, $0 \le b_\epsilon \le 1$. Similarly, we can show that w_ϵ, $h_\epsilon \ge 0$. Next we prove that h_ϵ is bounded from above. We first recall the definition of the negative and positive parts of a function f, namely $(f)_+ = \max\{f, 0\}$, $(f)_- = \max\{-f, 0\}$. We set, $\hat{h} = h_\epsilon - \bar{h}$, with $\bar{h}$ an arbitrary positive constant to be determined later. We multiply the equation for h_ϵ in (3.18), by $\hat{h}_+$ and integrate over Ω to obtain

$$\int_\Omega \frac{\partial h_\epsilon}{\partial t}\hat{h}_+\,dx - d_h\int_\Omega \Delta\phi_\epsilon(h_\epsilon)\hat{h}_+\,dx + \int_\Omega I(b_\epsilon)f_\epsilon(h_\epsilon)\hat{h}_+\,dx = \int_\Omega p_\epsilon\hat{h}_+\,dx, \quad (3.27)$$

which implies that

$$\frac{1}{2}\frac{d}{dt}\int_\Omega |\hat{h}_+|^2\,dx + d_h\int_\Omega \phi_\epsilon'(h_\epsilon)|\nabla\hat{h}_+|^2\,dx + \int_\Omega I(b_\epsilon)f_\epsilon(h_\epsilon)\hat{h}_+\,dx = \int_\Omega p_\epsilon\hat{h}_+\,dx. \quad (3.28)$$

From (3.13), (3.28) and the fact that, $\phi_\epsilon'(h_\epsilon) > 0$, $0 \le p_\epsilon(t,x) \le \|p\|_{L^\infty(Q_T)}$, we have that

$$\frac{1}{2}\frac{d}{dt}\int_\Omega |\hat{h}_+|^2 + I(0)\int_\Omega f_\epsilon(h_\epsilon)\hat{h}_+ \le \|p\|_{L^\infty(Q_T)}\int_\Omega \hat{h}_+\,dx, \quad (3.29)$$

from which we infer that

$$\begin{aligned}\frac{1}{2}\frac{d}{dt}\int_\Omega |\hat{h}_+|^2 + I(0)\int_\Omega \big(f_\epsilon(h_\epsilon) - f_\epsilon(\bar{h})\big)\,(h_\epsilon - \bar{h})_+ \\ \le \|p\|_{L^\infty(Q_T)}\int_\Omega \hat{h}_+\,dx,\end{aligned} \quad (3.30)$$

which we may write as

$$\begin{aligned}\frac{1}{2}\frac{d}{dt}\int_\Omega |\hat{h}_+|^2 + I(0)\int_\Omega \big(f_\epsilon(h_\epsilon) - f_\epsilon(\bar{h})\big)\,(h_\epsilon - \bar{h})_+ \\ \le \big(\|p\|_{L^\infty(Q_T)} - I(0)f_\epsilon(\bar{h})\big)\int_\Omega \hat{h}_+\,dx,\end{aligned} \quad (3.31)$$

Thanks to the monotonicity of $\phi_\epsilon(\cdot)$, the second term on the left hand side of the above inequality is nonnegative. Next, we look for $\bar{h} > \|h_0\|_{L^\infty(\Omega)}$ such that

$$\|p\|_{L^\infty(Q_T)} - I(0)f_\epsilon(\bar{h}) \le 0. \quad (3.32)$$

Since, $-f_\epsilon(\bar{h}) \le (1 - \bar{h}^\alpha)$, we may choose

$$\bar{h} := \max\left\{\left(\frac{\|p\|_{L^\infty(Q_T)}}{I(0)} + 1\right)^{1/\alpha}, \|h_0\|_{L^\infty(\Omega)}\right\}, \quad (3.33)$$

so that

$$\frac{d}{dt}\int_\Omega |\hat{h}_+|^2(t)\,dx \le 0, \tag{3.34}$$

which in turn implies that

$$|\hat{h}_+(t)|^2_{L^2(\Omega)} \le |\hat{h}_+(0)|^2_{L^2(\Omega)} = |(h_0-\bar{h})_+|^2_{L^2(\Omega)} = 0\,, \tag{3.35}$$

for $\bar{h}$ given by (3.33), and so,

$$h_\epsilon \le \bar{h} \text{ in } Q_T. \tag{3.36}$$

To obtain an upper bound for w_ϵ we work similarly. We set $\hat{w} = w_\epsilon - \bar{w}$, where $\bar{w}$ is a positive constant to be determined later, we multiply the equation for w_ϵ in (3.18) by $\hat{w}_+$ and integrate over Ω to obtain that

$$\begin{aligned}&\frac{1}{2}\frac{d}{dt}\int_\Omega |\hat{w}_+|^2\,dx + \delta_w\int_\Omega |\nabla\hat{w}_+|^2\,dx + \\ &+\int_\Omega (L(b_\epsilon)+G_2(b_\epsilon))(|\hat{w}_+|^2 + \bar{w}\hat{w}_+)\,dx = \int_\Omega I(b_\epsilon)f_\epsilon(h_\epsilon)\hat{w}_+\,dx.\end{aligned} \tag{3.37}$$

where we have used the equality $w_\epsilon = (w_\epsilon-\bar{w})_+ - (w_\epsilon-\bar{w})_- + \bar{w}$. Then, from (3.13), (3.36) and the fact that $f_\epsilon(s) \le s^\alpha$ for $s \ge 0$, we have that

$$\int_\Omega I(b_\epsilon)f_\epsilon(h_\epsilon)\hat{w}_+\,dx \le I(1)\bar{h}^\alpha\int_\Omega \hat{w}_+\,dx. \tag{3.38}$$

So, using (3.14) and dropping the appropriate non-negative terms on the left hand side of (3.37), we end up with

$$\frac{1}{2}\frac{d}{dt}\int_\Omega |\hat{w}_+|^2\,dx + \left(\bar{w}L(1) - I(1)\bar{h}^\alpha\right)\int_\Omega \hat{w}_+\,dx \le 0. \tag{3.39}$$

Therefore, arguing as before we may choose

$$\bar{w} := \max\left\{\frac{I(1)\bar{h}^\alpha}{L(1)}, \|w_0\|_{L^\infty(\Omega)}\right\},$$

so that

$$w_\epsilon \le \bar{w}, \text{ in } Q_T. \tag{3.40}$$

□

Next we remark that b_ϵ satisfies a problem of the form

$$\begin{cases} b_{\epsilon t} = d_b\Delta b_\epsilon + F_\epsilon & \text{in } Q_T \\ b_\epsilon = 0 & \text{on } S_T \\ b_\epsilon(x,0) = b_{0,\epsilon}(x) & \text{in } \Omega \end{cases} \tag{3.41}$$

where

$$0 \leq b_{0,\epsilon} \leq \|b_0\|_{L^\infty(\Omega)} \leq 1$$

and

$$F_\epsilon \in L^\infty(Q_T). \tag{3.42}$$

Multiplying the equation by b_ϵ and integrating by parts, we deduce that

$$\|b_\epsilon\|_{L^2(0,T;H_0^1(\Omega))} \leq C, \tag{3.43}$$

Further taking the duality product $< \cdot, \cdot >_{(H^{-1},H_0^1)}$ of $b_{\epsilon t}$ with an arbitrary test function from $L^2(0,T;H_0^1(\Omega))$, we deduce that

$$\|b_{\epsilon t}\|_{L^2(0,T;H^{-1}(\Omega))} \leq C, \tag{3.44}$$

Then, the inequalities (3.43) and (3.44) imply that

$$\{b_\epsilon\} \text{ is relative compact in } L^2(Q_T). \tag{3.45}$$

(cf. [73, Theorem 2.1 p. 27]. We deduce that there exist a function $b \in L^2(0,T;H_0^1(\Omega))$ with $b_t \in L^2(0,T;H^{-1}(\Omega))$ and a subsequence $\{b_{\epsilon_j}\}$ of $\{b_\epsilon\}$ such that

$$b_{\epsilon_j} \to b \text{ strongly in } L^2(Q_T) \tag{3.46}$$

$$b_{\epsilon_j t} \to b_t \text{ weakly in } L^2(0,T;H_0^1(\Omega)) \tag{3.47}$$

Moreover, it follows from [73, Lemma 1.2 p.260] that

$$b \in C([0,T];L^2(\Omega)). \tag{3.48}$$

Finally, it is clear that $0 \leq b \leq 1$ for all $t \in [0,T]$ and a.e. $x \in \Omega$. Since, w_ϵ satisfies the equation it follows in a similar way that w_ϵ converges along a subsequence to a limit w strongly in $L^2(Q_T)$ and weakly in $L^2(0,T;H_0^1(\Omega))$ as $\epsilon \to 0$ where $w \in C([0,T];L^2(\Omega))$ and $0 \leq w \leq \bar{w}$ for all $t \in [0,T]$ and a.e. $x \in \Omega$.

Next we consider the problem for h_ϵ, namely

$$\begin{cases} \partial_t h_\epsilon = \Delta\phi_\epsilon(h_\epsilon) - I(b_\epsilon)f_\epsilon(h_\epsilon) + p_\epsilon & \text{in } Q_T, \\ h_\epsilon = 0 & \text{on } S_T, \\ h_\epsilon(x,0) = h_{0,\epsilon}(x) & \text{for } x \in \Omega, \end{cases} \tag{3.49}$$

We first prove the following estimate

Lemma 1. *We have that*

$$\frac{1}{2}\int_\Omega (h_\epsilon)^2(t)\,dx + \int_0^T \int_\Omega |\nabla\psi_\epsilon(h_\epsilon)|^2\,dx\,dt \leq C(T) \tag{3.50}$$

where $\psi_\epsilon(s) = \int_0^s \sqrt{\phi'_\epsilon(s)}\, ds$, *which in turn implies that*

$$\int_0^T \int_\Omega |(\nabla \phi_\epsilon(h_\epsilon(t))|^2 \leq C(T) \tag{3.51}$$

Proof. The function h_ϵ satisfies the initial value problem

$$h_{\epsilon t} = d_h \Delta \phi_\epsilon(h_\epsilon) + G_\epsilon \tag{3.52}$$

together with zero Dirichlet boundary conditions where we have set $G_\epsilon = -I(b_\epsilon) f_\epsilon(h_\epsilon) + p_\epsilon$, and so $\|G_\epsilon\|_{L^\infty(Q_T)} \leq C$. We multiply the equation (3.52) by h_ϵ and integrate by parts to deduce that

$$\frac{1}{2}\frac{d}{dt}\int_\Omega (h_\epsilon)^2(t)\, dx + d_h \int_\Omega \nabla \phi_\epsilon(h_\epsilon) \cdot \nabla h_\epsilon \, dxdt = \int_\Omega G_\epsilon h_\epsilon \, dx \tag{3.53}$$

which implies that

$$\begin{aligned} &\int_\Omega (h_\epsilon)^2(t)\, dx + 2d_h \int_0^T \int_\Omega \phi'_\epsilon(h_\epsilon) |\nabla h_\epsilon|^2 \, dxdt \\ &\leq \int_\Omega G_\epsilon^2 \, dxdt + \int_0^T \int_\Omega h_\epsilon^2 \, dxdt + \int_\Omega h_{0\epsilon}^2 \, dx. \end{aligned} \tag{3.54}$$

Since

$$\int_0^T \int_\Omega \phi'_\epsilon(h_\epsilon) |\nabla h_\epsilon|^2 \, dxdt = \int_0^T \int_\Omega (\sqrt{\phi'_\epsilon(h_\epsilon)} \nabla h_\epsilon)^2 = \int_0^T \int_\Omega |\nabla \psi_\epsilon(h_\epsilon)|^2 \, dxdt, \tag{3.55}$$

we deduce that

$$\begin{aligned} \int_\Omega (h_\epsilon(T))^2 \, dx + 2d_h \int_0^T \int_\Omega |\nabla \psi_\epsilon(h_\epsilon)|^2 \leq \int_0^T \int_\Omega G_\epsilon^2 \, dxdt + \\ + \int_0^T \int_\Omega h_\epsilon^2 \, dxdt + \int_\Omega h_{0\epsilon}^2 \, dx, \end{aligned} \tag{3.56}$$

which in turn yields inequality (3.50). To prove (3.51), we observe that

$$\begin{aligned} \int_0^T \int_\Omega |(\nabla \phi_\epsilon(h_\epsilon(t))|^2 &= \int_0^T \int_\Omega \phi'_\epsilon(h_\epsilon(t))^2 |\nabla h_\epsilon(t)|^2 \, dxdt \\ &\leq \sup |\phi'_\epsilon(h_\epsilon(x,t))| \int_0^T \int_\Omega \phi'_\epsilon(h_\epsilon(t)) |\nabla h_\epsilon(t)|^2 \, dxdt \\ &\leq M \int_0^T \int_\Omega \left(\sqrt{\phi'_\epsilon(h_\epsilon(t))} \nabla h_\epsilon(t) \right)^2, \end{aligned} \tag{3.57}$$

where M is independent of ϵ and so (3.51) follows from (3.55) and (3.50). □

Next we set $U_\epsilon = \phi_\epsilon(h_\epsilon)$ and $\beta_\epsilon(\cdot) = \phi_\epsilon^{-1}(\cdot)$, to apply the result of [29, Theorem 6.2].

Lemma 2. *(i) For all $\tau > 0$, the function U_ϵ is equicontinuous in $\bar{Q}_T^\tau$. Precisely, there exists a continuous nondecreasing function $\omega_\tau(\cdot)$ with $\omega_\tau(0) = 0$, such that*

$$|U_\epsilon(x_1, t_1) - U_\epsilon(x_2, t_2)| \le \omega_\tau(|x_1 - x_2| + |t_1 - t_2|^{1/2}) \tag{3.58}$$

for all $(x_i, t_i) \in \bar{Q}_T^\tau$, $i = 1, 2$. The function ω_τ does not depend on ϵ.

(ii) if in addition $U(0, x) = U_0(x) \in C(\bar{\Omega})$, then $\{U_\epsilon\}$ is equicontinuous on $\bar{Q}_T$.

We deduce from Lemma 2(i) that for all $\tau > 0$, U_{ϵ_j} is precompact in $C(\bar{Q}_T^\tau)$ and thus there exists a subsequence that we denote again by U_{ϵ_j} and a function $\zeta \in C(\bar{Q}_T^\tau)$ such that

$$U_{\epsilon_j} \to \zeta,$$

uniformly in $\bar{Q}_T^\tau$ as $\epsilon_j \to 0$. Then,

$$\begin{aligned} |h_{\epsilon_j} - \zeta^{1/m}| &= |\beta_\epsilon(U_{\epsilon_j}) - \zeta^{1/m}| \\ &\le |\beta_{\epsilon_j}(U_{\epsilon_j}) - (U_{\epsilon_j})^{1/m}| + |(U_{\epsilon_j})^{1/m} - \zeta^{1/m}|, \end{aligned} \tag{3.59}$$

Therefore, since for all $\epsilon > 0$, $|\beta_\epsilon(U_\epsilon) - (U_\epsilon)^{1/m}| < 2\epsilon$, setting $h = \zeta^{1/m}$ we have that

$$\begin{aligned} h_{\epsilon_j} &\to h, \text{ uniformly in } \bar{Q}_T^\tau, \\ \phi_\epsilon(h_{\epsilon_j}) &\to h^m \text{ uniformly in } \bar{Q}_T^\tau, \end{aligned} \tag{3.60}$$

as $\epsilon_j \to 0$, for all $\tau > 0$. Moreover, from Lemma 1 there exists a subsequence of $\{h_{\epsilon_j}\}$ which we denote again by h_{ϵ_j} and a function $\chi \in L^2((0, T); H_0^1(\Omega))$ such that

$$\phi_{\epsilon_j}(h_{\epsilon_j}) \rightharpoonup \chi \text{ weakly in } L^2(0, T; H_0^1(\Omega)), \tag{3.61}$$

as $\epsilon_j \to 0$. Since, $L^2(\Omega) \subset H^{-1}(\Omega)$ we further deduce that $\phi_{\epsilon_j}(h_{\epsilon_j}) \rightharpoonup \chi$ weakly in $L^2(Q_T)$. On other hand, $\phi_{\epsilon_j}(h_{\epsilon_j}) \le (h_{\epsilon_j})^m \le \bar{h}^m$ and from (3.60) we have that $\phi_{\epsilon_j}(h_{\epsilon_j}) \to h^m$ a.e in Q_T. Then, by the dominated convergence theorem we deduce that $\phi_{\epsilon_j}(h_{\epsilon_j}) \to \phi(h)$ strongly in $L^2(Q_T)$. Therefore, $\phi(h_{\epsilon_j}) \rightharpoonup h^m$ weakly in $L^2(Q_T)$ and uniqueness of the weak limits implies that $\chi = h^m$. Hence, we conclude that

$$\phi_{\epsilon_j}(h_{\epsilon_j}) \rightharpoonup h^m \text{ weakly in } L^2(0, T; H_0^1(\Omega)), \tag{3.62}$$

as $\epsilon_j \to 0$.

Next we prove that (b, w, h) is a weak solution of Problem (P). We multiply the three partial differential equations in (3.18) by $\psi \in C^1(\overline{Q}_T) \cap L^2(0, T; H_0^1(\Omega))$

and integrate by parts to obtain (here for simplicity $\epsilon = \epsilon_j$)

$$\begin{aligned}\int_\Omega b_\epsilon(t)\psi(t) + d_b\int_0^t\int_\Omega \{\nabla b_\epsilon\cdot\nabla\psi - b_\epsilon\psi_t\}\,dxd\tau = \int_\Omega b_{0,\epsilon}\psi(0)+\\ \int_0^t\int_\Omega \{G_1(b_\epsilon)w_\epsilon(1-b_\epsilon)b_\epsilon - b_\epsilon\}\psi,\end{aligned} \tag{3.63}$$

$$\begin{aligned}\int_\Omega w_\epsilon(t)\psi(t) + d_w\int_0^t\int_\Omega \{\nabla w_\epsilon\cdot\nabla\psi - w_\epsilon\psi_t\}dxd\tau = \int_\Omega w_{0,\epsilon}\psi(0)+\\ \int_0^t\int_\Omega \{-\left(L(b_\epsilon)+G_2(b_\epsilon)\right)w_\epsilon + I(b_\epsilon)f_\epsilon(h_\epsilon)\}\psi,\end{aligned} \tag{3.64}$$

$$\begin{aligned}\int_\Omega h_\epsilon(t)\psi(t) + d_h\int_0^t\int_\Omega \{\nabla\phi_\epsilon(h_\epsilon)\cdot\nabla\psi - h_\epsilon\psi_t\}dxd\tau = \int_\Omega h_{0,\epsilon}\psi(0)+\\ \int_0^t\int_\Omega \{p_\epsilon - I(b_\epsilon)f_\epsilon(h_\epsilon)\}\psi\,dxd\tau.\end{aligned} \tag{3.65}$$

To summarize we have that b_ϵ,w_ϵ, h_ϵ are positive and bounded. Moreover, there exists and a subsequence of $(b_\epsilon, w_\epsilon, h_\epsilon)$, which converges strongly to (b, w, h) in $(L^2(Q_T))^3$, and a.e in Q_T, and $(b_\epsilon, w_\epsilon, \phi_\epsilon(h_\epsilon))$ converges weakly to $(b, w, \phi(h))$ in $(L^2(0,T;H_0^1))^3$. To pass to the limit in the terms involving $f_\epsilon(h_\epsilon)$ we notice that

$$|f_\epsilon(s) - s^\alpha| \le 2\epsilon^\alpha. \tag{3.66}$$

and thus,

$$\begin{aligned}|I(b_\epsilon)f_\epsilon(h_\epsilon) - I(b_\epsilon)f_\epsilon(h_\epsilon)| \le& |I(b_\epsilon)||(f_\epsilon(h_\epsilon) - f(h_\epsilon)| + |I(b_\epsilon) - I(b)||f(h_\epsilon)|\\ &+ |I(b)||f(h_\epsilon) - f(h)|\\ \le& 2I(1)\epsilon^\alpha + |I(b_\epsilon) - I(b)||f(\bar{h})|\\ &+ |I(1)||f(h_\epsilon) - f(h)|\,.\end{aligned} \tag{3.67}$$

Moreover, recalling (3.23) and (3.24), we can let $\epsilon \to 0$ in (3.63)-(3.65), to obtain the integral identities (3.15)-(3.17). Finally, if $h_0 \in C(\bar{\Omega})$ from Lemma 2(ii) $h \in C(\bar{Q}_T)$.

In fact, a weak solution of Problem (P_D) exists even if h_0 is just essentially bounded, since working as above we know that there exists $h \in C((0,T],(L^1(\Omega))$. We would also like to know is $\|h(t)\|_{L^1(\Omega)}$ is continuous at 0. To this end let $h_{0,n}$ be a sequence of smooth bounded functions which converges to h_0 in $L^1(\Omega)$. Working as above and using Lemma 2(ii) there exists a solution of the system, denoted by h_n, obtained as a limit of the approximating system such that $h_n \in C(\bar{Q}_T)$. Next note that

$$\|h(t) - h_0\|_{L_1(\Omega)} \le \|h(t) - h_n(t)\|_{L_1(\Omega)} + \|h_n(t) - h_{0,n}\|_{L_1(\Omega)} + \|h_{0,n} - h_0\|_{L_1(\Omega)} \tag{3.68}$$

where the second term on the right hand side goes to zero as t tends to 0, while the last term becomes arbitrarily small for n large enough. On the other hand, for any $\epsilon > 0$ and $h_1(0)$ and $h_2(0)$ smooth initial data, the solutions $h_{1,\epsilon}$ and $h_{2,\epsilon}$ of the corresponding approximating problems satisfy

$$\begin{aligned}\|h_{1,\epsilon}(t) - h_{2,\epsilon}(t)\|_{L^1(\Omega)} &\leq \|h_{1,\epsilon}(0) - h_{2,\epsilon}(0)\|_{L^1(\Omega)} + \int_0^t \|b_{1,\epsilon}(s) - b_{2,\epsilon}(s)\|_{L^1(\Omega)}\, ds \\ &\leq \|h_{1,\epsilon}(0) - h_{2,\epsilon}(0)\|_{L^1(\Omega)} + tD.\end{aligned}$$

where D is a positive constant. Letting $\epsilon \to 0$, this in turn implies that

$$\|h_1(t) - h_2(t)\|_{L^1(\Omega)} \leq \|h_1(0) - h_2(0)\|_{L^1(\Omega)} + tD \tag{3.69}$$

Finally, by (3.68) and (3.69)

$$\begin{aligned}\|h(t) - h_0\|_{L_1(\Omega)} \leq &\|h(0) - h_n(0)\|_{L^1(\Omega)} \\ &+ tD + \|h_n(t) - h_{0,n}\|_{L_1(\Omega)} + \|h_{0,n} - h_0\|_{L_1(\Omega)}\end{aligned} \tag{3.70}$$

thus $t \mapsto \|h(t)\|_{L^1(\Omega)}$ is continuous at zero and so $h \in C([0,T]; L^1(\Omega))$. We thus have the following result

Theorem 7. *If the initial condition (h_0, b_0, w_0) satisfies (3.7) and (3.8), then there exists a weak solution (b, w, h) of Problem (P_D) such that $0 \leq b \leq 1$, $0 \leq w \leq \bar{w}$ and $0 \leq h \leq \bar{h}$. If in addition $h_0, b_0, w_0 \in C(\bar{\Omega})$, then $h \in C(\bar{Q}_T)$ and $b, w \in C(\bar{\Omega} \times [\delta, T])$ for all $\delta > 0$.*

Proof. To complete the proof we note that from (3.42) and [45, Theorem 9.1 p. 341] it follows that [2]

$$\|b_\epsilon\|_{W_q^{2,1}(Q_T^\delta)} \leq C(\delta, T, q, \Omega) \tag{3.71}$$

for all $\delta \in (0,T)$ and all $q \in (1,\infty)$, where $Q_\delta^T = (\delta, T) \times \Omega$. This in turn implies that

$$\|b_\epsilon\|_{C^{\alpha, \frac{\alpha}{2}}(\bar{\Omega} \times [\delta, T])} \leq C, \tag{3.72}$$

for $\alpha = 2 - \frac{N+2}{q}$ and $q \neq N+2$ [11, Lemma 3.5]. Therefore, we can conclude (passing if necessary to another subsequence) that $b_{\epsilon_j} \to b$ uniformly in $\bar{Q}_T^\delta$ for all $\delta > 0$ and so $b \in C(\bar{\Omega} \times [\delta, T])$. Similarly, $w \in C(\bar{\Omega} \times [\delta, T])$. □

3.2.2 The case of Neumann Boundary conditions (P_N)

Although the above strategy can also be adapted to obtain the existence of weak solutions in the case of the Neumann problem (P_N), in this section, we exploit a different approach which is based on a fixed point argument.

[2] Here, $W_q^{2,1}(Q_\delta^T) = W^{1,q}(\delta, T; L^q(\Omega)) \cap L^q(\delta, T; W^{2,q}(\Omega) \cap W_0^{1,q}(\Omega))$

Theorem 8. *There exists a weak solution of Problem P_N.*

Before, giving the proof of Theorem 8 it is useful to state a lemma related to the problem

$$\begin{cases} \partial_t u - \Delta\varphi(u) = v & \text{in } Q_T, \\ \frac{\partial\varphi(u)}{\partial n} = 0 & \text{on } S_T, \\ u(x,0) = u_0(x) & \text{for } x \in \Omega. \end{cases} \tag{3.73}$$

where $\varphi : \mathbb{R} \to \mathbb{R}$ is nondecreasing continuous function with $\varphi(0) = 0$, $u_0 \in L^1(\Omega)$ and $v \in L^1(0,T;L^1(\Omega))$. It is known that system (3.73) possesses a unique weak solution [7]. For fixed u_0, let as denote by u_v the unique weak solution of (3.73) for some $v \in L^1(0,T;L^1(\Omega))$.

Lemma 3. *Suppose that $\varphi : \mathbb{R} \to \mathbb{R}$ is strictly increasing continuous function with $\varphi(0) = 0$, then*

(i) for each fixed $u_0 \in L^1(\Omega)$ and a weakly relatively compact set $\mathcal{K}$ in $L^1(0,T;L^1(\Omega))$, the set $\{u_v : v \in \mathcal{K}\}$ is relatively compact in $C([0,T];L^1(\Omega))$.

(ii) for each fixed $u_0 \in L^\infty(\Omega)$ and a bounded set $\mathcal{K}$ in $L^\infty(0,T;L^\infty(\Omega))$ the mapping $v \mapsto u_v$, is sequentially continuous from $\mathcal{K}$ endowed with the weak topology of $L^1(0,T;L^1(\Omega))$ into $C([0,T];L^p(\Omega))$ endowed with the strong topology, for all $p \in [1,\infty)$.

For the proof of Lemma 3 (i) we refer to the results of Diaz-Vrabie [26, 27]. It must be pointed out that although the compactness results of the above references concern the case of Dirichlet boundary conditions, the arguments are identical for the case of Neumann boundary conditions (see [27, Section 2] and [7]). On the other hand Lemma 3 (ii) is a consequence of the counterpart (i) thanks to the uniqueness of the weak solution (for details see [28, Corollary 1, Section 2] or [28, Corollary 3.1] for the case $p = 1$).

For convenience in what follows, if $\mathbf{u} = (u_1, u_2, u_3)$ is a vector function with $u_i \in X$, where X is a Banach space, we shall make use of the notation $\|\mathbf{u}\|_X := \max_{i=1,2,3}\{\|u_i\|_X\}$.

Proof of Theorem 8. Let us start with the existence of a local (in time) weak solution of (P_N). We introduce the reaction functions $\mathbf{R} : \mathbb{R}^3 \to \mathbb{R}^3$ given by

$$\mathbf{R}(b,w,h) = (R_1(b,w,h), R_2(b,w,h), R_3(b,w,h))$$

with

$$\begin{cases} R_1(b,w,h) = wG_1(b)(1-b)b - b \\ R_2(b,w,h) = -(\tilde{L}(b) + G_2(b))w + \tilde{I}(b)h|h|^{\alpha-1} \\ R_3(b,w,h) = -\tilde{I}(b)h|h|^{\alpha-1}. \end{cases} \tag{3.74}$$

where $\tilde{I}(b)$ (respectively $\tilde{L}(b)$) is a truncation of $I(b)$ (respectively $L(b)$) extending it continuously by a constant equal to $I(0)$ (respectively $L(0)$) for $b < 0$. We choose $K > 0$ such that

$$\max(\|b_0\|_{L^\infty(\Omega)}, \|w_0\|_{L^\infty(\Omega)}, \|h_0\|_{L^\infty(\Omega)}) + 1 \leq K.$$

Since the functions $R_i : \mathbb{R}^3 \to \mathbb{R}$ are continuous it is possible to find $M > 0$, such that

$$\max\{|R_1(b,w,h)|, |R_2(b,w,h)|, |R_3(b,w,h)| + \|p\|_{L^\infty(Q_T)}\} \leq M$$

assumed that

$$0 \leq b, w, h \leq K.$$

Now we define the "solution operator" $\mathcal{S} : L^1(0,T : L^1(\Omega))^3 \to C([0,T]; L^2(\Omega))^3$ by $\mathcal{S}(f,g,v) = (b,w,h)$ where b, w, h are the unique weak solutions of the decoupled system

$$\begin{cases} \partial_t b - d_b \Delta b = f & \text{in } Q_T, \\ \partial_t w - d_w \Delta w = g & \text{in } Q_T, \\ \partial_t h - d_h \Delta h^m = v & \text{in } Q_T, \\ \frac{\partial b}{\partial n} = \frac{\partial w}{\partial n} = \frac{\partial h}{\partial n} = 0 & \text{on } S_T, \\ b(x,0) = b_0(x),\ w(x,0) = w_0(x),\ h(x,0) = h_0(x) & \text{for } x \in \Omega. \end{cases}$$

Next to control some a priori estimates it is useful to introduce the following convex set (adapted to the reaction terms $\mathbf{R}(b,w,h)$):

$$\mathcal{K}_{r,T_0} = \{(f,g,v) : f,g,v \in L^1(0,T_0 : L^1(\Omega)), \|(f,\, g,\, v)\|_{L^\infty(Q_{T_0})} \leq r\},$$

where $Q_{T_0} := (0,T_0) \times \Omega$, $r \geq M$ and $T_0 \in (0,T]$ is such that

$$\mathcal{S}(\mathcal{K}_{r,T_0}) \subset B_{L^\infty(Q_{T_0})}(\mathbf{0},K)$$

with $B_{L^\infty(Q_{T_0})}(\mathbf{0},K) := \{\mathbf{u} \in L^\infty(Q_{T_0})^3 : \|\mathbf{u}\|_{L^\infty(Q_{T_0})}) \leq K\}$. Recall that M depends on K through the properties of $\mathbf{R}$. Moreover, it is not difficult to see that $\mathcal{K}_{r,T_0}$ is nonempty and weakly compact in $(L^1(0,T_0 : L^1(\Omega)))^3$. Next let us define the restriction of the solution operator on $\mathcal{K}_{r,T_0}$:

$$\widehat{\mathcal{S}} = \mathcal{S}|_{\mathcal{K}_{r,T_0}} : \mathcal{K}_{r,T_0} \to L^\infty(Q_{T_0})^3.$$

We also define the composition of the realization operator associated to $\mathbf{R}$ and $\widehat{\mathcal{S}}$, namely, the operator $\mathcal{R} : \mathcal{K}_{r,T_0} \to C([0,T]; L^2(\Omega))^3$ defined by

$$\mathcal{R}(f,g,v) = (R_1(\widehat{\mathcal{S}}(f,g,v)), R_2(\widehat{\mathcal{S}}(f,g,v)), R_3(\widehat{\mathcal{S}}(f,g,v)) + p)$$

i.e. $\mathcal{R}(f,g,v) = \mathbf{R}(b,w,h)$ with $(b,w,h) = \widehat{\mathcal{S}}(f,g,v)$. Then, from the choice of the set $\mathcal{K}_{r,T_0}$ we know that $\mathcal{R}$ maps $\mathcal{K}_{r,T_0}$ into $\mathcal{K}_{r,T_0}$.

Next we prove that there exists at least one fixed point of $\mathcal{R} : \mathcal{K}_{r,T_0} \to \mathcal{K}_{r,T_0}$. This will be a consequence of a variant of the Schauder fixed point theorem given in [82, Theorem 1.2.11 (Arino, Gautier and Penot)], which requires $\mathcal{R}$ to be weakly-weakly sequentially continuous. It is actually enough to show that the graph of $\mathcal{R}$, is weakly-weakly sequentially closed [82, Corollary 1.2.5]. To this end, let $\{(f_n,g_n,v_n)\}_{n\in\mathbb{N}} \in \mathcal{K}_{r,T_0}$ and $\{(F_n,G_n,V_n)\}_{n\in\mathbb{N}} \in \mathcal{R}(f_n,g_n,v_n)$ be sequences which converge weakly in $(L^1((0,T);L^1(\Omega)))^3$ to (f,g,v) and (F,G,V), respectively. Then from Lemma 3 (ii) $\widehat{\mathcal{S}}$ is weakly-strongly sequentially continuous from $L^1(0,T_0;L^1(\Omega))$ into $C([0,T_0];L^p(\Omega))$ and so we may assume without loss of generality (taking a subsequence if necessary) that

$$\widehat{\mathcal{S}}(f_n,g_n,v_n) \to \widehat{\mathcal{S}}(f,g,v) \text{ a.e in } Q_{T_0}, \tag{3.75}$$

which, by continuity of R_i, implies that

$$R_i(\widehat{\mathcal{S}}(f_n,g_n,v_n)) \to R_i(\widehat{\mathcal{S}}(f,g,v)) \text{ a.e in } Q_{T_0}. \tag{3.76}$$

Moreover, $R_i(\widehat{\mathcal{S}}(f_n,g_n,v_n))$ is a.e bounded in Q_{T_0} and therefore by the dominated convergence theorem we have that $\mathcal{R}(f_n,g_n,v_n) \to \mathcal{R}(f,g,v)$ strongly in $(L^1(Q_{T_0}))^3$. Consequently, by uniqueness of weak limits we conclude that $(F,G,V) = \mathcal{R}(f,g,v)$. Therefore, the graph of $\mathcal{R}$ is weakly-weakly sequentially closed and so $\mathcal{R}$ has at least one fixed point (f,g,v). Since $(b,w,h) = \widehat{\mathcal{S}}(f,g,v)$ we conclude that (b,w,h) is a weak solution of the problem (P_N) on the cylinder $Q_{T_0} := (0,T_0)\times\Omega$, i.e. a local (in time) solution of (P_N) on Q_{T_0}.

Now it only remains to prove that no possible blow-up of the norm in $C([0,T];L^2(\Omega))^3$ may arise to get the continuation of the local weak solution to the whole cylinder Q_T. But for the reaction terms $\mathbf{R}(b,w,h)$ given by (3.74) and for positive initial conditions satisfying (3.7), (3.8) this is an easy task: indeed, similar arguments to the ones of the proof of Theorem 1 show that the local weak solution satisfies that

$$0 \le b \le 1, 0 \le w \le \overline{C} \text{ a.e. in } Q_{T_0},$$

where $\overline{C} > 0$ is independent of T_0 and, by well-known estimates for the porous medium with monotone absorption

$$0 \le h \le \|h_0\|_{L^\infty(\Omega)} + T\|p\|_{L^\infty(Q_T)} \text{ a.e. in } Q_{T_0}$$

which is also independent of T_0. Therefore, the local weak solution can be extended, by taking T_0 as initial time and the values of b,w,h, at $t = T_0$ as new initial data, to the complete cylinder Q_T producing at least one global weak solution of (P_N) in view of the fact that b,w,h are nonnegative. □

Remark. The above type of arguments can be applied to prove the convergence of some numerical algorithms that relies in suitable decoupling of the system and applying the Diaz-Vrabie 1989 *ad hoc* compactness argument. For instance we can consider the following iterative argument: we solve the uniformly parabolic equations by prescribing the h-component

$$\begin{cases} \partial_t b_n = d_b \Delta b_n + w_n G_1(b_n)(1-b_n)b_n - b_n & \text{in } Q_T, \\ \partial_t w_n = d_w \Delta w_n - (L(b_n) + G_2(b_n))w_n + I(b_n)h_{n-1}^{\alpha} & \text{in } Q_T, \end{cases} \tag{3.77}$$

together with the initial conditions,

$$b_n(x,0) = b_0(x),\ w_n(x,0) = w_0(x),\ \text{ for } x \in \Omega, \tag{3.78}$$

and Neumann boundary conditions

$$\frac{\partial b_n}{\partial n} = \frac{\partial w_n}{\partial n} = 0,\ \text{on } \partial\Omega \times (0,T). \tag{3.79}$$

Then we solve the degenerate equation by prescribing the b-component

$$(P_{h,n}) = \begin{cases} \partial_t h_n = d_h \Delta h_n^m - I(b_{n-1})h_n^{\alpha} + p & \text{in } Q_T, \\ \frac{\partial h_n}{\partial n} = 0 & \text{on } \partial\Omega \times (0,T), \\ h_n(x,0) = h_0(x) & \text{for } x \in \Omega. \end{cases}$$

Obviously the iteration starts with the initial data. The existence of weak solutions for the decoupled problems are easy modifications of previous results in the literature (or they can be obtained by following some ideas of the preceding section for the treatment of the Dirichlet case). The convergence of the algorithm is a small variant of the proof of Theorem 3.

3.3 Properties of the surface water component

In this section, we focus on the qualitative properties of the surface water component h investigating the impact of dry periods on the zeroes set of h. Precisely, we assume that precipitation is negligible, if not absent, for sufficiently long time, that is

$$p(t) = 0 \text{ for } t \in (0,T), \tag{3.80}$$

with T large enough. Then, we can show that h vanishes after a finite time for the Dirichlet boundary conditions. In addition, for certain range of the parameters and a compacted supported initial condition, h expands its support by forming a free boundary during the dry period.

In what follows, without loss of generality we suppose that $\delta_h = 1$. We let (b, w, h) be a solution of system (3.2) for a non-negative and bounded initial datum

(b_0, w_0, h_0), with $0 \leq b_0 \leq 1$. In order to determine the properties of h it suffices to study the following scalar equation

$$\partial_t h - \Delta h^m + I(b(t,x))h^\alpha = 0 \text{ in } Q_T, \tag{3.81}$$

which involves the bounded solution component b. We consider (3.81), subject to the homogeneous Dirichlet boundary conditions

$$h(t,x) = 0, \forall (t,x) \in [0,T) \times \partial\Omega, \tag{3.82}$$

and a given non-negative initial datum

$$h_0 = h(0,x),\ x \in \Omega. \tag{3.83}$$

At the end of the section some remarks are given concerning the homogeneous Newmann boundary conditions as well as the non-homogeneous Dirichlet boundary conditions.

3.3.1 Extinction in finite time

We recall that $0 \leq b_0 \leq 1$ implies $0 \leq b \leq 1$, and thus $I(0) \leq I(b(t,x) \leq I(1)$. Therefore, if h satisfies (3.81)–(3.83) and $\bar{U}$ is such that

$$\begin{cases} \dfrac{\partial \bar{U}}{\partial t} - \Delta \bar{U}^m + I(0)\bar{U}^\alpha \geq 0 & \text{in } \Omega \\ \bar{U}(t,x) \geq h(t,x) & \text{on } (0,T) \times \Omega \\ \bar{U}(0,x) \geq h(0,x) & \text{in } \Omega \end{cases} \tag{3.84}$$

since

$$\frac{\partial h}{\partial t} - \Delta h^m + I(0)h^\alpha \leq \frac{\partial h}{\partial t} - \Delta h^\kappa + I(b(t,x))h^\alpha = 0. \tag{3.85}$$

by comparison we have that $h \leq \bar{U}$ in Q_T [24]. This simple observation leads to the following

Theorem 9. *Let (3.80) hold true and let (b, w, h) be a solution of problem (3.2)–(3.4) in the time interval $(0,T)$. Then, if $T > 0$ is large enough, there exists $T^* \in (0,T)$ such that $h(t,x) = 0$ for all $t > T^*$.*

Proof. Let U be uniform in space satisfying the non-linear ODE:

$$\begin{cases} \dfrac{\partial U}{\partial t} + \lambda U^\alpha = 0, \\ U(0) = \|h_0\|_{L^\infty(\Omega)}, \end{cases} \tag{3.86}$$

for $\lambda > 0$. Then, for $\alpha < 1$, (3.86) possesses the following explicit solution

$$U(t;\lambda) = \left(\max\{0, \|h_0\|^{1-\alpha}_{L^\infty(\Omega)} - \lambda(1-\alpha)t\}\right)^{1/(1-\alpha)}, \tag{3.87}$$

Obviously, $U(t; I(0)) = \bar{U}(t)$ satisfies (3.84). As a result, letting

$$T^*(\|h_0\|_{L^\infty(\Omega)}, I(0), \alpha) = \frac{(\|h_0\|_{L^\infty(\Omega)})^{(1-\alpha)}}{I(0)(1-\alpha)},$$

by comparison $0 \leq h(t) \leq \bar{U}(t)$, $h(t) = 0$ for all $t \geq T^*(\|h_0\|_{L^\infty(\Omega)}, I(0), \alpha)$. □

3.3.2 Estimates for the zeroes set of h

First, let us introduce the following notation. If f is a real-valued function defined on Ω, we denote by $\text{supp}(f)$ the support of f in Ω, that is

$$\text{supp}(f) := \overline{\{x \in \Omega |\, f(x) \neq 0\}},$$

and by $N(f)$ the complement of the support, namely,

$$N(f) := \bar{\Omega} - \text{supp}(f).$$

Next we estimate the location of the zeros of h in Ω for all t in $(0, T)$.

Theorem 10. *Let $\sigma = \alpha/m < 1$ and suppose that $h_0 \in L^\infty(\Omega)$ is a nonnegative and compacted supported initial datum. Then $N(h(t,x) \subset N(h_0(x))$ for all $t \in (0,T)$. In particular, if we set $M = \|h_0\|_{L^\infty(\Omega)}$, $L^* = \left(\frac{M^m}{K}\right)^{\frac{2}{1-\sigma}}$ and $K = \left(\frac{I(0)(1-\sigma)^2}{2(2\sigma+N(1-\sigma))}\right)^{\frac{1}{1-\sigma}}$, we have that*

$$N(h(t,x)) \subset \{x \in (\Omega - supp(h(0,x))) \; s.t \; dist(x, supp(h(0,x))) \geq L^*\}.$$

Proof. We look for local sup-solutions which may vanish at points of the zero set of the initial datum h_0. Letting $\sigma = \alpha/\kappa$, we have that for $0 < \sigma < 1$ and $\lambda > 0$, the function $V(x) = K(\lambda)|x - x_0|^{\frac{2}{1-\sigma}}$, with $K(\lambda) = \left(\frac{\lambda(1-\sigma)^2}{2(2\sigma+N(1-\sigma))}\right)^{\frac{1}{1-\sigma}}$ satisfies the equation $-\Delta V + \lambda V^\sigma = 0$ (see [23]). Now, let $x_0 \in \Omega - \text{supp}(h_0)$, $R := \text{dist}\{x_0, \text{supp}(h_0)\}$ and $\tilde{\Omega} := (B_R(x_0) \cap \Omega)$. Then for $\bar{u}(t,x) = (V(x))^{1/m}$ we have that

$$\begin{cases} \partial_t \bar{u} - \Delta \bar{u}^m + I(0)\bar{u}^\sigma = 0 & \text{in } (0,T) \times \tilde{\Omega}, \\ \bar{u}(x) \geq 0 = h_0(x) & \text{on } \tilde{\Omega}, \end{cases} \tag{3.88}$$

and

$$\bar{u} \geq 0 \text{ on } (0,T) \times (\partial\Omega \cap \tilde{\Omega}). \tag{3.89}$$

By (3.85), $\bar{u}$ is a local super solution of (3.81) as long as the inequality $h(t,x) \leq \bar{u}(t,x)$ is also satisfied for all x in $\partial B_R(x_0) \cap \text{int}\,(\Omega)$ and $t \in (0,T)$. In fact, since $|x - x_0| = R$ on $\partial B_R(x_0)$, if

$$R \geq \left(\frac{M_h^m}{K(I(0))}\right)^{\frac{1-\sigma}{2}} \tag{3.90}$$

and $\|h\|_{L^\infty(0,T;\Omega)} \leq M_h$, we have that $\left(K(I(0))R^{\frac{2}{1-\sigma}}\right)^{1/\kappa} \geq M_h$ which in turn implies that

$$\bar{u} \geq h, \text{ on } (0,T) \times \partial\tilde{\Omega} - \partial\Omega. \tag{3.91}$$

Therefore, when (3.90) holds true, $\bar{u}$ is a local sup-solution thanks to (3.85), (3.88), (3.89) and (3.91). Finally, $\|h\|_{L^\infty(0,t;\Omega)} \leq \|h_0\|_{L^\infty(\Omega)}$, so we may set $M_h = \|h_0\|_{L^\infty(\Omega)}$ and since $0 \leq h(x_0) \leq \bar{u}(x_0) = 0$ the result follows. □

Remark 5. *In the case of homogeneous Neumann boundary conditions, a similar result is true due to the local nature of the supersolutions. In particular, in the proof above we may take $R := dist\{x_0, supp(h_0) \cup \partial\Omega\}$ so that the ball $B_R(x_0)$ for $x_0 \in \Omega - supp(h_0)$ is entirely contained in Ω, then if (3.90) is satisfied, (3.85), along with (3.88) and (3.91) ensure that the super-solution is appropriately defined.*

Remark 6. *The same result holds true for the problem with compacted supported inhomogeneous Dirichlet boundary conditions, i.e when $h(t,x) = g(t,x) \geq 0$ on $(0,T) \times (\partial\Omega \cap \tilde{\Omega})$ with $g(t,\cdot) > 0$ on a compact subset of $\partial\Omega$. In this case, we may take $R := dist\{x_0, supp(h_0) \cup (\cup_{\tau>0} supp\,(g(\tau,\cdot)))\}$.*

Bibliography

[1] H. Amann. Fixed point equations and nonlinear eigenvalue problems in ordered Banach spaces. *SIAM Review*, 18(4):620–709, 1976.

[2] A. Ambrosetti and A. Malchiodi. *Nonlinear Analysis and Semilinear Elliptic Problems*. Cambridge studies in Advanced Mathematics, 2007.

[3] O. Arino, S. Gautier, and J. P. Penot. A fixed point theorem for sequentially continuous mappings with application to ordinary differential equations. *Funkcial. Ekvac*, 27(3):273–279, 1984.

[4] J. B. L. Bard. A model for generating aspects of zebra and other mammalian coat patterns. *Journal of Theoretical Biology*, 93(2):363–385, 1981.

[5] M. Baudena and M. Rietkerk. Complexity and coexistence in a simple spatial model for arid savanna ecosystems. *Theoretical Ecology*, 6(2):131–141, 2013.

[6] M. Beck, J. Knobloch, D. Lloyd, B. Sandstede, and T. Wagenknecht. Snakes, ladders, and isolas of localized patterns. *SIAM Journal on Mathematical Analysis*, 41(3):936–972, 2009.

[7] P. Benilan. *Equations d'évolution dans un espace de Banach quelconque et applications*. PhD thesis, Université Paris XI, 1972.

[8] J. Blat and K. Brown. Global bifurcation of positive solutions in some systems of elliptic equations. *SIAM Journal on Mathematical Analysis*, 17(6):1339–1353, 1986.

[9] F. Borgogno, P. D'Odorico, F. Laio, and L. Ridolfi. Mathematical models of vegetation pattern formation in ecohydrology. *Reviews of Geophysics*, 47:RG1005, 2009.

[10] U. Bortolozzo, M. G. Clerc, and S. Residori. Local theory of the slanted homoclinic snaking bifurcation diagram. *Phys. Rev. E*, 78:036214, Sep 2008.

[11] D. Brochet, D. Hilhorst, and X. Chen. Finite dimensional exponential attractor for the phase field model. *Applicable Analysis: An International Journal*, 49(3-4):197–212, 1993.

[12] K. J. Brown and F. A. Davidson. Global bifurcation in the brusselator system. *Nonlinear Analysis: Theory, Methods & Applications*, 24(12):1713–1725, 1995.

[13] F. Cartenì, A. Marasco, G. Bonanomi, S. Mazzoleni, M. Rietkerk, and F. Giannino. Negative plant soil feedback explaining ring formation in clonal plants. *Journal of theoretical biology*, 313:153–161, 2012.

[14] M. D. Cramer and N. N. Barger. *PLoS ONE*, 8:e70876, 2013.

[15] M. G. Crandall and P. H. Rabinowitz. Bifurcation from simple eigenvalues. *Journal of Functional Analysis*, 8(2):321–340, 1971.

[16] M. C. Cross and P. C. Hohenberg. Pattern formation outside of equilibrium. *Reviews of modern physics*, 65(3):851, 1993.

[17] E. Dancer. Global solution branches for positive mappings. *Arch. Rational Mech. Anal.*, 52:181–192, 1973.

[18] J. H. P. Dawes. Localized pattern formation with a large-scale mode: Slanted snaking. *SIAM J. Applied Dynamical Systems*, 7:186–206, 2008.

[19] V. Deblauwe, N. Barbier, P. Couteron, O. Lejeune, and J. Bogaert. The global biogeography of semi-arid periodic vegetation patterns. *Global Ecology and Biogeography*, 17(6):715–723, Nov. 2008.

[20] V. Deblauwe and J. Bogaert. Modulation des structures de végétation auto-organisées en milieu aride/self-organized vegetation pattern modulation in arid climates. 2010.

[21] G. T. Dee and W. van Saarloos. Bistable systems with propagating fronts leading to pattern formation. *Physical review letters*, 60(25):2641–2644, 1988.

[22] J. M. d'Herbès, C. Valentin, D. J. Tongway, and J. C. Leprun. Banded vegetation patterns and related structures. In *Banded vegetation patterning in arid and semiarid environments*, pages 1–19. Springer, 2001.

[23] J. I. Díaz. *Nonlinear partial differential equations and free boundaries*. Pitman Advanced Publishing Program, 1985.

[24] J. I. Diaz and F. de Thelin. On a nonlinear parabolic problem arising in some models related to turbulent flows. *SIAM J. Math. Anal.*, 25(4):1085–1111, 1994.

[25] J. I. Díaz, J. Hernández, and L. Tello. On the multiplicity of equilibrium solutions to a nonlinear diffusion equation on a manifold arising in climatology. *Mathematical Analysis and Applications*, 216(AY975691):593–613, 1997.

[26] J. I. Díaz and I. I. Vrabie. Propriétés de compacité de l'opérateur de green généralisé pour l'équation des milieux poreux. *Comptes rendus de l'Académie des sciences. Série 1, Mathématique*, 309(4):221–223, 1989.

[27] J. I. Díaz and I. I. Vrabie. Compactness of the green operator of nonlinear diffusion equations: application to boussinesq type systems in fluid mechanics. *Topol. Methods in Nonlinear Anal*, 4:399–416, 1994.

[28] J. I. Díaz and I. I. Vrabie. Existence for reaction diffusion systems. a compactness method approach. *Journal of mathematical analysis and applications*, 188(2):521–540, 1994.

[29] E. DiBenedetto. Continuity of weak solutions to a general porous medium equation. *Indiana University Journal*, (32):83–118, 1983.

[30] E. Doedel, R. C. Paffenroth, A. R. Champneys, T. F. Fairgrieve, Y. A. Kuznetsov, B. E. Oldeman, B. Sandstede, and X. Wang. Auto2000. Technical report, Concordia University, 2002.

[31] D. J. Eldridge, E. Zaady, and S. M. Infiltration through three contrasting biological soil crusts in patterned landscapes in the negev, israel. *J Stat Phys*, 148:723–739, 2012.

[32] C. B. Field, V. Barros, T. F. Stocker, D. Qin, D. J. Dokken, L. L. Ebi, M. D. Mastrandrea, K. J. Mach, G.-K. Plattner, S. K. Allen, M. Tignor, and P. M. Midgley. Managing the risks of extreme events and disasters to advance climate change adaptation: A special report of the intergovernmental panel on climate change. Technical report, Cambridge University Press, Cambridge, UK, and New York, NY, USA, 2013.

[33] A. Gierer and H. Meinhardt. A theory of biological pattern formation. *Kybernetik*, 12(1):30–39, 1972.

[34] E. Gilad, M. Shachak, and E. Meron. Dynamics and spatial organization of plant communities in water-limited systems. *Theoretical Population Biology*, 72:214–230, 2007.

[35] E. Gilad, J. von Hardenberg, A. Provenzale, M. Shachak, and E. Meron. Ecosystem engineers: from pattern formation to habitat creation. *Physical Review Letters*, 93(9):098105–098105, 2004.

[36] E. Gilad, J. von Hardenberg, A. Provenzale, M. Shachak, and E. Meron. A mathematical model of plants as ecosystem engineers. *Journal of Theoretical Biology*, 244:680–691, 2007.

[37] E. Gilad, J. von Hardenberg, A. Provenzale, M. Shachak, and E. Meron. A mathematical model of plants as ecosystem engineers. *Journal of Theoretical Biology*, 244:680–691, 2007.

[38] P. Gray and S. K. Scott. Autocatalytic reactions in the isothermal, continuous stirred tank reactor: Isolas and other forms of multistability. *Chemical Engineering Science*, 38(1):29 – 43, 1983.

[39] C. Holzapfel, K. Tielbörger, H. Parag, J. Kigel, and M. Sternberg. Annual plant-shrub interactions along an aridity gradient. *Basic and Applied Ecology*, 7:268–279, 2006.

[40] C. Jones, J. Lawton, and M. Shachak. Organisms as ecosystem engineers. *Oikos*, 69:373–386, 1994.

[41] C. Jones, J. Lawton, and M. Shachak. Positive and negative efects of organisms as ecosystem engineers. *Ecology*, 78:1946–1957, 1997.

[42] S. Kéfi, M. Rietkerk, C. L. Alados, Y. Pueyo, V. P. Papanastasis, A. Elaich, and P. C. de Ruiter. Spatial vegetation patterns and imminent desertification in Mediterranean arid ecosystems. *Nature*, 449(7159):213–7, Sept. 2007.

[43] C. A. Klausmeier. Regular and irregular patterns in semiarid vegetation. *Science*, 284(5421):1826–1828, 1999.

[44] E. Knobloch. Spatially localized structures in dissipative systems: open problems. *Nonlinearity*, 21(4):T45, 2008.

[45] O. A. Ladyzhenskaya, V. A. Solonnikov, and N. N. Uraltseva. *Linear and quasilinear equations of parabolic type*, volume 23 of *Translations of Mathematical Monographs*. American Mathematical Society, Providence, R.I., 1967.

[46] R. Lefever and O. Lejeune. On the origin of tiger bush. *Bulletin of Mathematical Biology*, 59:263–294, 1997.

[47] O. Lejeune, M. Tlidi, and P. Couteron. Localized vegetation patches: A self-organized response to resource scarcity. *Physical Review E*, 66(1):10901, 2002.

[48] T. Ma and S. Wang. *Bifurcation theory and applications*, volume 53. World Scientific, 2005.

[49] F. Maestre, F. Valladares, and J. Reynolds. Is the change of plant-plant interactions with abiotic stress predictable? a meta-analysis of field results in arid environments. *J. Ecol.*, 93:748–757, 2005.

[50] E. Meron. Modeling dryland landscapes. *Math. Model. Nat. Phenom.*, 6:163–187, 2011.

[51] E. Meron. Pattern-formation approach to modelling spatially extended ecosystems. *Ecological Modelling*, 234:70–82, 2012.

[52] E. Meron, H. Yizhaq, and E. Gilad. Localized structures in dryland vegetation: Forms and functions. *Chaos*, 17(037109), 2007.

[53] J. D. Murray. *Mathematical Biology II: Spatial Models and Biomedical Applications*, volume 18 of *Interdisciplinary Applied Mathematics*. Springer New York, 2003.

[54] J. Nathan, J. von Hardenberg, and E. Meron. Spatial instabilities untie the exclusion-principle constraint on species coexistence. *Journal of Theoretical Biology*, 335:198 – 204, 2013.

[55] L. A. Peletier and W. C. Troy. Spatial patterns described by the extended fisher–kolmogorov equation: Periodic solutions. *SIAM Journal on Mathematical Analysis*, 28(6):1317–1353, 1997.

[56] L. Pismen. *Patterns and Interfaces in Dissipative Dynamics*. Springer Series in Synergetics. Springer, 2006.

[57] Y. Pomeau. Front motion, metastability and subcritical bifurcations in hydrodynamics. *Physica D*, 23:3–11, 1986.

[58] F. I. Pugnaire and M. T. Luque. Changes in plant interactions along a gradient of environmental stress. *Oikos*, 93:42–49, 2001.

[59] P. H. Rabinowitz. Some global results for nonlinear eigenvalue problems. *Journal of functional analysis*, 7(3):487–513, 1971.

[60] M. Rietkerk, M. C. Boerlijst, F. van Langevelde, R. HilleRisLambers, J. van de Koppel, L. Kumar, H. H. T. Prins, and A. M. D. Roos. Self-organization of vegetation in arid ecosystems. *American Naturalist*, 160:524–530, 2002.

[61] M. Rietkerk, S. C. Dekker, P. C. de Ruiter, and J. van de Koppel. Self-organized patchiness and catastrophic shifts in ecosystems. *Science*, 305:1926–1929, 2004.

[62] M. Rietkerk and J. van de Koppel. Regular pattern formation in real ecosystems. *Trends in Ecology and evolution*, 23(3):169–175, 2008.

[63] M. Sankaran, J. Ratnam, and N. P. Hanan. Tree–grass coexistence in savannas revisited – insights from an examination of assumptions and mechanisms invoked in existing models. *Ecology Letters*, 7(6):480–490, 2004.

[64] M. Scheffer, S. R. Carpenter, J. A. Foley, C. Folke, and B. Walker. Catastrophic shifts in ecosystems. *Nature*, 413:591–596, 2001.

[65] R. Scholes, P. Dowty, K. Caylor, D. Parsons, P. Frost, and H. Shugart. Trends in savanna structure and composition along an aridity gradient in the kalahari. *Journal of Vegetation Science*, 13:419–428, 2002.

[66] M. Shachak, J. R. Gosz, A. Perevolotsky, and S. T. A. Pickett. *Biodiversity in Drylands: Towards a Unified Framework*. Oxford University Press, 2005.

[67] E. Sheffer, J. von Hardenberg, H. Yizhaq, M. Shachak, and E. Meron. Emerged or imposed: a theory on the role of physical templates and self-organisation for vegetation patchiness. *Ecology Letters*, 16(2):127–139, 2013.

[68] E. Sheffer, H. Yizhaq, E. Gilad, M. Shachak, and E. Meron. Why do plants in resource deprived environments form rings? *Ecological Complexity*, 4:192–200, 2007.

[69] E. Sheffer, H. Yizhaq, M. Shachak, and E. Meron. Mechanisms of vegetation-ring formation in water-limited systems. *Journal of Theoretical Biology*, 273(1):138–146, 2011.

[70] J. A. Sherratt and G. J. Lord. Nonlinear dynamics and pattern bifurcations in a model for vegetation stripes in semi-arid environments. *Theoritical Population Biology*, 71:1–11, 2007.

[71] J. Smoller. Shock waves and reaction-diffusion equations. In *Research supported by the US Air Force and National Science Foundation. New York and Heidelberg, Springer-Verlag (Grundlehren der Mathematischen Wissenschaften. Volume 258), 1983, 600 p.*, volume 258, 1983.

[72] J. Swift and P. C. Hohenberg. Hydrodynamic fluctuations at the convective instability. *Phys. Rev. A*, 15:319–328, Jan 1977.

[73] R. Temam. *Navier–Stokes Equations and Nonlinear Functional Analysis*. Society for Industrial and Applied Mathematics, 1995.

[74] D. Tilman. *Resource competition and community structure*. Monographs in Population Biology. Princeton University Press, Princeton, New Jersey, USA, 1982.

[75] M. Tlidi, R. Lefever, and A. Vladimirov. On vegetation clustering, localized bare soil spots and fairy circles. In *Dissipative Solitons: From Optics to Biology and Medicine*, pages 1–22. Springer, 2008.

[76] D. J. Tongway, C. Valentin, J. Seghieri, and J.-C. Menaut, editors. *Banded Vegetation Patterning in Arid and Semiarid Environments: Ecological Processes and Consequences for Management.* Ecological Studies 149. Springer, 2001.

[77] A. M. Turing. The chemical basis of morphogenesis. *Philosophical Transactions of the Royal Society of London, series B*, 237:37–72, 1952.

[78] L. Turnbull, J. Wainwright, and R. E. Brazier. Changes in hydrology and erosion over a transition from grassland to shrubland. *Hydrological Processes*, 24(4):393–414, 2010.

[79] S. van der Stelt, A. Doelman, G. Hek, and J. D. M. Rademacher. Rise and fall of periodic patterns for a generalized klausmeier–gray–scott model. *Journal of nonlinear science*, 23(1):39–95, 2013.

[80] J. von Hardenberg, A. Y. Kletter, H. Yizhaq, J. Nathan, and E. Meron. Periodic versus scale-free patterns in dryland vegetation. *Proc. Roy. Soc. B*, 277:1771–1776, 2010.

[81] J. von Hardenberg, E. Meron, M. Shachak, and Y. Zarmi. Diversity of vegetation patterns and desertification. *Physical Review Letters*, 87:198101–1, 2001.

[82] I. I. Vrabie. *Compactness methods for nonlinear evolutions*, volume 75. CRC Press, 1995.

[83] L. Wang and M. Y. Li. Diffusion-driven instability in reaction–diffusion systems. *Journal of mathematical analysis and applications*, 254(1):138–153, 2001.

[84] N. E. West. Structure and functions of microphytic soil crusts in wildland ecosystems of arid to semi-arid regions. *Advances in ecological Research*, 20:179–223, 1990.

[85] E. Zeidler. *Nonlinear Functional Analysis and Its Applications*, volume II/B. Springer, 1990.

[86] Y. R. Zelnik, S. Kinast, H. Yizhaq, G. Bel, and E. Meron. Regime shifts in models of dryland vegetation. *Philosophical Transactions R. Soc. A*, 371:20120358, 2013.